

INVITED ARTICLE

Nonlinear waves in Bose–Einstein condensates: physical relevance and mathematical techniques

R Carretero-González^{1,4}, D J Frantzeskakis² and P G Kevrekidis³

¹ Nonlinear Dynamical Systems Group⁵, and Computational Science Research Center⁶,
Department of Mathematics and Statistics, San Diego State University, San Diego CA,
92182-7720, USA

² Department of Physics, University of Athens, Panepistimiopolis, Zografos, Athens 15784,
Greece

³ Department of Mathematics and Statistics, University of Massachusetts, Amherst MA
01003-4515, USA

Received 20 October 2006, in final form 12 March 2008

Published 10 June 2008

Online at stacks.iop.org/Non/21/R139

Recommended by J Lega

Abstract

The aim of this review is to introduce the reader to some of the physical notions and the mathematical methods that are relevant to the study of nonlinear waves in Bose–Einstein condensates (BECs). Upon introducing the general framework, we discuss the prototypical models that are relevant to this setting for different dimensions and different potentials confining the atoms. We analyse some of the model properties and explore their typical wave solutions (plane wave solutions, bright, dark, gap solitons as well as vortices). We then offer a collection of mathematical methods that can be used to understand the existence, stability and dynamics of nonlinear waves in such BECs, either directly or starting from different types of limits (e.g. the linear or the nonlinear limit or the discrete limit of the corresponding equation). Finally, we consider some special topics involving more recent developments, and experimental setups in which there is still considerable need for developing mathematical as well as computational tools.

PACS numbers: 03.75.Kk, 03.75.Lm, 05.45.Yv

(Some figures in this article are in colour only in the electronic version)

⁴ <http://rohan.sdsu.edu/~rcarretero/>

⁵ <http://nlds.sdsu.edu/>

⁶ <http://www.csrc.sdsu.edu/>

Abbreviations

AC	Anti-continuum (limit)
BEC	Bose–Einstein condensate
BdG	Bogoliubov–de Gennes (equations)
cqNLS	cubic-quintic NLS
DNLS	discrete nonlinear Schrödinger (equation)
EP	Ermakov–Pinney (equation)
GP	Gross–Pitaevskii (equation)
KdV	Korteweg–de Vries (equation)
LS	Lyapunov–Schmidt (technique)
MT	magnetic trap
NLS	nonlinear Schrödinger (equation)
NPSE	non-polynomial Schrödinger equation
ODE	ordinary differential equation
OL	optical lattice
PDE	partial differential equation
RPM	reductive perturbation method
TF	Thomas–Fermi

1. Introduction

The phenomenon of Bose–Einstein condensation is a quantum-phase transition originally predicted by Bose [1] and Einstein [2, 3] in 1924. In particular, it was shown that below a critical transition temperature T_c , a finite fraction of particles of a boson gas (i.e. whose particles obey the Bose statistics) *condenses* into the same quantum state, known as the *Bose–Einstein condensate* (BEC). Although Bose–Einstein condensation is known to be a fundamental phenomenon, connected, e.g. to superfluidity in liquid helium and superconductivity in metals (see, e.g., [4]), BECs were experimentally realized 70 years after their theoretical prediction: this major achievement took place in 1995, when different species of dilute alkali vapours confined in a magnetic trap (MT) were cooled down to extremely low temperatures [5–7], and has already been recognized through the 2001 Nobel prize in Physics [8, 9]. This first unambiguous manifestation of a macroscopic quantum state in a many-body system sparked an explosion of activity, as reflected by the publication of several thousand papers related to BECs since then. Nowadays there exist more than fifty experimental BEC groups around the world, while an enormous amount of theoretical work has followed and driven the experimental efforts, with an impressive impact on many branches of physics.

From a theoretical standpoint, and for experimentally relevant conditions, the static and dynamical properties of a BEC can be described by means of an effective mean-field equation known as the Gross–Pitaevskii (GP) equation [10, 11]. This is a variant of the famous nonlinear Schrödinger (NLS) equation [12] (incorporating an external potential used to confine the condensate), which is known to be a universal model describing the evolution of complex field envelopes in nonlinear dispersive media [13]. As such, the NLS equation is a key model appearing in a variety of physical contexts, ranging from optics [14–17], to fluid dynamics and plasma physics [18], while it has also attracted much interest from a mathematical viewpoint [12, 19, 20]. The relevance and importance of the NLS model is not limited to the case of conservative systems and the theory of solitons [13, 18, 21–23]; in fact, the NLS equation is directly connected to dissipative universal models, such as the complex Ginzburg–Landau

equation [24,25], which have been studied extensively in the context of pattern formation [26] (see also [27] for further discussion and applications).

In the case of BECs, the nonlinearity in the GP (NLS) model is introduced by the interatomic interactions, accounted for through an effective mean field. Importantly, the mean-field approach, and the study of the GP equation, allows the prediction and description of important, and experimentally relevant, nonlinear effects and nonlinear waves, such as solitons and vortices. These, so-called, *matter-wave* solitons and vortices can be viewed as fundamental nonlinear excitations of BECs, and as such have attracted considerable attention. Importantly, they have also been observed in many elegant experiments using various relevant techniques. These include, among others, phase engineering of the condensates in order to create vortices [28, 29] or dark matter-wave solitons in them [30–34], the stirring (or rotation) of the condensates providing angular momentum creating vortices [35,36] and vortex lattices [37–39], the change in scattering length (from repulsive to attractive via Feshbach resonances) to produce bright matter-wave solitons and soliton trains [40–43] in attractive condensates or set into motion a repulsive BEC trapped in a periodic optical potential referred to as optical lattice to create gap matter-wave solitons [44]. As far as vortices and vortex lattices are concerned, it should be noted that their description and connection to phenomena as rich and profound as superconductivity and superfluidity were one of the themes of the Nobel prize in Physics in 2003.

The aim of this paper is to give an overview of some physical and mathematical aspects of the theory of BECs. The fact that there exist already a relatively large number of reviews [45–51] and textbooks [4, 52–55] devoted in the physics of BECs, and given the space limitations of this paper, will not allow us to be all inclusive. Thus, this review naturally entails a personalized perspective on BECs, with a special emphasis on the nonlinear waves that arise in them. In particular, our aim here is to present an overview of both the physical setting and, perhaps more importantly, of the mathematical techniques from dynamical systems and nonlinear dynamics that can be used to address the dynamics of nonlinear waves in such a setting. This manuscript is organized as follows.

Section 2 is devoted to the mean-field description of BECs, the GP model and its properties. In particular, we present the GP equation and discuss its variants in the cases of repulsive and attractive interatomic interactions and how to control them via Feshbach resonances. We also describe the ground state properties of BECs and their small-amplitude excitations via the Bogoliubov–de Gennes equations. Additionally, we present the types of the external confining potential and how their form leads to specific types of simplified mean-field descriptions.

Section 3 describes the reduction of the spatial dimensionality of the BEC by means of effectively suppressing one or two transverse directions. This can be achieved by ‘tightening’ the external confining potential (usually a harmonic magnetic trap) along these directions. We introduce the basic nonlinear structures (dark and bright solitons) that are ubiquitous to one-dimensional settings. The different types of nonlinearities that arise from different approximations due to the dimensionality reduction are discussed. We also present the dimensionality reduction in the presence of external periodic potentials generated by the optical lattices (which are created as interference patterns of multiple laser beams) and the discrete limit, the discrete nonlinear Schrödinger equation, that they entail for strong potentials.

Section 4 deals with the mathematical methods used to describe nonlinear waves in BECs. The presentation concerns four categories of methods, depending on the particular features of the model at hand. The first one concern ‘direct’ methods, which analyse the nonlinear mean-field models directly, without employing techniques based on some appropriate, physically relevant and mathematically tractable limit. Such approaches include, for example, the method of moments, self-similarity and rescaling methods or the variational techniques among others.

The second one will concern methods that make detailed use of the understanding of the *linear limit* of the problem (e.g. the linear Schrödinger equation in the presence of a parabolic, periodic or a double-well potential). The third category of mathematical methods entails perturbation techniques from the *fully nonlinear limit* of the system (e.g. the integrable NLS equation), while the fourth one concerns discrete systems (relevant to BECs trapped in strong optical lattices), where perturbation methods from the so-called anti-continuum limit are extremely helpful.

Finally, in section 5 we present some special topics that have recently attracted much physical interest, both theoretical and experimental. These include multicomponent and spinor condensates described by systems of coupled GP equations, shock waves, as well as nonlinear structures arising in higher dimensions, such as vortices and vortex lattices in BECs, and multidimensional solitons (including dark and bright ones). We also briefly discuss the manipulation of matter waves by means of various techniques based on the appropriate control of the external potentials. In that same context, the effect of disorder on the matter waves is studied. Finally, we touch upon the description of BECs beyond mean-field theory, presenting relevant theoretical models that have recently attracted attention.

2. The Gross–Pitaevskii (GP) mean-field model

2.1. Origin and fundamental properties of the GP equation

We consider a sufficiently dilute ultracold atomic gas, composed by N interacting bosons of mass m confined by an external potential $V_{\text{ext}}(\mathbf{r})$. Then, the many-body Hamiltonian of the system is expressed, in second quantization form, through the boson annihilation and creation field operators, $\hat{\Psi}(\mathbf{r}, t)$ and $\hat{\Psi}^\dagger(\mathbf{r}, t)$, as [46, 53]

$$\hat{H} = \int d\mathbf{r} \hat{\Psi}^\dagger(\mathbf{r}, t) \hat{H}_0 \hat{\Psi}(\mathbf{r}, t) + \frac{1}{2} \int d\mathbf{r} d\mathbf{r}' \hat{\Psi}^\dagger(\mathbf{r}, t) \hat{\Psi}^\dagger(\mathbf{r}', t) V(\mathbf{r} - \mathbf{r}') \hat{\Psi}(\mathbf{r}', t) \hat{\Psi}(\mathbf{r}, t), \quad (1)$$

where $\hat{H}_0 = -(\hbar^2/2m)\nabla^2 + V_{\text{ext}}(\mathbf{r})$ is the ‘single-particle’ operator and $V(\mathbf{r} - \mathbf{r}')$ is the two-body interatomic potential. The mean-field approach is based on the so-called Bogoliubov approximation, first formulated by Bogoliubov in 1947 [56], according to which the condensate contribution is separated from the boson field operator as $\hat{\Psi}(\mathbf{r}, t) = \Psi(\mathbf{r}, t) + \hat{\Psi}'(\mathbf{r}, t)$. In this expression, the complex function $\Psi(\mathbf{r}, t) \equiv \langle \hat{\Psi}(\mathbf{r}, t) \rangle$ (i.e. the expectation value of the field operator), is commonly known as the *macroscopic wavefunction of the condensate*, while $\hat{\Psi}'(\mathbf{r}', t)$ describes the non-condensate part, which, at temperatures well below T_c , is actually negligible (for generalizations accounting for finite temperature effects see section 5.7). Then, the above prescription leads to a non-trivial zeroth-order theory for the BEC wavefunction as follows: first, from the Heisenberg evolution equation $i\hbar(\partial\hat{\Psi}/\partial t) = [\hat{\Psi}, \hat{H}]$ for the field operator $\hat{\Psi}(\mathbf{r}, t)$, the following equation is obtained:

$$i\hbar \frac{\partial}{\partial t} \hat{\Psi}(\mathbf{r}, t) = \left[\hat{H}_0 + \int d\mathbf{r}' \hat{\Psi}^\dagger(\mathbf{r}', t) V(\mathbf{r}' - \mathbf{r}) \hat{\Psi}(\mathbf{r}', t) \right] \hat{\Psi}(\mathbf{r}, t). \quad (2)$$

Next, considering the case of a dilute ultracold gas with binary collisions at low energy, characterized by the s-wave scattering length a , the interatomic potential can be replaced by an effective delta-function interaction potential, $V(\mathbf{r}' - \mathbf{r}) = g\delta(\mathbf{r}' - \mathbf{r})$ [46, 47, 52, 53], with the coupling constant (i.e. the nonlinear coefficient) g given by $g = 4\pi\hbar^2 a/m$. Finally, employing this effective interaction potential, and replacing the field operator $\hat{\Psi}$ with the classical field Ψ , equation (2) yields the GP equation,

$$i\hbar \frac{\partial}{\partial t} \Psi(\mathbf{r}, t) = \left[-\frac{\hbar^2}{2m} \nabla^2 + V_{\text{ext}}(\mathbf{r}) + g|\Psi(\mathbf{r}, t)|^2 \right] \Psi(\mathbf{r}, t). \quad (3)$$

The complex function Ψ in the GP equation (3) can be expressed in terms of the density $\rho(\mathbf{r}, t) \equiv |\Psi(\mathbf{r}, t)|^2$, and phase $S(\mathbf{r}, t)$ of the condensate as $\Psi(\mathbf{r}, t) = \sqrt{\rho(\mathbf{r}, t)} \exp[iS(\mathbf{r}, t)]$. Note that the current density $\mathbf{j} = (\hbar/2mi)(\Psi^*\nabla\Psi - \Psi\nabla\Psi^*)$ (asterisk denotes complex conjugate), assumes a hydrodynamic form $\mathbf{j} = \rho\mathbf{v}$, with an atomic velocity $\mathbf{v}(\mathbf{r}, t) = (\hbar/m)\nabla S(\mathbf{r}, t)$. The latter is irrotational (i.e. $\nabla \times \mathbf{v} = 0$), which is a typical feature of *superfluids*, and satisfies the famous Onsager–Feynman quantization condition $\oint_C \mathbf{dl} \cdot \mathbf{v} = (\hbar/m)\mathcal{N}$, where \mathcal{N} is the number of *vortices* enclosed by the contour C (the circulation is obviously zero for a simply connected geometry).

For time-independent external potentials, the GP model possesses two integrals of motion, namely, the total number of atoms,

$$N = \int |\Psi(\mathbf{r}, t)|^2 \mathbf{d}\mathbf{r}, \quad (4)$$

and the energy of the system,

$$E = \int \mathbf{d}\mathbf{r} \left[\frac{\hbar^2}{2m} |\nabla\Psi|^2 + V_{\text{ext}}|\Psi|^2 + \frac{1}{2}g|\Psi|^4 \right], \quad (5)$$

with the three terms in the right-hand side representing, respectively, the kinetic energy, the potential energy and the interaction energy.

A time-independent version of the GP equation (3) can readily be obtained upon expressing the condensate wave function as $\Psi(\mathbf{r}, t) = \Psi_0(\mathbf{r}) \exp(-i\mu t/\hbar)$, where Ψ_0 is a function normalized to the number of atoms ($N = \int \mathbf{d}\mathbf{r} |\Psi_0|^2$) and $\mu = \partial E/\partial N$ is the chemical potential. Substitution of the above expression into the GP equation (3) yields the following steady state equation for Ψ_0 :

$$\left[-\frac{\hbar^2}{2m} \nabla^2 + V_{\text{ext}}(\mathbf{r}) + g|\Psi_0|^2(\mathbf{r}) \right] \Psi_0(\mathbf{r}) = \mu\Psi_0(\mathbf{r}). \quad (6)$$

Equation (6) is useful for the derivation of stationary solutions of the GP equation, including the *ground state* of the system (see section 2.5).

2.2. The GP equation versus the full many-body quantum-mechanical problem

It is clear that the above mean-field approach and the analysis of the pertinent GP equation (3) is much simpler than a treatment of the full many-body Schrödinger equation. However, a quite important question is if the GP equation can be derived rigorously from a self-consistent treatment of the respective many-body quantum-mechanical problem. Although the GP equation is known from the early 1960s, this problem was successfully addressed only recently for the stationary GP equation (6) in [57]. In particular, in that work it was proved that the GP energy functional describes correctly the energy and the particle density of a trapped Bose gas to the leading order in the small parameter $\bar{\rho}|a|^3$, where $\bar{\rho}$ is the average density of the gas⁷. The above results were proved in the limit where the number of particles $N \rightarrow \infty$ and the scattering length $a \rightarrow 0$, such that Na is fixed. Importantly, although [57] referred to the full three-dimensional (3D) Bose gas, extensions of this work for lower dimensional settings were also reported (see the review [51] and references therein).

⁷ When $N|a|^3 \ll 1$, the Bose gas is called ‘dilute’ or ‘weakly interacting’. In fact, the smallness of this dimensionless parameter is required for the derivation of the GP equation (3); in typical BEC experiments this parameter takes values $N|a|^3 < 10^{-3}$ [46].

The starting point of the analysis of [57] is the effective Hamiltonian of N identical bosons. Choosing the units so that $\hbar = 2m = 1$, this Hamiltonian is expressed as (see also [52]),

$$H = \sum_{j=1}^N [-\nabla_j^2 + V_{\text{ext}}(\mathbf{r}_j)] + \sum_{i < j} v(|\mathbf{r}_i - \mathbf{r}_j|), \quad (7)$$

where $v(|\mathbf{r}|)$ is a general interaction potential assumed to be spherically symmetric and decaying faster than $|\mathbf{r}|^{-3}$ at infinity. Then, denoting the quantum-mechanical ground-state energy of the Hamiltonian (7) (which depends on the number of particles N and the dimensionless⁸ scattering length \tilde{a}) by $E_{\text{QM}}(N, \tilde{a})$, the main theorem proved in [57] is as follows:

- The GP energy is the dilute limit of the quantum-mechanical energy:

$$\forall \tilde{a}_1 > 0: \quad \lim_{n \rightarrow \infty} \frac{1}{N} E_{\text{QM}} \left(N, \frac{\tilde{a}_1}{n} \right) = E_{\text{GP}}(1, \tilde{a}_1), \quad (8)$$

where $E_{\text{GP}}(N, \tilde{a})$ is the energy of a solution of the dimensionless stationary GP equation (6) (in units such that $\hbar = 2m = 1$), and the convergence is uniform on bounded intervals of \tilde{a}_1 .

The above results (as well as the ones in [51]) were proved for stationary solutions of the GP equation, and, in particular, for the ground state solution. More recently, the time-dependent GP equation (3) was also analysed within a similar asymptotic limit ($N \rightarrow \infty$) in [58]. In this work, it was proved that the limit points of the k -particle density matrices of $\Psi_{N,t}$ (which is the solution of the N -particle Schrödinger equation) satisfy asymptotically the GP equation (and the associated hierarchy of equations) with a coupling constant given by $\int v(x) dx$, where $v(x)$ describes the interaction potential.

Thus, these recent rigorous results justify (under certain conditions) the use of the mean-field approach and the GP equation as a quite relevant model for the description of the static and dynamic properties of BECs.

2.3. Repulsive and attractive interatomic interactions. Feshbach resonance

Depending on the BEC species, the scattering length a (and, thus, the nonlinearity coefficient g in the GP equation (3)) may take either positive or negative values, accounting for repulsive or attractive interactions between the atoms, respectively. Examples of repulsive (attractive) BECs are formed by atomic vapours of ^{87}Rb and ^{23}Na (^{85}Rb and ^7Li), which are therefore described by a GP model with a defocusing (focusing) nonlinearity in the language of nonlinear optics [12, 17].

On the other hand, it is important to note that during atomic collisions, the atoms can stick together and form bound states in the form of molecules. If the magnetic moment of the molecular state is different from the one of atoms, one may use an external (magnetic, optical or dc-electric) field to controllably vary the energy difference between the atomic and molecular states. Then, at a so-called *Feshbach resonance* (see, e.g., [59] for a review), the energy of the molecular state becomes equal to that of the colliding atoms and, as a result, long-lived molecular states are formed. This way, as the aforementioned external field is varied through the Feshbach resonance, the scattering length is significantly increased, changes sign and is finally decreased. Thus, Feshbach resonance is a quite effective mechanism that can be used to manipulate the interatomic interaction (i.e. the magnitude and *sign* of the scattering length).

⁸ The dimensionless two-body scattering length is obtained from the solution $u(r)$ of the zero-energy scattering equation $-u''(r) + \frac{1}{2}v(r)u(r) = 0$ with $u(0) = 0$ and is given, by definition, as $\tilde{a} = \lim_{r \rightarrow \infty} (r - u(r)/u'(r))$ (see also [52, 53]).

Specifically, the behaviour of the scattering length near a Feshbach resonant magnetic field B_0 is typically of the form [60, 61],

$$a(B) = \hat{a} \left(1 - \frac{\Delta}{B - B_0} \right), \quad (9)$$

where \hat{a} is the value of the scattering length far from resonance and Δ represents the width of the resonance. Feshbach resonances were studied in a series of elegant experiments performed with sodium [62, 63] and rubidium [64, 65] condensates. Additionally, they have been used in many important experimental investigations, including, among others, the formation of bright matter-wave solitons [40–43].

2.4. The external potential in the GP model

The external potential $V_{\text{ext}}(\mathbf{r})$ in the GP equation (3) is used to trap and/or manipulate the condensate. In the first experiments, the BECs were confined by means of magnetic fields [8, 9], while later experiments demonstrated that optical confinement of BECs is also possible [66, 67], utilizing the so-called optical dipole traps [68, 69]. While magnetic traps are typically harmonic (see below), the shape of optical dipole traps is extremely flexible and controllable, as the dipole potential is directly proportional to the light intensity field [69]. An important example is the special case of periodic optical potentials called *optical lattices* (OLs), which have been used to reveal novel physical phenomena in BECs [70–72].

In the case of the ‘traditional’ magnetic trap, the external potential has the harmonic form

$$V_{\text{MT}}(\mathbf{r}) = \frac{1}{2}m(\omega_x^2 x^2 + \omega_y^2 y^2 + \omega_z^2 z^2), \quad (10)$$

where, in general, the trap frequencies ω_x , ω_y , ω_z along the three directions are different. On the other hand, the optical lattice is generated by a pair of laser beams forming a standing wave which induces a periodic potential. For example, a single periodic 1D standing wave of the form $E(z, t) = 2E_0 \cos(kz) \exp(-i\omega t)$ can be created by the superposition of the two identical beams, $E_{\pm}(z, t) = E_0 \exp[i(\pm kz - \omega t)]$, having the same polarization, amplitude E_0 , wavelength $\lambda = 2\pi/k$ and frequency ω . Since the dipole potential V_{dip} is proportional to the intensity $I \sim |E(z, t)|^2$ of the light field [69], this leads to an optical lattice of the form $V_{\text{dip}} \equiv V_{\text{OL}} = V_0 \cos^2(kz)$. In such a case, the lattice periodicity is $\lambda/2$ and the lattice height is given by $V_0 \sim I_{\text{max}}/\Delta\omega$, where I_{max} is the maximum intensity of the light field and $\Delta\omega \equiv \omega - \omega_0$ is the detuning of the lasers from the atomic transition frequency ω_0 . Note that atoms are trapped at the nodes (anti-nodes) of the optical lattice for blue- (red-) detuned laser beams or $\Delta\omega > 0$ ($\Delta\omega < 0$). In a more general 3D setting, the optical lattice potential can take the following form

$$V_{\text{OL}}(\mathbf{r}) = V_0 [\cos^2(k_x x + \phi_x) + \cos^2(k_y y + \phi_y) + \cos^2(k_z z + \phi_z)], \quad (11)$$

where $k_i = 2\pi/\lambda_i$ ($i \in \{x, y, z\}$), $\lambda_i = \lambda/[2 \sin(\theta_i/2)]$, θ_i are the (potentially variable) angles between the laser beams [70, 72] and ϕ_i are arbitrary phases.

It is also possible to realize experimentally an ‘optical superlattice’, characterized by two different periods. In particular, as demonstrated in [73], such a superlattice can be formed by the sequential creation of two lattice structures using four laser beams. A stationary 1D superlattice can be described as $V(z) = V_1 \cos(k_1 z) + V_2 \cos(k_2 z)$, where k_i and V_i denote, respectively, the wavenumbers and amplitudes of the sublattices. The experimental tunability of these parameters provides precise and flexible control over the shape and time variation of the external potential.

The magnetic or/and the optical dipole traps can be experimentally combined either with each other or with other potentials; an example concerns far off-resonant laser beams, which

can create effective repulsive or attractive localized potentials, for blue-detuned or red-detuned lasers, respectively. Such a combination of a harmonic trap with a repulsive localized potential located at the centre of the harmonic trap is the *double-well* potential, such as, e.g. the one used in the seminal interference experiment of [74]. Double-well potentials have also been created by a combination of a harmonic and a periodic optical potential [75]. Finally, other combinations, including, e.g., linear ramps of (gravitational) potential $V_{\text{ext}} = mgz$ have also been experimentally applied (see, e.g., [75, 76]). Additional recent possibilities include the design and implementation of external potentials, offered, e.g., by the so-called *atom chips* [77–79] (see also the review [80]). Importantly, the major flexibility for the creation of a wide variety of shapes and types of external potentials (e.g. stationary, time-dependent, etc), has inspired many interesting applications (see, for example, section 5.4).

2.5. Ground state

The ground state of the GP model of equation (3) can readily be found upon expressing the condensate wave function as $\Psi(\mathbf{r}, t) = \Psi_0(\mathbf{r}) \exp(-i\mu t/\hbar)$. If $g = 0$, equation (6) reduces to the usual Schrödinger equation with potential V_{ext} . Then, for a harmonic external trapping potential (see equation (10)), the ground state of the system is obtained when letting all non-interacting bosons occupy the lowest single-particle state; there, Ψ_0 has the Gaussian profile

$$\Psi_0(\mathbf{r}) = \sqrt{N} \left(\frac{m\omega_{\text{ho}}}{\pi\hbar} \right)^{3/4} \exp \left[-\frac{m}{2\hbar} (\omega_x x^2 + \omega_y y^2 + \omega_z z^2) \right], \quad (12)$$

where $\omega_{\text{ho}} = (\omega_x \omega_y \omega_z)^{1/3}$ is the geometric mean of the confining frequencies.

For repulsive interatomic forces ($g > 0$ or scattering length $a > 0$), if the number of atoms of the condensate is sufficiently large so that $Na/a_{\text{ho}} \gg 1$, the atoms are pushed towards the rims of the condensate, resulting in slow spatial variations of the density. Then the kinetic energy (gradient) term is small compared with the interaction and potential energies and becomes significant only close to the boundaries. Thus, the Laplacian kinetic energy term in equation (6) can safely be neglected. This results in the, so-called, Thomas–Fermi (TF) approximation [46, 52, 53] for the system’s ground state density profile:

$$\rho(\mathbf{r}) = |\Psi_0(\mathbf{r})|^2 = g^{-1} [\mu - V_{\text{ext}}(\mathbf{r})], \quad (13)$$

in the region where $\mu > V_{\text{ext}}(\mathbf{r})$ and $\rho = 0$ outside. For a spherically symmetric harmonic magnetic trap ($V_{\text{ext}} = V_{\text{MT}}$ with $\omega_{\text{ho}} = \omega_x = \omega_y = \omega_z$), the radius $R_{\text{TF}} = (2\mu/m)^{1/2}/\omega_{\text{ho}}$ for which $\rho(R_{\text{TF}}) = 0$ is the so-called Thomas–Fermi radius determining the size of the condensed cloud. Furthermore, the normalization condition connects μ and N through the equation $\mu = (\hbar\omega_{\text{ho}}/2)(15Na/a_{\text{ho}})^{2/5}$, where $a_{\text{ho}} = (\hbar/m\omega_{\text{ho}})^{1/2}$ is the harmonic oscillator length.

For attractive interatomic forces ($g < 0$ or $a < 0$), the density tends to increase at the trap centre, while the kinetic energy tends to balance this increase. However, if the number of atoms N in the condensate exceeds a critical value, i.e. $N > N_{\text{cr}}$, the system is subject to *collapse* in 2D or 3D settings [12, 52, 53]. Collapse was observed experimentally in both cases of the attractive ^7Li [81] and ^{85}Rb condensates [82]. In these experiments, it was demonstrated that during collapse the density grows and, as a result, the rate of collisions (both elastic and inelastic) is increased; these collisions cause atoms to be ejected from the condensate in an energetic explosion, which leads to a loss of mass that results in a smaller condensate. It should be noted that the behaviour of BECs close to collapse can be significantly affected by effects such as inelastic two- and three-body collisions that are not included in the original GP equation; such effects are briefly discussed below (see section 3.4).

The critical number of atoms necessary for collapse in a spherical BEC is determined by the equation $N_{\text{cr}}|a|/a_{\text{ho}} = 0.575$ [83], where $|a|$ is the absolute value of the scattering length. Importantly, collapse may not occur in a quasi-1D setting (see section 3.1), provided that the number of atoms does not exceed the critical value given by the equation $N_{\text{cr}}|a|/a_r = 0.676$, with a_r being the transverse harmonic oscillator length [84–86].

2.6. Small-amplitude linear excitations

We now consider small-amplitude excitations of the condensate, which can be found upon linearizing the time-dependent GP equation around the ground state. Specifically, solutions of equation (3) can be sought in the form

$$\Psi(\mathbf{r}, t) = e^{-i\mu t/\hbar} \left[\Psi_0(\mathbf{r}) + \sum_j (u_j(\mathbf{r})e^{-i\omega_j t} + v_j^*(\mathbf{r})e^{i\omega_j t}) \right], \quad (14)$$

where u_j, v_j are small (generally complex) perturbations, describing the components of the condensate's (linear) response to the external perturbations that oscillate at frequencies $\pm\omega_j$ (the latter are (generally complex) eigenfrequencies). Substituting equation (14) into equation (3), and keeping only the linear terms in u_j and v_j , the following set of equations is derived:

$$\begin{aligned} [\hat{H}_0 - \mu + 2g|\Psi_0|^2(\mathbf{r})]u_j(\mathbf{r}) + g\Psi_0^2(\mathbf{r})v_j(\mathbf{r}) &= \hbar\omega_j u_j(\mathbf{r}), \\ [\hat{H}_0 - \mu + 2g|\Psi_0|^2(\mathbf{r})]v_j(\mathbf{r}) + g\Psi_0^{*2}(\mathbf{r})u_j(\mathbf{r}) &= -\hbar\omega_j v_j(\mathbf{r}), \end{aligned} \quad (15)$$

where $\hat{H}_0 \equiv -(\hbar^2/2m)\nabla^2 + V_{\text{ext}}(\mathbf{r})$. Equations (15) are known as the *Bogoliubov–de Gennes* (BdG) equations. These equations can also be derived using a purely quantum-mechanical approach [46, 47, 52, 53] and can be used, apart from the ground state, for any state (including solitons and vortices) with the function Ψ_0 being modified accordingly.

The BdG equations are intimately connected to the stability of the state Ψ_0 . Specifically, suitable combinations of equations (15) yield

$$(\omega_j - \omega_j^*) \int (|u_j|^2 - |v_j|^2) d\mathbf{r} = 0. \quad (16)$$

This equation can be satisfied in two different ways: first, if $\omega_j - \omega_j^* = 0$, i.e. if the eigenfrequencies ω_j are real; if this is true for all j , the fact that $\text{Im}\{\omega_j\} = 0$ shows that the state Ψ_0 is *stable*. Note that, in this case, one can use the normalization condition for the eigenmodes u_j, v_j of the form $\int (|u_j|^2 - |v_j|^2) d\mathbf{r} = 1$. On the other hand, occurrence of imaginary or complex eigenfrequencies ω_j (i.e. if $\omega_j - \omega_j^* \neq 0$ or $\text{Im}\{\omega_j\} \neq 0$), indicates *dynamical instability* of the state Ψ_0 ; in such a case, equation (16) is satisfied only if $\int |u_j|^2 d\mathbf{r} = \int |v_j|^2 d\mathbf{r}$.

In the case of a uniform gas (i.e. for $V_{\text{ext}}(\mathbf{r}) = 0$ and $\Psi_0^2 = \rho = \text{const}$), the amplitudes u and v are plane waves $\sim e^{i\mathbf{k}\cdot\mathbf{r}}$ (of wavevector \mathbf{k}) and the BdG equations (15) lead to a dispersion relation, known as the *Bogoliubov spectrum*:

$$(\hbar\omega)^2 = \left(\frac{\hbar^2 \mathbf{k}^2}{2m} \right) \left(\frac{\hbar^2 \mathbf{k}^2}{2m} + 2g\rho \right). \quad (17)$$

For small momenta $\hbar\mathbf{k}$, equation (17) yields the phonon dispersion relation $\omega = cq$, where

$$c = \sqrt{g\rho/m} \quad (18)$$

is the *speed of sound*, while, for large momenta, the spectrum provides the free particle energy $\hbar^2 \mathbf{k}^2 / (2m)$; the ‘crossover’ between the two regimes occurs when the excitation wavelength is of the order of the healing length (see equation (19)).

In the case of attractive interatomic interactions ($g < 0$), the speed of sound becomes imaginary, which indicates that long wavelength perturbations grow or decay exponentially in time. This effect is directly connected to the *modulational instability*, which leads to delocalization in momentum space and, in turn, to localization in position space and the formation of solitary wave structures. Modulational instability is responsible for the formation of bright matter-wave solitons [40–42], as analysed by various theoretical works (see, e.g., [87–89] and the reviews [90, 91]).

3. Lower-dimensional BECs, solitons and reduced mean-field models

3.1. The shape of the condensate and length scales

In the case of the harmonic trapping potential (10), the flexibility over the choice of the three confining frequencies ω_j ($j \in \{x, y, z\}$) may be used to control the shape of the condensate: if $\omega_x = \omega_y \equiv \omega_r \approx \omega_z$ the trap is isotropic and the BEC is almost spherical, while the cases $\omega_z < \omega_r$ or $\omega_r < \omega_z$ describe anisotropic traps in which the BEC is, respectively, ‘cigar shaped’ or ‘disc-shaped’. The strongly anisotropic cases with $\omega_z \ll \omega_r$ or $\omega_r \ll \omega_z$ are particularly interesting as they are related to effectively quasi-one-dimensional (1D) and quasi-two-dimensional (2D) BECs, respectively. Such lower-dimensional BECs have been studied theoretically [92–98] (see also [51] for a rigorous mathematical analysis) and have been realized experimentally in optical and magnetic traps [99], in optical lattice potentials [100–103] and surface microtraps [78, 79].

The confining frequencies of the harmonic trapping potential set characteristic length scales for the spatial size of the condensate through the characteristic harmonic oscillator lengths $a_j \equiv (\hbar/m\omega_j)^{1/2}$. Another important length scale, introduced by the effective mean-field nonlinearity, is the healing length, which is the distance over which the kinetic energy and the interaction energy balance: if the BEC density grows from 0 to ρ over the distance ξ , the kinetic energy, $\sim \hbar^2/(2m\xi^2)$, and interaction energy, $\sim 4\pi\hbar^2 a\rho/m$, become equal at the value of ξ given by [46, 52, 53]

$$\xi = (8\pi\rho a)^{-1/2}. \quad (19)$$

Note that the name for ξ is coined from the fact that it is actually the distance over which the BEC wavefunction Ψ ‘heals’ over defects. Thus, the spatial widths of nonlinear excitations, such as dark solitons and vortices in BECs, are of $\mathcal{O}(\xi)$.

3.2. Lower-dimensional GP equations

Let us assume that $\omega_z \ll \omega_x = \omega_y \equiv \omega_r$. Then, if the transverse harmonic oscillator length $a_r \equiv \sqrt{\hbar/m\omega_r} < \xi$, the transverse confinement of the condensate is so tight that the dynamics of such a cigar-shaped BEC can be considered to be effectively 1D. This allows for a reduction of the fully 3D GP equation to an effectively 1D GP model, which can be done for sufficiently small trapping frequency ratios ω_z/ω_r . It should be stressed, however, that such a reduction should be only considered as the 1D limit of a 3D mean-field theory and *not* as a genuine 1D theory (see, e.g., [51] for a rigorous mathematical discussion). Similarly, a disc-shaped BEC with $a_z < \xi$ and sufficiently small frequency ratios ω_r/ω_z , can be described by an effective 2D GP model. Below, we focus on cigar-shaped BECs and briefly discuss the case of disc-shaped ones.

Following [84, 104, 105] (see also [91]), we assume a quasi-1D setting with $\omega_z \ll \omega_r$ and decompose the wavefunction Ψ into longitudinal (along z) and transverse (on the (x, y) plane)

components; then, we seek for solutions of equation (3) in the form

$$\Psi(\mathbf{r}, t) = \psi(z, t) \Phi(r; t), \quad (20)$$

where $\Phi(r; t) = \tilde{\Phi}_0(r) \exp(-i\gamma t)$, $r^2 \equiv x^2 + y^2$, while the chemical potential γ and the transverse wavefunction $\tilde{\Phi}(r)$ are involved in the auxiliary problem for the transverse quantum harmonic oscillator,

$$\frac{\hbar^2}{2m} \nabla_r^2 \tilde{\Phi}_0 - \frac{1}{2} m \omega_r^2 r^2 \tilde{\Phi}_0 + \gamma \tilde{\Phi}_0 = 0, \quad (21)$$

where $\nabla_r^2 \equiv \partial^2/\partial x^2 + \partial^2/\partial y^2$. Since the considered system is effectively 1D, it is natural to assume that the transverse condensate wavefunction $\Phi(r)$ remains in the ground state; in such a case $\tilde{\Phi}_0(r)$ takes the form $\tilde{\Phi}_0(r) = \pi^{-1/2} a_r^{-1} \exp(-r^2/2a_r^2)$ (note that when considering the reduction from 3D to 2D the transverse wave function takes the form $\tilde{\Phi}_0(r) = \pi^{-1/4} a_r^{-1/2} \exp(-r^2/2a_r^2)$). Then, substituting equation (20) into equation (3) and averaging the resulting equation in the r -direction (i.e. multiplying by Φ^* and integrating with respect to r), we finally obtain the following 1D GP equation:

$$i\hbar \frac{\partial}{\partial t} \psi(z, t) = \left[-\frac{\hbar^2}{2m} \frac{\partial^2}{\partial z^2} + V(z) + g_{1D} |\psi(z, t)|^2 \right] \psi(z, t), \quad (22)$$

where the effective 1D nonlinear coefficient is given by $g_{1D} = g/2\pi a_r^2 = 2a\hbar\omega_r$ and $V(z) = (1/2)m\omega_z^2 z^2$. On the other hand, in the 2D case of disc-shaped BECs, the respective $(2+1)$ -dimensional NLS equation has the form of equation (22), with ∂_z^2 being replaced by the Laplacian ∇_r^2 , the effectively 2D nonlinear coefficient is $g_{2D} = g/\sqrt{2\pi} a_z = 2\sqrt{2\pi} a a_z \hbar\omega_z$, while the potential is $V(x, y) = (1/2)m\omega_r^2(x^2 + y^2)$. Note that such dimensionality reductions based on the averaging method are commonly used in other disciplines, such as, e.g., in nonlinear fibre optics [17].

A similar reduction can be performed if, additionally, an optical lattice potential is present. In this case, it is possible (as, e.g., in the experiment of [44]) to tune ω_z so that it provides only a very weak trapping along the z -direction; this way, the shift in the potential trapping energies over the wells where the BEC is confined can be made practically negligible. In such a case, the potential in equation (22) is simply the 1D optical lattice $V(z) = V_0 \cos^2(kz)$. Similarly, an ‘egg-carton potential’ $V(x, y) = V_0[\cos^2(k_x x) + \cos^2(k_y y)]$ is relevant for disc-shaped condensates.

We note in passing that the dimensionality reduction of the GP equation can also be done self-consistently, using multiscale expansion techniques [106, 107]. It is also worth mentioning that more recently a rigorous derivation of the 1D GP equation was presented in [108], using energy and Strichartz estimates, as well as two anisotropic Sobolev inequalities.

3.3. Bright and dark matter-wave solitons

The 1D GP equation (22) can be reduced to the following dimensionless form

$$i \frac{\partial}{\partial t} \psi(z, t) = \left[-\frac{\partial^2}{\partial z^2} + V(z) + g |\psi(z, t)|^2 \right] \psi(z, t), \quad (23)$$

where the density $|\psi|^2$, length, time and energy are, respectively, measured in units of $4\pi|a|a_r^2$, a_r , ω_r^{-1} and $\hbar\omega_r$, while the nonlinear coefficient g is rescaled to unity (i.e. $g = \pm 1$ for repulsive and attractive interatomic interactions, respectively). In the case of a homogeneous BEC ($V(z) = 0$), equation (23) becomes the ‘traditional’ completely integrable NLS equation.

The latter is well known (see, e.g., [21]) to possess an infinite number of conserved quantities (integrals of motion), with the lowest-order ones being the number of particles:

$$N = \int_{-\infty}^{\infty} |\psi|^2 dz,$$

the momentum:

$$P = (i/2) \int_{-\infty}^{\infty} (\psi \psi_z^* - \psi^* \psi_z) dz$$

and the energy:

$$E = (1/2) \int_{-\infty}^{\infty} (|\psi_z|^2 + g|\psi|^4) dz,$$

where the subscripts denote partial derivatives.

The type of soliton solutions of the NLS equation depends on the parameter g . In particular, for *attractive* BECs ($g = -1$), the NLS equation possesses a *bright* soliton solution of the following form [109]

$$\psi_{bs}(z, t) = \eta \operatorname{sech}[\eta(z - vt)] \exp[i(kz - \omega t)], \quad (24)$$

where η is the amplitude and inverse spatial width of the soliton, while k , ω and $v \equiv \partial\omega/\partial k = k$ are the soliton wavenumber, frequency and velocity, respectively. The frequency and wavenumber of the soliton are connected through the ‘soliton dispersion relation’ $\omega = \frac{1}{2}(k^2 - \eta^2)$, which implies that the allowable region in the (k, ω) plane for bright solitons is located *below* the parabola $\omega = \frac{1}{2}k^2$, corresponding to the ‘elementary excitations’ (i.e. the linear wave solutions) of the NLS equation.

Introducing the solution (24) into the integrals of motion N , P and E it is readily found that

$$N = 2\eta, \quad P = 2\eta k, \quad E = \eta k^2 - \frac{1}{3}\eta^3. \quad (25)$$

These equations imply that the bright soliton behaves as a classical particle with effective mass M_{bs} , momentum P_{bs} and energy E_{bs} , respectively, given by $M_{bs} = 2\eta$, $P_{bs} = M_{bs}v$ and $E_{bs} = \frac{1}{2}M_{bs}v^2 - \frac{1}{24}M_{bs}^3$, where it is recalled that $v = k$. Note that in the equation for the energy, the first and second terms in the right-hand side are, respectively, the kinetic energy and the binding energy of the quasi-particles associated with the soliton [110]. Differentiating the soliton energy and momentum over the soliton velocity, the following relation is found:

$$\frac{\partial E_{bs}}{\partial P_{bs}} = v, \quad (26)$$

which underscores the particle-like nature of the bright soliton.

On the other hand, for *repulsive* BECs ($g = +1$), the NLS equation admits a dark soliton solution, which in this case is supported on a non-zero background $\psi = \psi_0 \exp[i(kz - \omega t)]$. The dark soliton may be expressed as [111]

$$\psi(z, t) = \psi_0 (\cos \varphi \tanh \zeta + i \sin \varphi) \exp[i(kz - \omega t)], \quad (27)$$

where $\zeta \equiv \psi_0 \cos \varphi (z - vt)$, $\omega = (1/2)k^2 + \psi_0^2$, while the remaining parameters v , φ and k are connected through the relation $v = \psi_0 \sin \varphi + k$. Here, φ is the so-called ‘soliton phase angle’ or, simply, the phase shift of the dark soliton ($|\varphi| < \pi/2$), which describes the *darkness* of the soliton through the relation, $|\psi|^2 = 1 - \cos^2 \varphi \operatorname{sech}^2 \zeta$; this way, the limiting cases $\varphi = 0$ and $\cos \varphi \ll 1$ correspond to the so-called *black* and *grey* solitons, respectively. The amplitude and velocity of the dark soliton are given by $\cos \varphi$ and $\sin \varphi$, respectively; thus, the black soliton, $\psi = \psi_0 \tanh(\psi_0 x) \exp(-i\mu t)$, is a stationary dark soliton ($v = 0$), while the

grey soliton moves with a velocity close to the speed of sound ($v \sim c \equiv \psi_0$ in our units). The dark soliton solution (27) has two independent parameters, for the background (ψ_0 and k) and for the soliton (φ). In fact, it should be mentioned that in both the bright and the dark solitons, there is also a freedom in selecting the initial location of the solitary wave z_0 (in the above formulae, z_0 has been set equal to zero)⁹. Also, it should be noted that as in this case the dispersion relation implies that $\omega > k^2$, the allowable region in the (k, ω) plane for dark solitons is located *above* the parabola $\omega = \frac{1}{2}k^2$.

As the integrals of motion of the NLS equation refer to *both* the background and the dark soliton, the integrals of motion for the dark soliton are *renormalized* so as to extract the contribution of the background [112–114]. In particular, the renormalized momentum and energy of the dark soliton (27) read (for $k = 0$):

$$P_{\text{ds}} = -2v(c^2 - v^2)^{1/2} + 2c^2 \tan^{-1} \left[\frac{(c^2 - v^2)^{1/2}}{v} \right], \quad (28)$$

$$E_{\text{ds}} = \frac{4}{3}(c^2 - v^2)^{3/2}. \quad (29)$$

Upon differentiating the above expressions over the soliton velocity v , it can readily be found that

$$\frac{\partial E_{\text{ds}}}{\partial P_{\text{ds}}} = v, \quad (30)$$

which shows that, similarly to the bright soliton, the dark soliton effectively behaves like a classical particle. Note that, usually, dark matter-wave solitons are considered in the simpler case where the background is at rest, i.e. $k = 0$; then, the frequency ω actually plays the role of a normalized one-dimensional chemical potential, namely, $\mu \equiv \psi_0^2$, which is determined by the number of atoms of the condensate. Moreover, it should be mentioned that in the case of a harmonically confined condensate, i.e. for $V(z) = \frac{1}{2}\Omega^2 z^2$ (with $\Omega = \omega_z/\omega_r$ being the normalized trap strength) in equation (23), the background of the dark soliton is actually the ground state of the BEC which can be approximated by the Thomas–Fermi cloud (see equation (13)); thus, the ‘composite’ wavefunction (containing both the background and the dark soliton) can be approximated, e.g., by the form $\psi = \psi_{\text{TF}}(z) \exp(-i\psi_0^2 t) \psi_{\text{ds}}(z, t)$, where $\psi_{\text{ds}}(z, t)$ is the dark soliton of equation (27).

Both types of matter-wave solitons, namely, the bright and the dark ones, have been observed in a series of experiments. In particular, the formation of quasi-1D bright solitons and bright soliton trains has been observed in ⁷Li [40, 41] and ⁸⁵Rb [42] atoms upon tuning the interatomic interaction within the stable BEC from repulsive to attractive via the Feshbach resonance mechanism (discussed in section 3.3). On the other hand, quasi-1D dark solitons were observed in ²³Na [30, 31] and ⁸⁷Rb [32–34] atoms upon employing quantum-phase engineering techniques or by dragging a moving impurity (namely a laser beam) through the condensate. Note that multidimensional solitons (and vortices) as well as many interesting applications based on the particle-like nature of matter-wave solitons highlighted here are discussed in section 5.

3.4. Mean-field models with non-cubic nonlinearities

Mean-field models with non-cubic nonlinearities have also been derived and used in various studies, concerning either the effect of dimensionality on the dynamics of cigar-shaped BECs or the effect of the three-body collisions irrespective of the dimensionality of the system.

⁹ Recall that the underlying model, namely, the completely integrable NLS equation, has infinitely many symmetries, including translational and Galilean invariance.

Let us first discuss the former case, i.e. consider a condensate confined in a highly anisotropic trap with, e.g., $\omega_z \ll \omega_r$, and examine the effect of the deviation from one-dimensionality on the longitudinal condensate dynamics. Following [115–119], one may factorize the wavefunction as per equation (20), but with the transverse wavefunction Φ depending also on the longitudinal variable z . Then, one may employ an *adiabatic approximation* to separate the fast transverse and slow longitudinal dynamics (i.e. neglecting derivatives of Φ with respect to the slow variables z and t). This way, assuming that the external potential is separable, $V_{\text{ext}}(\mathbf{r}) = U(r) + V(z)$, the following system of equations is obtained from the 3D GP equation (3):

$$i\hbar \frac{\partial \psi}{\partial t} = -\frac{\hbar^2}{2m} \frac{\partial^2 \psi}{\partial z^2} + V(z)\psi + \mu_r(\rho)\psi, \quad (31)$$

$$\mu_r(\rho)\Phi = -\frac{\hbar^2}{2m} \nabla_r^2 \Phi + U(r)\Phi + g\rho|\Phi|^2\Phi, \quad (32)$$

where the transverse local chemical potential $\mu_r(\rho)$ (which depends on the longitudinal density $\rho(z, t) = |\psi(z, t)|^2$) is determined by the ground state solution of equation (32). An approximate solution of the above system of equations (31) and (32) was found in [115] (see also [116, 117]) as follows. As the system is close to 1D, it is natural to assume that the transverse wave function is *close* to the ground state of the transverse harmonic oscillator, and can be expanded in terms of the radial eigenmodes $\tilde{\Phi}_j$, i.e. $\Phi(r; z) = \tilde{\Phi}_0(r) + \sum_j C_j(z)\tilde{\Phi}_j(r)$. Accordingly, expanding the chemical potential $\mu_r(\rho)$ in terms of the density as $\mu_r(\rho) = \hbar\omega_r + g_1\rho - g_2\rho^2 + \dots$, the following NLS equation is obtained:

$$i\hbar \frac{\partial \psi}{\partial t} = \left[-\frac{\hbar^2}{2m} \frac{\partial^2}{\partial z^2} + V(z) + f(\rho) \right] \psi, \quad (33)$$

with the nonlinearity function given by

$$f(\rho) = g_1\rho - g_2\rho^2. \quad (34)$$

It is clear that equation (33) is a *cubic–quintic* NLS (cqNLS) equation, with the coefficient of the linear and quadratic term being given in [115]: $g_1 = g_{1\text{D}} = 2a\hbar\omega_r$ and $g_2 = 24 \ln(4/3)a^2\hbar\omega_r$, respectively. In the effectively 1D case discussed in section 3.2, this cqNLS equation is reduced to the 1D GP equation (22). Note that the cqNLS model has been used in studies of the dynamics of dark [115] and bright [116, 117] matter-wave solitons in elongated BECs.

The transverse chemical potential μ_r of an elongated condensate was also derived recently by Muñoz Mateo and Delgado [118] as a function of the longitudinal density ρ . This way, the same authors presented in the recent work of [119] the effective 1D NLS equation (33), but with the nonlinearity function given by

$$f(\rho) = \sqrt{1 + 4aN\rho}, \quad (35)$$

where a is the scattering length and N is the number of atoms¹⁰. Note that in the weakly interacting limit, $4aN\rho \ll 1$, the resulting NLS equation has the form of equation (22), with the same nonlinear coefficient $g_{1\text{D}}$. This model, which was originally suggested in [120], predicts accurately ground state properties of the condensate, such as the chemical potential, the axial density profile and the speed of sound.

Other approaches to the derivation of effective lower-dimensional mean-field models have also been proposed in earlier works, leading (as in the case of [118–120]) to NLS-type equations with *generalized nonlinearities* [121–125]. Among these models, the so-called

¹⁰ Note that the number of atoms N appears in the nonlinearity function $f(\rho)$ due to the fact that the wavefunction is now normalized to 1 rather than to N , as in the GP equation (22).

non-polynomial Schrödinger equation (NPSE) has attracted considerable attention. The latter was obtained by Salasnich *et al* [121] by employing the following ansatz for the transverse wavefunction, $\Phi(r; t) = [\exp(-r^2/2\sigma^2(z, t))]/[\pi^{1/2}\sigma(z, t)]$; then, the variational equations related to the minimization of the action functional (from which the 3D GP equation can be derived as the associated Euler–Lagrange equation) led to equation (33) with a nonlinearity function

$$f(\rho) = \frac{gN}{2\pi a_r^2} \frac{\rho}{\sqrt{1+2aN\rho}} + \frac{\hbar\omega_r}{2} \left(\frac{1}{\sqrt{1+2aN\rho}} + \sqrt{1+2aN\rho} \right), \quad (36)$$

and to the following equation for the transverse width σ : $\sigma^2 = a_r^2 \sqrt{1+2aN\rho}$. Note that in the weakly interacting limit of $aN\rho \ll 1$, equation (33) becomes again equivalent to the 1D GP equation (22), while the width σ becomes equal to the transverse harmonic oscillator length a_r . The NPSE (33) has been found to predict accurately static and dynamic properties of cigar-shaped BECs (such as the density profiles, the speed of sound and the collapse threshold of attractive BECs) [126], while its solitonic solutions have been derived in [121]. Generalizations of the NPSE model in applications involving time-dependent potentials [124, 127] or the description of spin-1 atomic condensates [125], have also been presented. Moreover, it is worth mentioning that the NPSE has been found to predict accurately the BEC dynamics in recent experiments [75].

On the other hand, as mentioned above, mean-field models with non-cubic nonlinearities, and particularly the cqNLS equation in a 1D, 2D or a 3D setting, may have a different physical interpretation, namely, to take into account three-body interactions. In this context, and in the most general case, the coefficients g_1 and g_2 in equation (34) are complex, with the imaginary parts describing *inelastic* two- and three-body collisions, respectively [128]. As concerns the three-body collision process, it occurs at interparticle distances of order of the characteristic radius of interaction between atoms and, generally, results in the decrease of the density that can be achieved in traps. Particularly, the rate of this process is given by $(d\rho/dt) = -L\rho^3$ [52], where ρ is the density and L is the loss rate, which is of order of 10^{-27} – 10^{-30} cm⁶ s⁻¹ for various species of alkali atoms [129]. Accordingly, the decrease in the density is equivalent to the term $-(L/2)|\Psi|^4\Psi$ in the time-dependent GP equation, i.e. to the above mentioned quintic term.

The cqNLS model has been studied in various works, mainly in the context of attractive BECs (scattering length $a < 0$ or $g_1 < 0$). Particularly, in studies concerning collapse, both cases with real g_2 [130], and with imaginary g_2 [131, 132] were considered. Additionally, relevant lower-dimensional (and in particular 1D) models were also analysed in [133, 134]. The latter works present also realistic values for these 1D cubic–quintic NLS models, including also estimations for the three-body collision parameter g_2 (see also [135–137] in which the coefficient g_2 was assumed to be real). Additionally, *periodic potentials* were also considered in such cubic–quintic models and various properties and excitations of the BECs, such as ground state and localized excitations [135] or band-gap structure and stability [136], were studied. Moreover, studies of modulational instability in the continuous model with the dissipative quintic term [138] or the respective discrete model with a conservative quintic term [137] were also reported.

3.5. Weakly and strongly interacting 1D Bose gases. The Tonks–Girardeau gas

In the previous subsections we discussed the case of ultracold *weakly interacting* quasi-1D BECs, which, in the absence of thermal or quantum fluctuations, are described by an effectively 1D GP equation (cf equation (22)). On the other hand, and in the same context of 1D Bose gases, there exists the opposite limit of *strong interatomic coupling* [92, 93, 139]. In this case,

the collisional properties of the bosonic atoms are significantly modified, with the interacting bosonic gas behaving like a system of free fermions; such, so-called, *Tonks–Girardeau* gases of impenetrable bosons [140, 141] have recently been observed experimentally [142, 143]. The transition between the weakly and strongly interacting regimes is usually characterized by a single parameter $\gamma = 2/(\rho a_{1D})$ [92, 93], with $a_{1D} \equiv a_r^2/a_{3D}$ and a_{3D} being the effective 1D and the usual 3D scattering lengths, respectively (a_r is the transverse harmonic oscillator length) [53]. This parameter quantifies the ratio of the average interaction energy to the kinetic energy calculated with mean-field theory. Note that γ varies smoothly as the interatomic coupling is increased from values $\gamma \ll 1$ for a weakly interacting 1D Bose gas, to $\gamma \gg 1$ for the strongly interacting Tonks–Girardeau gas, with an approximate ‘crossover regime’ being around $\gamma \sim \mathcal{O}(1)$, attained experimentally as well [144, 145].

The above mentioned weakly and strongly interacting 1D Bose gases can effectively be described by a generalized 1D NLS of the form of equation (33). In such a case, while the functional dependence of $f(\rho)$ on γ (and its analytical asymptotics) are known [146], its precise values in the crossover regime can only be evaluated numerically. Such intermediate values have been tabulated in [139], and subsequently discussed by various authors in the framework of the local density approximation [147, 148]. Note that following the methodology of [121], Salasnich *et al* have proposed a model different from the NPSE, but still of the form of equation (33), with the nonlinearity function depending on the density $|\psi|^2$ and the transverse width σ of the gas, to describe the weakly and the strongly interacting regimes, as well as the crossover regime [149]. Finally, it is noted that a much simpler approximate model (with $f(\rho)$ being an explicit function of the density), which also refers to these three regimes, was recently proposed in [150].

Coming back to the case of the Tonks–Girardeau gas, it has been suggested that an effective mean-field description of this limiting case can be based on a 1D *quintic* NLS equation, i.e. an equation of the form (33) with a nonlinearity function [151]:

$$f(\rho) = \frac{\pi^2 \hbar^2}{2m} \rho^2. \quad (37)$$

The quintic NLS equation was originally derived by Kolomeisky *et al* [152] from a renormalization group approach, and then by other groups, using different techniques [153–155]; it is also worth noting that its time-independent version has been rigorously derived from the many-body Schrödinger equation [156]. Although the applicability of the quintic NLS equation has been criticized (as in certain regimes it fails to predict correctly the coherence properties of the strongly interacting 1D Bose gases [157]), the corresponding hydrodynamic equations for the density ρ and the phase S arising from this equation are well-documented in the context of the local density approximation [139, 147]. In fact, this equation is expected to be valid as long as the number of atoms exceeds a certain minimum value (typically much larger than 10), for which oscillations in the density profiles become essentially suppressed [151, 154, 158]; in other words, the density variations should occur on a length scale which is larger than the Fermi healing length $\xi_F \equiv 1/(\pi \rho_p)$ (where ρ_p is the peak density of the trapped gas).

The quintic NLS model has been used in various studies [151, 159–161], basically connected to the dynamics of dark solitons in the Tonks–Girardeau gas, and in the aforementioned crossover regime of $\gamma \sim \mathcal{O}(1)$ [150]. In this connection, it is relevant to note that in the above works it was found that, towards the strongly interacting regime, the dark soliton oscillation frequency is up-shifted, which may be used as a possible diagnostic tool of the system being in a particular interaction regime.

3.6. Reduced mean-field models for BECs in optical lattices

Useful reduced mean-field models can also be derived in the case where the BECs are confined in periodic (optical lattice) potentials. Here, we discuss both continuous and discrete variants of such models, focusing—as in the previous subsections—on the 1D case (generalizations to higher-dimensional settings are also discussed). We start our exposition upon considering that the external potential in equation (22) is of the form $V(z) = V_0 \sin^2(kz)$, i.e. an optical lattice of periodicity $L = \pi/k$. Then, measuring length, energy and time in units of $a_L = L/\pi$, $E_L = 2E_{\text{rec}} = \hbar^2/ma_L^2$ (where the recoil energy E_{rec} is the kinetic energy gained by an atom when it absorbs a photon from the optical lattice), and $\omega_L^{-1} = \hbar/E_L$, respectively, we express equation (22) in the dimensionless form of equation (23) with $V(z) = \sin^2(z)$.

Generally, the stationary states of equation (23) can be found upon employing the usual ansatz, $\psi(z, t) = F(z) \exp(-i\mu t)$, where μ is the dimensionless chemical potential. In the limiting case $g \rightarrow 0$ (i.e. for a non-interacting condensate) where the Bloch–Floquet theory is relevant, the function $F(x)$ can be expressed as [162] $F(z) = u_{k,\alpha}(z) \exp(ikz)$, where the functions $u_{k,\alpha}(z)$ share the periodicity of the optical lattice, i.e. $u_{k,\alpha}(z) = u_{k,\alpha}(z + nL)$ where n is an integer. If the Floquet exponent (also called ‘quasimomentum’ in the physics context) k is real, the wavefunction ψ has the form of an infinitely extended wave, known as a *Bloch wave*. Such waves exist in *bands* (which are labelled by the index α introduced above), while they do not exist in *gaps*, which are spectral regions characterized by $\text{Im}(k) \neq 0$.

The concept of Bloch waves can also be extended in the nonlinear case ($g \neq 0$) [163–170]. In particular, when the nonlinear coefficient is small, the nonlinear band-gap spectrum and the nonlinear Bloch waves are similar to the ones in the linear case [166]. However, when the nonlinear coefficient is increased (or, physically speaking, the local BEC density grows), the chemical potential of the nonlinear Bloch wave is increased (decreased) for $g > 0$ ($g < 0$) and, thus, the nonlinearity effectively ‘shifts’ the edges of the linear band. In this respect, it is relevant to note that for a sufficiently strong nonlinearity, ‘swallowtails’ (or loops) appear in the band-gap structure, both at the boundary of the Brillouin zone and at the zone centre. This was effectively explained in [170], where an adiabatic tuning of a second lattice with half period was considered. Swallowtails in the spectrum are related to several interesting effects, such as a non-zero Landau–Zener tunnelling probability [163], the existence of two nonlinear complex Bloch waves (which are complex conjugates of each other) at the edge of the Brillouin zone [165, 166], as well as the existence of period-doubled states (in the case of sufficiently strong optical lattices—see section 3.6.2), also related to periodic trains of solitons [169] in this setting. We finally note that experimentally it is possible to load a BEC into the ground or excited Bloch state with unprecedented control over both the lattice and the atoms [103].

3.6.1. Weak optical lattices. Let us first consider the case of weak optical lattices, with $V_0 \ll \mu$. In this case, and in connection to the above discussion, a quite relevant issue is the possibility of nonlinear localization of matter-waves in the gaps of the linear spectrum, i.e. the formation of fundamental nonlinear structures in the form of *gap solitons*, as observed in the experiment [44]. The underlying mechanism can effectively be described by means of the so-called Bloch-wave envelope approximation near the band edge, first formulated in the context of optics [171], and then used in the BEC context as well [106, 172, 173] (see also [174] and the review [175]). In particular, a multiscale asymptotic method was used to show that the BEC wave function can effectively be described as $\psi(z, t) = U(z, t)u_{k,0}(z) \exp(ikz)$, where $u_{k,0}(z) \exp(ikz)$ represents the Bloch state in the lowest band $\alpha = 0$ (at the corresponding central quasimomentum k), while the envelope function $U(z, t)$ is governed by the following

dimensionless NLS equation:

$$i \frac{\partial U}{\partial t} = -\frac{1}{2m_{\text{eff}}} \frac{\partial^2 U}{\partial z^2} + g'_{\text{1D}} |U|^2 U, \quad (38)$$

where g'_{1D} is a renormalized (due to the presence of the optical lattice) effectively 1D nonlinear coefficient, and m_{eff} is the effective mass. Importantly, the latter is proportional to the inverse effective diffraction coefficient $\partial^2 \mu / \partial k^2$ whose sign may change, as it is actually determined by the curvature of the band structure of the linear Bloch waves. Obviously, the NLS equation (38) directly highlights the abovementioned nonlinear localization and soliton formation, which occurs for $m_{\text{eff}} g'_{\text{1D}} < 0$. Note that the above envelope can be extended in higher-dimensional (2D and 3D) settings [176], in which the effective mass becomes a tensor. In such a case, and for repulsive BECs ($g < 0$), all components of the tensor have to be negative for the formation of multidimensional gap solitons [177, 178].

Coupled-mode theory originally used in the optics context [171, 179], has also been used to describe BECs in optical lattices [180–184]. According to this approach, and in the same case of weak optical lattice strengths, the wavefunction is decomposed into forward and backward propagating waves, $A(z, t)$ and $B(z, t)$, with momenta $k = +1$ and $k = -1$, respectively, namely,

$$\psi(z, t) = [A(z, t) \exp(ix) + B(z, t) \exp(-ix)] \exp(-i\mu t).$$

This way, equation (23) can be reduced to the following system of coupled-mode equations (see also the recent work [185] for a rigorous derivation):

$$i \left(\frac{\partial A}{\partial t} + 2 \frac{\partial A}{\partial x} \right) = V_0 B + g(|A|^2 + 2|B|^2) A, \quad (39)$$

$$i \left(\frac{\partial B}{\partial t} - 2 \frac{\partial B}{\partial x} \right) = V_0 A + g(2|A|^2 + |B|^2) B. \quad (40)$$

Note that equations (39) and (40) are valid at the edge of the first Brillouin zone, i.e. in the first spectral gap of the underlying linear problem (with $g = 0$). There, the assumption of weak localization of the wave function (which is written as a superposition of just two momentum components) is quite relevant: for example, a gap soliton near the edge of a gap can indeed be approximated by a modulated Bloch wave, which itself is a superposition of forward and backward propagating waves [171]. Thus, coupled-mode theory was successfully used to describe matter-wave gap solitons in [180–184]. Note that the coupled-mode equations (39) and (40) can be directly connected by a NLS equation of the form (38) by means of a formal asymptotic method [183] that uses the distance from the band edges as a small parameter. We finally mention that the coupled-mode equations can formally be extended in higher dimensions [185].

3.6.2. Strong optical lattices and the discrete nonlinear Schrödinger equation. Another useful reduction, which is relevant to deep optical lattice potentials with $V_0 \gg \mu$, is the one of the GP equation to a genuinely discrete model, the so-called *discrete NLS* (DNLS) equation [186]. Such a reduction has been introduced in the context of arrays of BEC droplets confined in the wells of an optical lattice in [187, 188] and further elaborated in [189]; we follow the latter below.

When the optical lattice is very deep, the strongly spatially localized wave functions at the wells of the optical lattice can be approximated by Wannier functions, i.e. the Fourier transform of the Bloch functions. Due to the completeness of the Wannier basis, any solution of equation (23) can be expressed as $\psi(z, t) = \sum_{n,\alpha} c_{n,\alpha}(t) w_{n,\alpha}(z)$, where n and α label wells

and bands, respectively. Substituting the above expression into equation (23), and using the orthonormality of the Wannier basis, we obtain a set of differential equations for the coefficients. Upon suitable decay of the Fourier coefficients and the Wannier functions' prefactors (which can be systematically checked for given potential parameters), the model can be reduced to

$$i \frac{dc_{n,\alpha}}{dt} = \hat{\omega}_{0,\alpha} c_{n,\alpha} + \hat{\omega}_{1,\alpha} (c_{n-1,\alpha} + c_{n+1,\alpha}) + g \sum_{\alpha_1, \alpha_2, \alpha_3} W_{\alpha\alpha_1\alpha_2\alpha_3}^{nnnn} c_{n,\alpha_1}^* c_{n,\alpha_2} c_{n,\alpha_3}, \quad (41)$$

where $W_{\alpha\alpha_1\alpha_2\alpha_3}^{nn_1n_2n_3} = \int_{-\infty}^{\infty} w_{n,\alpha} w_{n_1,\alpha_1} w_{n_2,\alpha_2} w_{n_3,\alpha_3} dx$. The latter equation degenerates into the so-called tight-binding model [187, 188],

$$i \frac{dc_{n,\alpha}}{dt} = \hat{\omega}_{0,\alpha} c_{n,\alpha} + \hat{\omega}_{1,\alpha} (c_{n-1,\alpha} + c_{n+1,\alpha}) + g W_{1111}^{nnnn} |c_{n,\alpha}|^2 c_{n,\alpha}, \quad (42)$$

if one restricts consideration only to the first band. Equation (42) is precisely the reduction of the GP equation to its discrete counterpart, namely, the DNLS equation. Higher-dimensional versions of the latter are of course physically relevant models and have, therefore, been used in various studies concerning quasi-2D and 3D BECs confined in strong optical lattices (see subsequent sections).

4. Some mathematical tools for the analysis of BECs

Our aim in this section is to present an overview of the wide array of mathematical techniques that have emerged in the study of BECs. Rather naturally, one can envision multiple possible partitions of the relevant methods, e.g. based on the type of nonlinearity (repulsive or attractive, depending on the sign of the scattering length) or based on the type of external potential (periodic, decaying or confining) involved in the problem. However, in this review, we will classify the mathematical methods based on the mathematical nature of the underlying considerations. We focus, in particular, on four categories of methods. The first one concerns 'direct' methods which analyse the mean-field model directly, without initiating the analysis at some appropriate, mathematically tractable limit. Such approaches include, e.g., the method of moments, self-similarity and rescaling methods or the variational techniques among others. The second one concerns methods that make detailed use of the understanding of the linear limit of the problem (in a parabolic or a periodic potential or in combinations thereof including, e.g. a double-well potential). The third entails perturbations from the nonlinear limit of the system (such as, e.g., the integrable NLS equation), while the fourth one concerns discrete systems where perturbation methods from the so-called anti-continuum limit of uncoupled sites are extremely helpful.

4.1. Direct methods

Perhaps one of the most commonly used direct methods in BEC is the so-called variational approximation (see [190] for a detailed review). It consists of using an appropriate ansatz, often a solitonic one or a Gaussian one (for reasons of tractability of the ensuing integrations) in the Lagrangian or the Hamiltonian of the model at hand, with some temporally dependent variational parameters. Often these parameters are the amplitude and/or the width of the BEC wavefunction. Then, subsequent derivation of the Euler–Lagrange equations leads to ordinary differential equations (ODEs) for such variational parameters which can be studied either analytically or numerically shedding light on the detailed dynamics of the BEC system. Such methods have been extensively used in examining very diverse features of BECs: these include collective excitations [191], BEC dynamics in 1D optical lattices [187], collapse or absence

thereof in higher-dimensional settings (see, e.g., [192] and references therein), BEC dynamics in settings with space- or time-dependent nonlinearity settings (see, e.g., [193]) and so on. However, both due to the very widespread use of the method and due to the fact that detailed reviews of it already exist [190, 194], we will not focus on reviewing it here. Instead, we direct the interested reader to the above works and references therein. We also note in passing one of the concerns about the validity of the variational method, which consists of its strong restriction of the infinite-dimensional GP dynamics to a small finite-dimensional subspace (freezing the remaining directions by virtue of the selected ansatz). This restriction is well known to potentially lead to invalid results [195]; it is worth noting, however, that there are efforts underway to systematically compute corrections to the variational approximation [196], thereby increasing the accuracy of the method.

Another very useful tool for analysing BEC dynamics is the so-called moment method [197], whereby appropriate moments of the wavefunction $\psi = \sqrt{\rho} \exp(i\phi)$ (where $\rho = |\psi|^2$ and ϕ are the BEC density and phase, respectively) are defined such as $N = \int \rho \, d\mathbf{r}$ (the number of atoms), $X_i = \int x_i \rho \, d\mathbf{r}$ (the centre of mass location), $\tilde{V}_i = \int \rho \partial\phi / \partial x_i \, d\mathbf{r}$ (the centre speed), $W_i = \int x_i^2 \rho \, d\mathbf{r}$ (the width of the wavefunction), $B_i = 2 \int x_i \rho \partial\phi / \partial x_i \, d\mathbf{r}$ (the growth speed), $K_i = -(1/2) \int \psi^* \partial^2 \phi / \partial x_i^2 \, d\mathbf{r}$ (the kinetic energy) and $J = \int G(\rho) \, d\mathbf{r}$ (the interaction energy, see below). Note that in the above expressions the subscript i denotes the i th direction. Then for the rather general GP-type mean-field model of the form:

$$i \frac{\partial \psi}{\partial t} = -\frac{1}{2} \Delta \psi + V(\mathbf{r})\psi + g(|\psi|^2, t)\psi - i\sigma(|\psi|^2, t)\psi, \quad (43)$$

with a generalized nonlinearity $g(\rho) = \partial G / \partial \rho$, the generalized dissipation σ and, say, the typical parabolic potential of the form $V(\mathbf{r}) = \sum_k (1/2) \omega_k^2 x_k^2$, the moment equations read [197]:

$$\frac{dN}{dt} = -2 \int \sigma \rho \, d\mathbf{r}, \quad (44)$$

$$\frac{dX_i}{dt} = \tilde{V}_i - 2 \int \sigma x_i \rho \, d\mathbf{r}, \quad (45)$$

$$\frac{d\tilde{V}_i}{dt} = -\omega_i X_i - 2 \int \sigma \frac{\partial \phi}{\partial x_i} \rho \, d\mathbf{r}, \quad (46)$$

$$\frac{dW_i}{dt} = B_i - 2 \int \sigma x_i^2 \rho \, d\mathbf{r}, \quad (47)$$

$$\frac{dB_i}{dt} = 4K_i - 2\omega_i^2 W_i - 2 \int \delta G \, d\mathbf{r} - 4 \int \sigma \rho \partial\phi / \partial x_i \, d\mathbf{r}, \quad (48)$$

$$\frac{dK_i}{dt} = -\frac{1}{2} \omega_i^2 B_i - \int \delta G \frac{\partial^2 \phi}{\partial x_i^2} \, d\mathbf{r} + \int \sigma \left[\sqrt{\rho} \frac{\partial^2 \sqrt{\rho}}{\partial x_i^2} - \rho \left(\frac{\partial \phi}{\partial x_i} \right)^2 \right] \, d\mathbf{r}, \quad (49)$$

$$\frac{dJ}{dt} = \sum_i \int \delta G \frac{\partial^2 \phi}{\partial x_i^2} \, d\mathbf{r} - 2 \int g \sigma \rho \, d\mathbf{r} + \int \frac{\partial G}{\partial t} \, d\mathbf{r}, \quad (50)$$

where $\delta G \equiv G(\rho) - \rho g(\rho)$. One can then extract, for parabolic potentials, a closed-form exact ODE describing the motion of the centre of mass (assuming that the dissipation does not depend on ρ) of the form

$$\frac{d^2 X_i}{dt^2} = -\omega^2(t) X_i - 2\sigma(t) \frac{dX_i}{dt} - 2\sigma(t) X_i. \quad (51)$$

In the absence of dissipation (and for constant in time magnetic trap frequencies), this yields a simple harmonic oscillator for the centre of mass of the condensate. This is the so-called Kohn mode [198], which has been observed experimentally (see, e.g., [52, 53]). In fact, more generally, for conservative potentials one obtains a general Newtonian equation of the form [199]

$$\frac{d^2 X_i}{dt^2} = - \int \frac{\partial V}{\partial x_i} \rho \, d\mathbf{r}, \quad (52)$$

which is the analogue of the linear quantum-mechanical Ehrenfest theorem.

There are some simple dissipationless (i.e. with $\sigma = 0$) cases for which the equations (44)–(50) close. For example, if the potential is spherically symmetric ($\omega_i(t) = \omega(t)$), one can close the equations for $R = \sqrt{W}$, together with the equation for K into the so-called Ermakov–Pinney (EP) equation [200] of the form

$$\frac{d^2 R}{dt^2} = -\omega(t)R + \frac{M}{R^3}, \quad (53)$$

where M is a constant depending only on the initial data and the interaction strength U (the equations close only for the two-dimensional case and for $G = U\rho^2$). One of the remarkable features of such EP equations [200] is that they can be solved analytically provided that the underlying linear Schrödinger problem $d^2 R/dt^2 = -\omega(t)R$ is explicitly solvable with linearly independent solutions $R_1(t)$ and $R_2(t)$. In that case, the EP equation has a general solution of the form $(AR_1^2 + BR_2^2 + 2CR_1R_2)^{1/2}$, where the constants satisfy $AB - C^2 = M/w^2$ and w is the Wronskian of the solutions R_1 and R_2 . Such EP equations have also been used to examine the presence of parametric resonances for time-dependent frequencies (such that the linear Schrödinger problem has parametric resonances) in [201, 202]. Another place where such EP approach has been quite relevant is in the examination of BECs with temporal variation of the scattering length; the role of the latter in preventing collapse has been studied in the EP framework in [203]. It has also been studied in the context of producing exact solutions of the second moment of the wavefunction, which is associated with the width of the BEC, which are either oscillatory (breathing condensates) or decreasing in time (collapsing condensates) or increasing in time (dispersing BECs) in [204]. It should be mentioned that when the scattering length is time dependent the EP equation (53) is no longer exact, but rather an approximate equation, relying on the assumption of a quadratic spatial dependence of the condensate phase. Another case where exact results can be obtained for the moment equations is when the nonlinearity g is time-independent and the phase satisfies Laplace's equation $\Delta\phi = 0$, in which case vortex-line solutions can be found for the wavefunction ψ [197].

It should also be mentioned in passing that such moment methods are also used in deriving rigorous conditions for avoiding collapse in NLS equations more generally, where this class of methods is known under the general frame of variance identities (see, e.g., the detailed discussion of section 5.1 in [12]).

Another comment regarding the above discussion is that Newtonian dynamical equations of the form of equation (52) are more generally desirable in describing the dynamics not only of the full wavefunction but also of localized modes (nonlinear waves), such as bright solitons. This approach can be rigorously developed for small potentials $V(x) = \epsilon W(x)$ or wide potentials $V(x) = W(\epsilon x)$ in comparison with the length scale of the soliton. In such settings, it can be proved [205] that the motion of the soliton is governed by an equation of the form

$$m_{\text{eff}} \frac{d^2 s}{dt^2} = -\nabla U(s), \quad (54)$$

where m_{eff} is an effective mass (found to be $1/2$ independently of dimension in [205]) and the effective potential is given by

$$U(s) = \frac{\int V(\mathbf{r})\psi_0^2(\mathbf{r}-s) d\mathbf{r}}{\int \psi_0^2(\mathbf{r}) d\mathbf{r}}. \quad (55)$$

In 1D, equation (55) can be used to characterize not only the dynamics of the solitary wave but also its stability around stationary points such that $U'(s_0) = 0$. It is natural to expect that its motion will comprise stable oscillations if $U''(s_0) > 0$, while it will be unstable for $U''(s_0) < 0$. In the case of multiple such fixed points, the equation provides global information on the stability of each equilibrium configuration and local dynamics in the neighbourhood of all equilibria. In higher dimensions, an approach such as the one yielding equation (54) is not applicable due to the instability of the corresponding multidimensional (bright) solitary waves to collapse [12]. This type of dynamical equation was originally developed formally using asymptotic multiscale expansions as, e.g., in [206, 207]. We return to a more detailed discussion of such techniques characterizing the dynamics of the nonlinear wave in sections 4.3.2 and 4.3.3.

Another class of methods that can be used to obtain reduced ODE information from the original GP partial differential equation (PDE) concerns scaling transformations, such as the so-called lens transformation [12]. An example of this sort with

$$\psi(x, t) = \frac{1}{l(t)} \exp(i f(t) r^2) u\left(\frac{x}{L(t)}, \tau(t)\right), \quad (56)$$

has been used in [208] to convert the more general (with time-dependent coefficients) form of the d -dimensional GP equation

$$i \frac{\partial \psi}{\partial t} = -\frac{\alpha(t)}{2} \Delta \psi + \frac{1}{2} \Omega(t) r^2 \psi + g(t) \psi - i\sigma(t) \psi, \quad (57)$$

into the simpler form with time *independent* coefficients:

$$i \frac{\partial u}{\partial \tau} = -\frac{1}{2} \Delta_\eta u + s|u|^2 u, \quad (58)$$

where $\eta = x/L(t)$ and $s = \pm 1$. This happens if the temporally dependent functions $l(t)$, $f(t)$, $L(t)$ and $\tau(t)$ satisfy the similarity conditions:

$$\frac{dl}{dt} = \alpha(t)l + \sigma(t), \quad (59)$$

$$\frac{df}{dt} = -2\alpha(t)f^2 - \frac{1}{2}\Omega(t), \quad (60)$$

$$\frac{dL}{dt} = 2\alpha(t)fL, \quad (61)$$

$$\frac{d\tau}{dt} = \frac{\alpha(t)}{L^2}, \quad (62)$$

$$\frac{\alpha(t)}{L^2} = \sigma \frac{g(t)}{l^2}. \quad (63)$$

Some of these ODEs can be immediately solved, e.g.

$$L(t) = \exp\left(2 \int_0^t \alpha(t') f(t') dt'\right), \quad (64)$$

$$l(t) = \Gamma(t) \exp\left(d \int_0^t \alpha(t') f(t') dt'\right) = \Gamma(t) L(t)^{\frac{d}{2}}, \quad (65)$$

$$g(t) = s\alpha(t)\Gamma(t)L(t)^{d-2}, \quad (66)$$

where $\Gamma(t) = \exp(\int_0^t \sigma(t') dt')$. Note that this indicates that $\alpha(t)$, $g(t)$ and $\sigma(t)$ are interdependent through equation (66). While, unfortunately, equation (60) cannot be solved in general, it can be integrated in special cases, such as, e.g., $\Omega(t) = 0$. Note that in that case, periodic $\alpha(t)$ with zero average, i.e. $\int_0^T \alpha(t') dt' = 0$, implies that $L(t)$, $l(t)$ and $f(t)$ will also be periodic. In other settings the above equations can be used to construct collapsing solutions or to produce pulsating two-dimensional profiles, as is the case, e.g., for $\Omega(t) = m(1 - 2\text{sn}^2(t, m))$ in the form

$$\psi = \frac{1}{\text{dn}(t, m)} U \left(\frac{x}{\text{dn}(t, m), \tau(t)} \right) \exp \left(i\tau(t) - ir^2 \frac{m \text{cn}(t, m) \text{sn}(t, m)}{2 \text{dn}(t, m)} \right), \tag{67}$$

where $U(\eta)$ is the well-known 2D Townes soliton (see also section 5.4.2) profile and $\tau(t) = \int_0^t \text{dn}(t', m)^{-2} dt'$. Similar types of lens transformations were used to study collapse type phenomena [209, 210] and to examine modulational instabilities in the presence of parabolic potentials [87].

In the same way as the above class of transformation methods one can classify also the scaling methods that arise from the consideration of Lie group theory and canonical transformations [211] of nonlinear Schrödinger equations with spatially inhomogeneous nonlinearities of the form (for the stationary problem)

$$-\psi_{xx} + V(x)\psi + g(x)\psi^3 = \mu\psi. \tag{68}$$

Considering the generator of translational invariance motivates the scaling of the form $U(x) = b(x)^{-1/2}\psi$ and $X = \int_0^x [1/b(s)] ds$ with $g(x) = g_0/b(x)^3$. Then, U satisfies the regular 1D NLS equation (whose solutions are known from the inverse scattering method [21]) and b satisfies

$$b'''(x) - 2b(x)V'(x) + 4b'(x)\mu - 4b'(x)V(x) = 0, \tag{69}$$

which can remarkably be converted to an EP equation, upon the scaling $\tilde{b}(x) = b^{1/2}(x)$. Then, combining the knowledge of solvable EP cases (as per the discussion above) with that of the spatial profiles of the various (plane wave, solitary wave and elliptic function) solutions of the standard NLS equation for U , we can obtain special cases of $g(x)$ for which explicit analytical solutions are available [211].

4.2. Methods from the linear limit

When considering the GP equation as a perturbation problem, one way to do so is to consider the underlying linear Schrödinger problem, obtain its eigenvalues and eigenfunctions; subsequently one can consider the cubic nonlinear term within the realm of Lyapunov–Schmidt (LS) theory (see chapter 7 in [212]), to identify the nonlinear solutions bifurcating from the linear limit.

We discuss this approach in a general 1D problem, with both a magnetic trap and an optical lattice potential,

$$V(x) = V_{\text{MT}}(x) + V_{\text{OL}}(x) \equiv \frac{1}{2}\Omega^2 x^2 + V_0 \cos(2x), \tag{70}$$

following the approach of [213]. Considering the linear problem of the GP equation, using $\psi(x, t) = \exp(-iEt)u(x)$ (where E is the linear eigenvalue) and rescaling spatial variables by $\Omega^{1/2}$ one obtains

$$\mathcal{L}u = -\frac{1}{2} \frac{d^2 u}{dx^2} + \frac{1}{2} x^2 u + \frac{V_0}{\Omega} \cos \left(2 \frac{x}{\Omega^{1/2}} \right) u = \frac{E}{\Omega} u. \tag{71}$$

If we work in the physically relevant regime of $0 < \Omega \ll 1$ and for $V_0/\Omega = \mathcal{O}(1)$, then one can use $\mu = \Omega^{1/2}$ as a small parameter and develop methods of multiple scales and homogenization

techniques [213] in order to obtain analytical predictions for the linear spectrum. In particular, the one-dimensional eigenvalue problem using as fast variable $X = x/\mu$ and setting $\lambda = E_1/\Omega$ becomes

$$\left[\mu^2 \mathcal{L}_{\text{MT}} - \mu \frac{\partial^2}{\partial x \partial X} + \mathcal{L}_{\text{OL}} \right] u = \mu^2 \lambda u, \quad (72)$$

where

$$\mathcal{L}_{\text{MT}} = -\frac{1}{2} \frac{\partial^2}{\partial x^2} + \frac{1}{2} x^2, \quad (73)$$

$$\mathcal{L}_{\text{OL}} = -\frac{1}{2} \frac{\partial^2}{\partial X^2} + V_0 \cos(2X). \quad (74)$$

One can then use a formal series expansion (in μ) for u and λ

$$u = u_0 + \mu u_1 + \mu^2 u_2 + \dots, \quad (75)$$

$$\lambda = \frac{\lambda_{-2}}{\mu^2} + \frac{\lambda_{-1}}{\mu} + \lambda_0 + \dots \quad (76)$$

Substitution of this expansion in the eigenvalue problem of equation (72), and after tedious but straightforward algebraic manipulations and use of solvability conditions for the first three orders of the expansion ($\mathcal{O}(1)$, $\mathcal{O}(\mu)$ and $\mathcal{O}(\mu^2)$), yields the following result for the eigenvalue and the corresponding eigenfunction of the eigenvalue problem of the original operator. The relevant eigenvalue of the n th mode is approximated by

$$E^{(n)} = -\frac{1}{4} V_0^2 + \left(1 - \frac{1}{4} V_0^2\right) \Omega \left(n + \frac{1}{2}\right), \quad (77)$$

and the corresponding eigenfunction is given by

$$u^{(n)}(x) = c_n H_n \left(\frac{x}{\sqrt{1 - (V_0^2/4)}} \right) e^{-x^2/(2 - (V_0^2/2))} \times \frac{1}{\sqrt{\pi}} \left[1 - \frac{V_0}{2} \cos \left(\frac{2x}{\Omega^{1/2}} \right) \right], \quad (78)$$

where $c_n = (2^n n! \sqrt{\pi})^{-(1/2)}$ is the normalization factor and $H_n(x) = e^{-x^2} (-1)^n (d^n/dx^n) e^{x^2}$ are the Hermite polynomials.

Considering now the nonlinear problem $\mathcal{L}u = -su^3$ through LS theory, we obtain the bifurcation function

$$G(\mu, \Delta E) = -\Delta E \mu + s \langle (u^{(n)})^2, (u^{(n)})^2 \rangle \mu^3, \quad (79)$$

for bifurcating solutions $U_n = \mu u^{(n)}$, which bifurcate from the linear limit of $E = E^{(n)}$, with $\Delta E = E - E^{(n)}$. The notation $\langle f, g \rangle = \int f(x)g(x) dx$ is used to denote the inner product of f and g . This calculation shows that a non-trivial solution exists only if $s\Delta E > 0$ (i.e. the branches bend to the left for attractive nonlinearities with $s = -1$ and to the right for repulsive ones with $s = 1$) and the nonlinear solutions are created via a pitchfork bifurcation (given the symmetry $u \rightarrow -u$) from the linear solution. The bifurcation is subcritical for $s = -1$ and supercritical for $s = 1$. Typical examples of the relevant solutions of the linear problem (from which the nonlinear states bifurcate) are shown in figure 1.

Note that for $V_0 = 0$ the problem becomes the linear quantum harmonic oscillator (parabolic potential) whose eigenvalues and eigenfunctions are known explicitly and are a special case of those of equations (77) and (78) for $V_0 = 0$. This perspective has been used in numerous studies as a starting point for numerical computation, e.g. in 1D [105, 214, 215], as well as in higher dimensions [216].

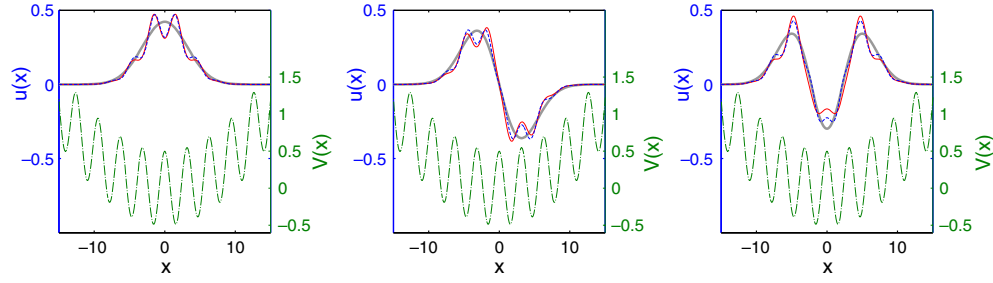


Figure 1. The first three (left to right) eigenfunctions of the linear Schrödinger equation with the potential of equation (70). The thick (grey) solid line corresponds to the eigenfunction for the case of $V_{MT}(x)$, while the thin (red) solid and (blue) dashed lines correspond to the eigenfunction for $V_{MT}(x) + V_{OL}(x)$, as computed numerically and theoretically (see equation (78)), respectively. The full potential $V_{MT}(x) + V_{OL}(x)$ (shifted for visibility, see scale on the right axis) is illustrated by the (green) dashed-dotted line. The parameters used in this example correspond to $V_0 = 0.5$ and $\Omega = 0.1$.

It is natural to subsequently examine the stability of the ensuing nonlinear states, stemming from the linear problem. This can be done through the linearization of the problem around the nonlinear continuation of the solutions $u^{(n)}$, with a perturbation $\tilde{u} = w + iv$. Then, the ensuing linearized equations for the eigenvalue λ and the eigenfunction \tilde{u} can be written in the standard (for NLS equations) L_+ , L_- form

$$L_+ w = \left[\mathcal{L} + 3s (u^{(n)})^2 \right] w = -\lambda v, \quad (80)$$

$$L_- v = \left[\mathcal{L} + s (u^{(n)})^2 \right] v = \lambda u. \quad (81)$$

Then, define $n(L)$ and $z(L)$ as the number of negative and zero eigenvalues, respectively, of operator L , k_r , k_i^- and k_c as the number of eigenvalues with, respectively, real positive, imaginary with positive imaginary part and negative Krein sign (see below) and complex with positive real and imaginary part. The Krein signature of an eigenvalue λ is the sign $(\langle w, L_+ w \rangle)$. One can then use the recently proven theorem for general Hamiltonian systems of the NLS type of [217] based on the earlier work of [218–221] (see also [222]) according to which

$$k_r + 2k_i^- + 2k_c = n(L_+) + n(L_-) - n(D), \quad (82)$$

where $D = dN/dE$ (N is the number of atoms of the state of interest). Then from Sturm–Liouville theory and given that $u^{(n)}$ is the only eigenfunction of L_- with eigenvalue 0 (by construction), we obtain $n(L_-) = j$ and $z(L_-) = 1$ for the eigenstate $U = \mu u^{(j)}$ (since it possesses j nodes). Similarly, using the nature of the bifurcation, one obtains $n(L_+) = j$ and $n(D) = 0$ if $s = 1$, while $n(L_+) = j + 1$ and $n(L_-) = 1$ if $s = -1$. Combining these results one has that $k_r + 2k_i^- + 2k_c = 2j$. More detailed considerations in the vicinity of the linear limit [213] in fact show that the resulting eigenvalues have to be simple and purely imaginary, i.e. $k_r = k_c = 0$, and, hence, each of the waves bifurcating from the linear limit is *spectrally stable* close to that limit. However, the nonlinear wave bifurcating from the j th linear eigenstate has j eigenvalues with negative Krein signature which may result in instability if these collide with other eigenvalues (of opposite sign). That is to say, the state $u^{(j)}$ has j potentially unstable eigendirections.

While the above results give a detailed handle on the stability of the structures near the linear limit, it is important to also quantify the bifurcations that may occur (which may also, in turn, alter the stability of the nonlinear states), as well as to examine the dynamics of the

relevant waves further away from that limit. A reduction approach that may be used to address both of these issues is that of projecting the dynamics to a full basis of eigenmodes of the underlying linear operator. Note that we have seen this method before in the reduction of the GP equation in the presence of a strong OL to the DNLS equation. Considering the problem $i u_t = \mathcal{L}u + s|u|^2 u - \omega u$, we can use the decomposition $u(x) = \sum_{j=0}^M c_j(t) q_j(x)$, where $q_j(x)$ are the orthonormalized eigenstates of the linear operator \mathcal{L} . Setting $a_{klm}^j = \langle q_k q_l q_m, q_j \rangle$ and following [223] straightforwardly yields

$$i \dot{c}_j = (\mu_j - \omega) c_j + s \sum_{k,l,m=0}^M a_{klm}^j c_k c_l c_m^*, \quad (83)$$

where μ_j are the corresponding eigenvalues of the eigenstates $q_j(x)$. It is interesting to note that this system with $M \rightarrow \infty$ is equivalent to the original dynamical system, but is practically considered for finite M , constituting a Galerkin truncation of the original GP PDE. This system preserves both the Hamiltonian structure of the original equation, as well as additional conservation laws such as the L^2 norm $\|u\|_{L^2}^2 = \sum_{j=0}^M |c_j|^2$.

A relevant question is then how many modes one should consider to obtain a useful/interesting/faithful description of the original infinite-dimensional dynamical system. The answer, naturally, depends on the form of the potential. The above reduction has been extremely successful in tackling double-well potentials in BECs [223–225], as well as in optical systems [226]. In this simplest case, a two-mode description is sufficient to extract the prototypical dynamics of the system with $M = 2$. Then the relevant dynamical equations become

$$i \dot{c}_0 = (\mu_0 - \omega) c_0 + s a_{000}^0 |c_0|^2 c_0 + s a_{110}^0 (2|c_1|^2 c_0 + c_1^2 c_0^*), \quad (84)$$

$$i \dot{c}_1 = (\mu_1 - \omega) c_1 + s a_{111}^1 |c_1|^2 c_1 + s a_{110}^0 (2|c_0|^2 c_1 + c_0^2 c_1^*), \quad (85)$$

where we have assumed a symmetric double-well potential so that terms such as a_{000}^1 or a_{111}^0 disappear and $a_{001}^0 = a_{010}^0 = a_{101}^0 = \dots = \int q_0^2 q_1^2 dx$. None of these assumptions is binding and the general cases have in fact been treated in [223, 224]. An angle-action variable decomposition $c_j = \rho_j e^{i\phi_j}$ leads to

$$\dot{\rho}_0 = s a_{110}^0 \rho_1^2 \rho_0 \sin(2\delta\phi), \quad (86)$$

$$\dot{\delta\phi} = -\Delta\mu + s(a_{000}^0 \rho_0^2 - a_{111}^1 \rho_1^2) - s a_{110}^0 (2 + 2 \cos(\delta\phi)) (\rho_0^2 - \rho_1^2), \quad (87)$$

where $\delta\phi$ is the relative phase between the modes. Straightforwardly analysing the ensuing equations (particularly equation (86)), we observe that the nonlinear problem can support states with $\rho_1 = 0$ and $\rho_0 \neq 0$ (symmetric ones, respecting the symmetry of the ground state of the double-well potential). It can also support ones with $\rho_0 = 0$ and $\rho_1 \neq 0$ (antisymmetric ones); these states are not a surprise since they existed even at the linear limit. However, in addition to these two, the nonlinear problem can support states with $\rho_0 \neq 0$ and $\rho_1 \neq 0$, provided that $\sin(2\delta\phi) = 0$. These are *asymmetric* states that have to bifurcate because of the presence of nonlinearity. A more detailed study of the second equation shows that, typically, the bifurcation occurs for $\|u\|_{L^2}^2 > N_c = \Delta\mu / (3a_{110}^0 - a_{000}^0)$ for $s = -1$ (attractive case) and is a bifurcation from the symmetric ground state branch, while it happens for $\|u\|_{L^2}^2 > N_c = \Delta\mu / (3a_{110}^0 - a_{111}^1)$ in the $s = 1$ (repulsive case) and is a bifurcation from the antisymmetric first excited state (see also figure 2 which shows the relevant states and bifurcation diagram). Note that this is a pitchfork bifurcation (since there are two asymmetric states born at the critical point, each having principally support over each of the two wells). It should be mentioned that although this bifurcation is established for the two-mode reduction, it has been systematically

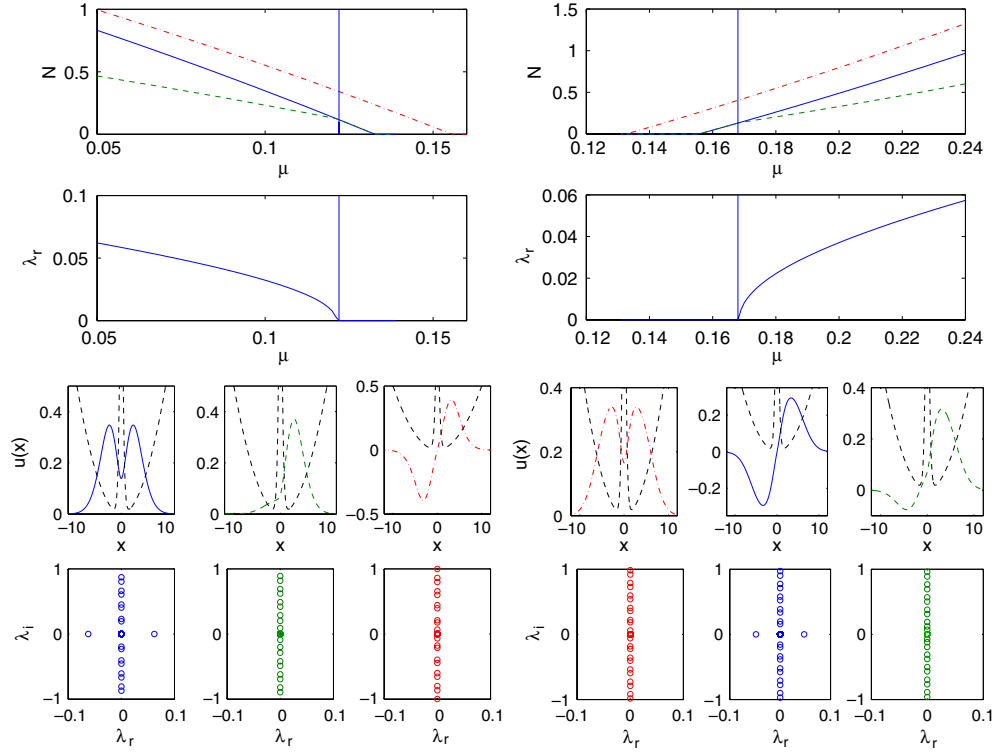


Figure 2. The left panels illustrate a typical double-well problem in the focusing case, while the right ones in the defocusing case. The top row shows the squared L^2 norm of the solutions (N) as a function of the eigenvalue parameter μ (illustrating in each case the bifurcation of a new asymmetric branch). The second row shows the instability of the solid (blue) branch (symmetric on the left and antisymmetric on the right) past the critical point through the appearance of a real eigenvalue. The third row shows a particular example of the profiles for each branch and the fourth row shows the spectral plane of the linearization around them (absence of a real eigenvalue indicates stability).

confirmed by numerical analysis of the GP PDE in [223, 224] for the case of a magnetic trap and an optical lattice or a magnetic trap and a defect, respectively, and it has been rigorously proved for a decaying at infinity double-well potential in [225] (in the latter the corrections to the above mentioned N_c were estimated). Based on the nature of the bifurcation (but this can also be proved within the two-mode reduction and rigorously from the GP equation), we expect the ensuing asymmetric solutions to be stable, destabilizing the branch from which they are stemming, as is confirmed in the numerical linear stability results of figure 2. It is also worthwhile to point out that such predictions (e.g. the stabilization of an asymmetric state beyond a critical power) have been directly confirmed in optical experiments [226] in photorefractive crystals, and also have a direct bearing on relevant BEC experiments analysed in [75]. We note in passing that in the physics literature, the problem is often tackled using wavefunctions that are localized in each of the wells of the double-well potential (as linear combinations of the states q_1 and q_2 used herein) [227–229], especially to study Josephson tunnelling (but also to examine self-trapping) [75]. We refer the interested reader to these publications for more details.

Such a few-mode approximation has also been successfully used in the case of three wells (in connection to applications in experiments in photorefractive crystals) in [230]. Naturally in that case, one uses three modes for the relevant decomposition and the corresponding dynamical equations grow in complexity very rapidly (as numerous additional overlap terms become relevant and the analysis becomes almost intractable). Similarly, such Galerkin approaches can also be used in the case where there is only a magnetic trap, in which case the underlying basis of expansion becomes that of the Hermite–Gauss polynomials [231]. In that case, in addition to the persistence of the linear states and a detailed quantitative analysis of their linearization spectrum that becomes available near the linear limit, one can importantly predict the formation of new types of solutions. An example of this type consists of the space-localized, time-periodic (i.e. breathing) solutions in the neighbourhood of, for example, the first excited state (which has the form of a dark soliton) of the harmonically confined linear problem [231].

Finally, we indicate that such methods from the linear limit can equally straightforwardly be applied to higher-dimensional settings and be used to extract complex nonlinear states. For instance, considering the problem

$$-\frac{\partial^2 u}{\partial r^2} - \frac{1}{r} \frac{\partial u}{\partial r} - \frac{1}{r^2} \frac{\partial^2 u}{\partial \theta^2} + i\Omega \frac{\partial u}{\partial \theta} + r^2 u + s|u|^2 u = \omega u, \quad (88)$$

where also a rotational stirring term (frequently used in condensate experiments [52, 53]) is included, one can use a decomposition into the linear states $q_{m,l}(r) \exp(il\theta)$ [232], where m is the number of nodes of $q_{m,l}$. Then the underlying linear problem has eigenvalues $\lambda_{m,l} = 2(|l| + 1) + 4m + l\Omega$ and, for example, for solutions bifurcating from $\lambda = 6$, one can write

$$u = (x_1 q_{1,0}(r) + y_1 q_{0,l'} \cos(l'\theta) + iy_2 q_{0,l'} \sin(l'\theta)) \epsilon^{1/2}, \quad (89)$$

together with $\omega = 6 + \epsilon\delta\omega$, and derive algebraic equations for x_1 , y_1 and y_2 :

$$0 = x_1 [\mu + 2x_1^2 + g_1(2|y_1|^2 + y_1^2 + y_2^2)], \quad (90)$$

$$0 = c_g \mu y_1 + g_2 x_1^2 (2y_1 + y_1^*) + \frac{3}{4} |y_1|^2 y_1 + \frac{1}{4} y_2^2 (2y_1 - y_1^*), \quad (91)$$

$$0 = y_2 [c_g \mu + g_2 x_1^2 + \frac{1}{4} (2|y_1|^2 - y_1^2) + \frac{3}{4} y_2^2], \quad (92)$$

where $\mu = -s\delta\omega/(g_0\pi)$, $g_1 = g_{0,l'}/g_0$, $g_2 = g_{0,l'}/g_{l'}$ and $c_g = g_2/g_1$ and $g_1 = \int r q_{1,0}^4 dr$, $g_{l'} = \int r q_{0,l'}^4 dr$, $g_{0,l'} = \int r q_{1,0}^2 q_{0,l'}^2 dr$. From these equations one can find real solutions containing only x_1 (ring solutions), only y_1 (multipole solutions), both x_1 and y_1 (soliton necklaces), as well as complex solutions also involving $y_2 \neq 0$ such as vortices and vortex necklaces. A sampler of these solutions is illustrated in figure 3; more details can be found in [232], where the stability of such states is also analysed, leading to the conclusion that the most robust among them are the (soliton and vortex) necklace and the vortex states.

4.3. Methods from the nonlinear limit

We partition our consideration of such methods into ones that tackle the stationary problem (in connection to the existence and the stability of the solutions) and ones that address the dynamics of the perturbed solitary waves.

4.3.1. Existence and stability methods. Consider a general Hamiltonian system of the form

$$\frac{dv}{dt} = JE'(v), \quad (93)$$

where the J matrix has the standard symplectic structure ($J^2 = -I$) and $E = \int (1/2)[|v_x|^2 + s|v|^4] dx$ for the case of the GP equation without external potential (although the formalism

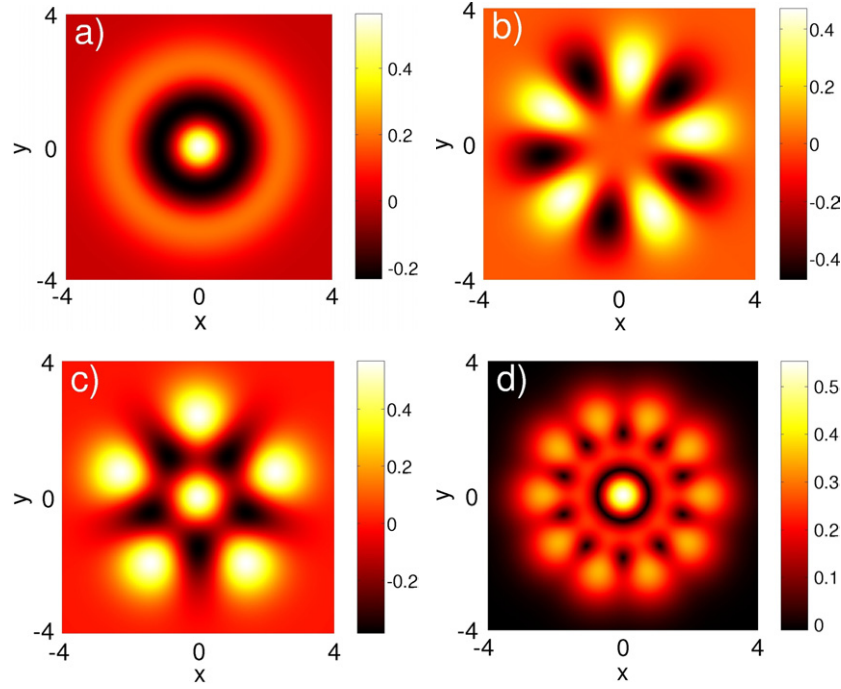


Figure 3. A typical ring solution (top left), multipole solution (top right), soliton necklace (bottom left) and vortex necklace (bottom right) that can be obtained from the near-linear analysis of the 2D problem through equations (90)–(92). Reprinted from [232], Copyright (2007), with permission from Elsevier.

presented below is very general [217, 233, 234]). Given that the above model in the case of the GP equation has certain invariances (e.g. with respect to translation and phase shift), one can use the generator T_ω of the corresponding semigroup $T(\exp(\omega t))$ of the relevant symmetry to make a change of variables $v(t) = T(\exp(\omega t))u(t)$, which in turn leads to $du/dt = JE'_0(u; \omega)$, where $E'_0(u; \omega) = E'(u) - J^{-1}T_\omega u$. Defining then the appropriate conserved functional $Q_\omega = (1/2)\langle J^{-1}T_\omega u, u \rangle$, we note that relative equilibria satisfying $E'_0(u; \omega) = 0$ will be critical points of $E_0(u; \omega) = E(u) - Q_\omega(u)$. Then the linearization problem around such a stationary wave u_0 reads

$$JE''_0(u_0; \omega)w = \lambda w. \tag{94}$$

Given the symmetries of the problem, this linearization operator has a non-vanishing kernel since

$$JE''_0(u_0; \omega)T_{\omega_i}u_0 = 0, \tag{95}$$

$$JE''_0(u_0; \omega)\partial_{\omega_i}u_0 = T_{\omega_i}u_0, \tag{96}$$

where each i corresponds to one of the relevant symmetries and the latter equation provides the generalized eigenvectors of the operator.

The consideration of the perturbed Hamiltonian problem with a Hamiltonian perturbation such that the perturbed energy is $E_0(u) + \epsilon E_1(u)$ was considered in [217, 222, 233, 234] and a number of conclusions were reached regarding the existence and stability of the ensuing solitary waves. Firstly, a necessary condition for the persistence of the wave is

$$\langle E'_1(u_0; \omega), T_{\omega_i}u_0 \rangle = 0, \tag{97}$$

for all i pertaining to the original symmetries. This is a rather natural condition intuitively since it implies that the perturbed wave is a stationary solution if it is a critical point of the perturbation energy functional. The condition is also sufficient if the number of zero eigenvalues $z(M)$ of the matrix $M_{ij} = \langle T_{\omega_i} u_0, E_1''(u_0; \omega) T_{\omega_j} u_0 \rangle$ is given by $n - k_s$, where n is the multiplicity of the original symmetries and k_s the number of symmetries broken by the perturbation.

As a result of the perturbation, $2k_s$ eigenvalues (corresponding to the k_s broken symmetries) will leave the origin, and can be tracked by the following result proved by means of LS reductions in [217]. The eigenvalues are $\lambda = \sqrt{\epsilon} \lambda_1 + \mathcal{O}(\epsilon)$, where the correction λ_1 is given by the generalized eigenvalue problem:

$$(D_0 \lambda_1^2 + M_1) v = 0, \quad (98)$$

where the matrix of symmetries $(D_0)_{ij} = \langle \partial_{\omega_i} u_0, E_0''(u_0; \omega) \partial_{\omega_j} u_0 \rangle$.

In addition to this perturbative result on the eigenvalues, one can obtain a general count on the number of unstable eigendirections of a Hamiltonian system [217], using the functional analytic framework of [218–220, 221] (see also [222] for a different approach). In particular, for a linearization operator $\mathcal{L}_\omega = E''(u) - J^{-1} T_\omega$ and a symmetry matrix $D_{ij} = \langle \partial_{\omega_i} u, \mathcal{L}_\omega \partial_{\omega_j} u \rangle$,

$$k_r + 2k_i^- + 2k_c = n(\mathcal{L}_\omega) - n(D) - z(D), \quad (99)$$

where the relevant symbolism has been introduced in section 4.2. In fact, the latter subsection constitutes a special case example of this formula, in the case of the form of

$$\mathcal{L}_\omega = \begin{pmatrix} L_+ & 0 \\ 0 & L_- \end{pmatrix}. \quad (100)$$

We now give a special case example of the application of the theory in the presence of a linear and a nonlinear lattice potential of the form [235]

$$iu_t = -\frac{1}{2}u_{xx} - (1 + \epsilon n_1(x)) |u|^2 u + \epsilon n_2(x) u. \quad (101)$$

Then the problem can be rephrased in the above formalism with

$$E_1(u) = \int_{-\infty}^{+\infty} (n_2(x) |u|^2 - \frac{1}{2} n_1(x) |u|^4) dx. \quad (102)$$

Therefore, as indicated above, the persistence of the stationary bright solitary wave of the form $u_0 = \sqrt{\mu} \operatorname{sech}[\sqrt{\mu}(x - \xi)] e^{i\delta}$ (with $\delta = \mu/2$) is tantamount to $\nabla_\xi E_1(u) = 0$. This implies that the wave is going to persist only if centred at the parameter-selected extrema of the energy (which are now going to form, at best, a countably infinite set of solutions, as opposed to the one-parameter infinity of solutions previously allowed by the translational invariance).

Furthermore, the stability of the perturbed wave is determined by the location of the eigenvalues associated with the translational invariance; previously, the relevant eigenvalue pair was located at the origin $\lambda = 0$ of the spectral plane of eigenvalues $\lambda = \lambda_r + i\lambda_i$. On the other hand, we expect the eigenvalues associated with the U(1) invariance (i.e. the phase invariance associated with the L^2 conservation) to remain at the origin, given the preservation of the latter symmetry under the perturbations considered herein. Adapting the framework of [217], we have that the matrices that arise in equation (98) are given by

$$D_0 = \begin{pmatrix} (\partial_x u_0, -x u_0) & 0 \\ 0 & 2(u_0, \partial_\mu u_0) \end{pmatrix} = \begin{pmatrix} \mu^{1/2} & 0 \\ 0 & -\mu^{-1/2} \end{pmatrix} \quad (103)$$

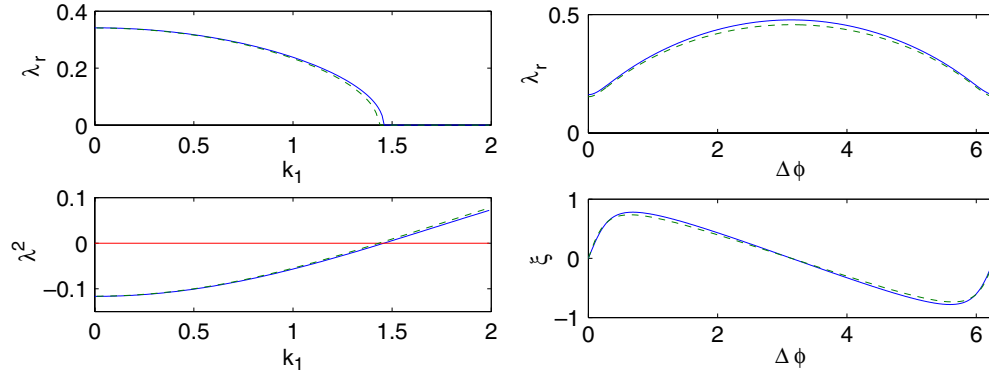


Figure 4. Typical examples of the translational eigenvalue as obtained numerically (solid/blue line) versus the analytical prediction (dashed/green line). The linear and nonlinear potentials are $n_1(x) = A \cos(k_1 x)$ and $n_2(x) = B \cos(k_2 x + \Delta\phi)$. In the left panels we assume that $A = B = 1$, and fix $k_2 = 2\pi/5$ and $\Delta\phi = 0$ and examine the relevant translational eigenvalue (its real part and its square) as a function of k_1 . Note that there is a transition from instability to stability as k_1 is increased. In the right panels we select $A = B = 1$ and $k_1 = k_2 = 2\pi/5$ and vary $\Delta\phi \in [0, 2\pi]$. Note that in the latter case the (critical point associated with the stationary) location of the solitary wave also changes with $\Delta\phi$ and its theoretical and numerical values are also given (again in dashed and solid lines, respectively). Note in all the cases the accuracy of the theoretical prediction. Adapted from [235].

(This figure is in colour only in the electronic version)

and

$$\begin{aligned}
 M_1 &= \begin{pmatrix} \frac{\partial}{\partial \xi} \left(\frac{\partial E_1}{\partial u_0^*}, \partial_\xi u_0 \right) & 0 \\ 0 & 0 \end{pmatrix} \\
 &= \begin{pmatrix} \int \left(\frac{1}{2} \frac{d^2 n_2}{dx^2} (u_0)^2 - \frac{1}{4} \frac{d^2 n_1}{dx^2} (u_0)^4 \right) dx & 0 \\ 0 & 0 \end{pmatrix}. \quad (104)
 \end{aligned}$$

One can then use the above along with equation (98) to obtain the relevant translational eigenvalue as

$$\lambda^2 = -\frac{\epsilon}{\mu^{1/2}} \int \left(\frac{1}{2} \frac{d^2 n_2}{dx^2} (u_0)^2 - \frac{1}{4} \frac{d^2 n_1}{dx^2} (u_0)^4 \right) dx. \quad (105)$$

Based on this expression, the corresponding eigenvalue can be directly evaluated, provided that the extrema of the effective energy landscape E_1 are evaluated first. This effective energy landscape $V_{\text{eff}}(\xi) = \epsilon E_1$ is a function of the solitary wave location ξ . The physical intuition of the above results is that the stability or instability of the configuration is associated with the convexity or concavity, respectively, of this effective energy landscape. Some examples of the accuracy of such a prediction are provided in figure 4, for specific forms of $n_1(x)$ and $n_2(x)$.

This class of techniques has been applied to different problems with spatial variation of the linear [236] or nonlinear [237] potential. They can also be applied to multicomponent problems [233] or to problems with different nonlinearity exponents [238] or higher dimensions [239]. We note in passing that in addition to these methods, for periodic variations of the potential, and for appropriate regimes (for details see [238–240]), one can develop multiple-scale techniques exploiting the disparity in spatial scales between the solution and the potential. We refer the

interested reader to the above references for further technical details. This type of averaging technique is popular not only when the linear or nonlinear potential presents spatial variations of a characteristic scale, but also similarly when these variations are temporal [241–243], especially because it is more straightforward in the averaged equations to extract conclusions about the possible existence or potential collapse or dispersion of the solutions [238, 239, 244].

A similar approach can be used in the case of dark solitons in examining the persistence and stability of the waves in the presence of external potentials; however in the latter case, it is a much harder task to control the linearization spectrum of the problem since it encompasses the origin. This complication has allowed this problem to be tackled only recently at the nonlinear limit [245] and perturbatively away from that limit [246]. The main result of [245] is that by using the limit

$$\lim_{\lambda \rightarrow 0} g(\lambda) = \lim_{\lambda \rightarrow 0} \langle (L - \lambda)^{-1} u', u' \rangle, \quad (106)$$

one can infer the stability of the black soliton, since if this quantity is positive the soliton will have a real eigenvalue and will be unstable, while if non-positive, it will be stable. However, one of the problems with this expression is that even when the soliton is analytically available, it is relatively hard to evaluate (see, e.g., the example of the integrable cubic case worked out in [245]). On the other hand, although there exist results on the orbital stability of dark solitons [247] and of other structures such as bubbles (black solitons with zero phase shift) [248] (see [246] for a more detailed discussion of earlier works), the work of [246] was the first one to establish detailed estimates on the relevant eigenvalues, using once again the technique of Lyapunov–Schmidt reductions in the limit of small potential perturbations. The main results can be summarized as follows. For the equation:

$$i u_t = -\frac{1}{2} u_{xx} + f(|u|^2)u + \epsilon V(x)u. \quad (107)$$

(i) The analogous condition to the persistence condition (97) is now

$$M'(\xi) = \int V'(x)[q_0 - u_0^2(x - \xi)] dx = 0, \quad (108)$$

where the unperturbed solution u_0 asymptotes to $\pm\sqrt{q_0}$ at $\pm\infty$; i.e. the background of the solution is now appropriately incorporated in equation (108) (in comparison with equation (97)).

(ii) The dark soliton will be spectrally unstable in the GP equation with exactly one real eigenvalue (for small ϵ) in the case where

$$M''(\xi) = \int V''(x)[q_0 - u_0^2(x - \xi)] dx < 0, \quad (109)$$

while it will be unstable due to two complex-conjugate eigenvalues with positive real part if $M''(\xi) > 0$. This is the analogous condition to the curvature of the effective potential; however, note the disparity of this condition from what would be expected intuitively based on the notion of convexity/concavity. The latter result is a direct byproduct of the nature of the essential spectrum (encompassing the origin in this defocusing case), which upon bifurcation of the translational eigenvalue along the imaginary axis makes it directly complex (case of $M''(\xi) > 0$). The location of the relevant eigenvalue in the GP case of cubic nonlinearity is given to leading order by

$$\lambda^2 + \frac{\epsilon}{4} M''(\xi) \left(1 - \frac{\lambda}{2}\right) = 0, \quad (110)$$

which is consonant with the above result. A form of this expression for general nonlinearities was also obtained in [246].

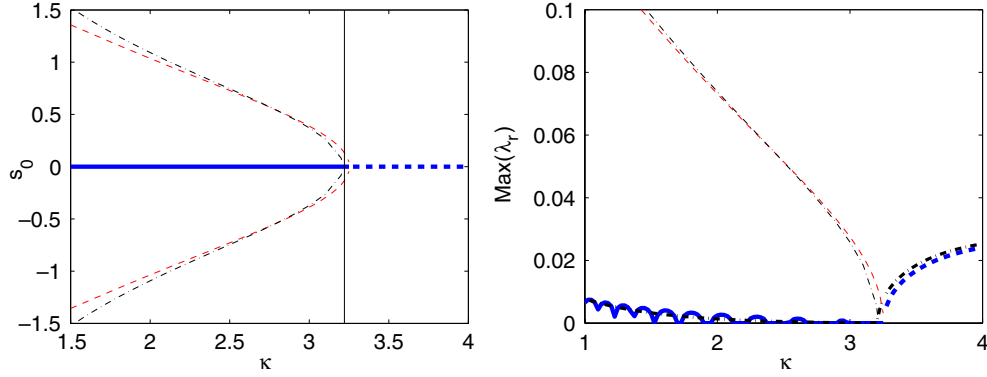


Figure 5. An example of a subcritical pitchfork bifurcation in the parameter κ of the potential $V(x) = x^2 \exp(-\kappa|x|)$ for fixed $\epsilon = 0.2$ in equation (107). The left panel shows the centre of mass $s_0 \equiv \xi$ of the dark soliton kink modes ($s_0 \neq 0$ by dashed line, $s_0 = 0$ by thick solid and dashed lines). The theoretical predictions of s_0 based on equation (108) are shown by dashed–dotted line. The vertical line gives the theoretical prediction for the bifurcation point $\kappa = \kappa_0 = 3.21$. The right panel shows the real part of the unstable eigenvalues for the corresponding solutions, using the same symbolism as the left panel. The theoretical predictions of eigenvalues are shown by thick and thin dashed–dotted lines, respectively, for the branches with $s_0 = 0$ and $s_0 \neq 0$. Note that for the quartet of eigenvalues of the branch centred at the origin, the small jumps are due to the finite size of the computational domain (see [246] for details).

A case example of the possible dark soliton solutions for a potential of the form $V(x) = x^2 \exp(-\kappa|x|)$ is shown in figure 5, illustrating the quantitative accuracy of equations (108)–(110). In this case, the formalism elucidates a subcritical pitchfork bifurcation whereby three dark soliton solutions (one centred at $\xi = 0$ and two symmetrically at $\xi \neq 0$) eventually merge into a single unstable kink centred at $\xi = 0$.

One of the fundamental limitations of this result is its being dependent upon the decaying nature of the potential at $\pm\infty$. The fundamentally different nature of the spectrum in the presence of parabolic or periodic potentials (or both) makes it much harder to provide such considerations in the latter cases. While this can be done in some special limits (such as the Thomas–Fermi, large chemical potential limit of the appendix of [231]), in that setting it is generally easier to use the linear limit approach of section 4.2.

4.3.2. Perturbation theory for solitons. Dynamics of either bright or dark matter-wave solitons can be studied by means of the perturbation theory for solitons [249–252] (see also [253] for a review). Here, we briefly discuss an application of this approach upon considering the example of soliton dynamics in BECs confined in an external potential, say $V(x)$, which is smooth and slowly varying on the soliton scale. This means that in the case, e.g., of the conventional parabolic trap $V(x) = (1/2)\Omega^2 x^2$, the effective trap strength is taken to be $\Omega \sim \epsilon$, where $\epsilon \ll 1$ is a formal small (perturbation) parameter. Taking into regard the above, we consider the following perturbed NLS equation:

$$i \frac{\partial u}{\partial t} + \frac{1}{2} \frac{\partial^2 u}{\partial x^2} - g|u|^2 u = R(u), \quad (111)$$

with the perturbation being the potential term $R(u) \equiv V(x)u$, and $g = \pm 1$ corresponding to repulsive and attractive interactions. Soliton dynamics in the framework of equation (111) can then be treated perturbatively, assuming that a perturbed soliton solution can be expressed as

$$u(x, t) = u_s(x, t) + \epsilon u_d(x, t) + \epsilon u_r(x, t). \quad (112)$$

Here, $u_s(x, t)$ has the same functional form as the soliton solutions (24) for $g = -1$ and (27) for $g = +1$, but with the soliton parameters depending on time. On the other hand, u_d is a function localized near the soliton, describing the deformation of the soliton (i.e. the change in the soliton shape) and u_r is the radiation (in the form of sound waves) emitted by the soliton. In fact, for this class of potentials, the effect described by u_d is not significant, as the small change in the soliton shape does not modify its motion, while the emission of radiation may be neglected for sufficiently weak perturbations. Thus, here we consider solely the first term in equation (112), which corresponds to the so-called *adiabatic approximation* of the perturbation theory for solitons [253].

First we discuss the dynamics of bright solitons in external potentials. Taking into regard that for $g = -1$ and $R(u) = 0$, equation (111) has a bright soliton solution of the form given in equation (24), we assume that in the perturbed case with $R(u) \neq 0$ a soliton solution can be expressed as

$$u(x, t) = \eta \operatorname{sech}[\eta(x - x_0)] \exp[i(kx - \phi(t))], \quad (113)$$

where x_0 is the soliton centre, the parameter $k = dx_0/dt$ defines both the soliton wavenumber and velocity, and $\phi(t) = (1/2)(k^2 - \eta^2)t$ is the soliton phase. In the case under consideration, the soliton parameters η , k and x_0 are considered to be unknown, slowly varying functions of time t . Then, from equation (111), it is found that the number of atoms N and the momentum P (which are integrals of motion of the unperturbed system), evolve, in the presence of the perturbation, according to the following equations:

$$\frac{dN}{dt} = -2 \operatorname{Im} \left[\int_{-\infty}^{+\infty} R(u) u^* dx \right], \quad \frac{dP}{dt} = 2 \operatorname{Re} \left[\int_{-\infty}^{+\infty} R(u) \frac{\partial u^*}{\partial x} dx \right]. \quad (114)$$

We now substitute the ansatz (113) (but with the soliton parameters being functions of time) into equations (114) and obtain the evolution equations for $\eta(t)$ and $k(t)$,

$$\frac{d\eta}{dt} = 0, \quad \frac{dk}{dt} = -\frac{\partial U}{\partial x_0}, \quad (115)$$

where $U(x_0)$ is given by the expression of equation (55). In the case, however, of slow variation of the potential on the scale of the solitary wave (the case of interest here), a simple Taylor expansion yields the same equation but with $U \equiv V$, i.e. the trapping potential.

Now, recalling that $dx_0/dt = k$, we may combine the above equations (115) to derive the following equation of motion for the soliton centre:

$$\frac{d^2 x_0}{dt^2} = -\frac{\partial V}{\partial x_0}, \quad (116)$$

which shows that the bright matter-wave soliton behaves effectively like a Newtonian particle. Note that in the case of a parabolic trapping potential, i.e. $V(x) = (1/2)\Omega^2 x^2$, equation (116) implies that the frequency of oscillation is Ω ; this result is consistent with the Ehrenfest theorem of the quantum mechanics or the so-called Kohn theorem [198], implying that the motion of the centre of mass of a cloud of particles trapped in a parabolic potential is decoupled from the internal excitations. Note that the result of equation (116) can be obtained by other methods, such as the WKB approximation [254] or other perturbative techniques [255–257].

We now turn to the dynamics of dark matter-wave solitons in the framework of equation (111) for $g = +1$. First, the background wavefunction is sought in the form $u = \Phi(x) \exp(-i\mu t)$ (μ being the normalized chemical potential), where the unknown function $\Phi(x)$ satisfies the following real equation:

$$\mu \Phi + \frac{1}{2} \frac{d^2 \Phi}{dx^2} - \Phi^3 = V(x) \Phi. \quad (117)$$

Then, following the analysis of [258], we seek for a dark soliton solution of equation (111) on top of the inhomogeneous background satisfying equation (117), namely, $u = \Phi(x) \exp(-i\mu t)v(x, t)$, where the unknown wavefunction $v(x, t)$ represents a dark soliton. This way, employing equation (117), the following evolution equation for the dark soliton wave function is readily obtained:

$$i \frac{\partial v}{\partial t} + \frac{1}{2} \frac{\partial^2 v}{\partial x^2} - \Phi^2(|v|^2 - 1)v = -\frac{d}{dx} \ln(\Phi) \frac{\partial v}{\partial x}. \tag{118}$$

Taking into regard the fact that in the framework of the Thomas–Fermi approximation the profile can be simply approximated by equation (117), equation (118) can be simplified to the following defocusing perturbed NLS equation:

$$i \frac{\partial v}{\partial t} + \frac{1}{2} \frac{\partial^2 v}{\partial x^2} - \mu(|v|^2 - 1)v = Q(v), \tag{119}$$

with the perturbation $Q(v)$ being of the form

$$Q(v) = (1 - |v|^2) vV + \frac{1}{2(\mu - V)} \frac{dV}{dx} \frac{\partial v}{\partial x}. \tag{120}$$

In the absence of the perturbation, equation (119) has the dark soliton solution (for $\mu = 1$) $v(x, t) = \cos \varphi \tanh \zeta + i \sin \varphi$, where $\zeta \equiv \cos \varphi [x - (\sin \varphi)t]$ (recall that $\cos \varphi$ and $\sin \varphi$ are the soliton amplitude and velocity, respectively, and φ is the soliton phase angle). To treat analytically the effect of the perturbation (120) on the dark soliton, we employ the adiabatic perturbation theory devised in [114]. Assuming, as in the case of bright solitons, that the dark soliton parameters become slowly varying unknown functions of t , the soliton phase angle becomes $\varphi \rightarrow \varphi(t)$ and, as a result, the soliton coordinate becomes $\zeta \rightarrow \zeta = \cos \varphi(t)[x - x_0(t)]$, where $x_0(t) = \int_0^t \sin \varphi(t') dt'$ is the soliton centre. Then, the evolution of the parameter φ is governed by [114]

$$\frac{d\varphi}{dt} = \frac{1}{2 \cos^2 \varphi \sin \varphi} \text{Re} \left[\int_{-\infty}^{+\infty} Q(v) \frac{\partial v^*}{\partial t} dx \right], \tag{121}$$

which, in turn, yields for the perturbation in equation (120):

$$\frac{d\phi}{dt} = -\frac{1}{2} \cos \varphi \frac{\partial V}{\partial x_0}. \tag{122}$$

To this end, combining equation (122) with the definition of the dark soliton centre, we obtain the following equation of motion (for nearly stationary dark solitons with $\cos \varphi \approx 1$):

$$\frac{d^2 x_0}{dt^2} = -\frac{1}{2} \frac{\partial V}{\partial x_0}. \tag{123}$$

Equation (123) implies that the dark soliton, similarly to the bright one, behaves like a Newtonian particle. However, in an harmonic potential with strength Ω , the dark soliton oscillates with another frequency, namely $\Omega/\sqrt{2}$, a result that may be considered as the Ehrenfest theorem for dark solitons. The oscillations of dark solitons in trapped BECs has been a subject that has attracted much interest; in fact, many relevant analytical works have been devoted to this subject, in which various different perturbative approaches have been employed [259–263]. It should also be mentioned that a more general Newtonian equation of motion, similar to equation (123) but also valid for a wider class of confining potentials, was recently discussed in [246].

Perturbation theory for dark solitons may also be applied for dark solitons with radial symmetry, i.e. for ring or spherical dark solitons described by a GP equation of the form

$$i \frac{\partial \psi}{\partial t} = -\frac{1}{2} \nabla^2 \psi + |\psi|^2 \psi + V(r)\psi, \tag{124}$$

where $\nabla^2 = \partial_r^2 + (D-1)r^{-1}\partial_r$ is the transverse Laplacian, $V(r) = (1/2)\Omega^2 r^2$ and $D = 2, 3$ correspond to the cylindrical and spherical case, respectively. In this case, equation (124) can be treated as a perturbed 1D defocusing NLS equation provided that the potential term and the term $\sim r^{-1}$ can be considered as small perturbations; this case is physically relevant for weak trapping potentials with $\Omega \ll 1$, and radially symmetric solitons of large radius r_0 . Then, it can be found [264] (see also [262]) that the radius r_0 of the radially symmetric dark solitons is governed by the following Newtonian equation of motion:

$$\frac{d^2 r_0}{dt^2} = -\frac{\partial V_{\text{eff}}}{\partial r_0}, \quad (125)$$

where the effective potential is given by $V_{\text{eff}}(r_0) = (1/4)\Omega^2 r_0^2 - \ln r_0^{(D-1)/3}$ (note that in the 1D limit of $D = 1$, equation (125) is reduced to equation (123)). Clearly, in this higher-dimensional setting the equation of the soliton motion becomes nonlinear, even for nearly black solitons, due to the presence of the repulsive curvature-induced logarithmic potential. We finally note that such radially symmetric solitons are generally found to be unstable, as they either decay to radiation (the small-amplitude ones) or are subject to the snaking instability (the moderate- and large-amplitude ones), giving rise to the formation of vortex necklaces [264].

4.3.3. The reductive perturbation method. Another useful tool in the analysis of the dynamics of matter-wave solitons (and especially the dark ones) is the so-called reductive perturbation method (RPM) [265]. Applying this asymptotic method, one usually introduces proper ‘stretched’ (slow) variables to show that *small-amplitude* nonlinear structures governed by a specific nonlinear evolution equation can effectively be described by another equation. Such a formal connection between soliton equations was demonstrated for integrable systems in [266], and then extended to the reduction of non-integrable models to integrable ones, first in applications in optics (see, e.g., [267–269]) and later in BECs. Here, we briefly describe this method upon considering, as an example, an inhomogeneous generalized NLS equation similar to equation (107), namely,

$$iu_t = -\frac{1}{2}u_{xx} + V(X)u + g(\rho)u, \quad (126)$$

which is characterized by a general nonlinearity $g(\rho)$ (depending on the density $\rho = |u|^2$), and a slowly varying external potential $V(X)$, depending on a slow variable $X \equiv \epsilon^{3/2}x$ (with ϵ being a formal small parameter). Our main purpose is to show that this rather general NLS-type mean-field model can be reduced to the much simpler Korteweg–de Vries (KdV) equation with variable coefficients. The latter has been used in the past to describe shallow water-waves over variable depth or ion-acoustic solitons in inhomogeneous plasmas [270], and, as we discuss below, it provides an effective description of the dark soliton dynamics in BECs.

Following the analysis of [150], we first derive from equation (126) hydrodynamic equations for the density ρ and the phase ϕ , arising from the Madelung transformation $u = \sqrt{\rho} \exp(i\phi)$, and then introduce the following asymptotic expansions:

$$\rho = \rho_0(X) + \epsilon \rho_1(X, T) + \epsilon^2 \rho_2(X, T) + \dots, \quad (127)$$

$$\phi = -\mu_0 t + \epsilon^{1/2} \phi_1(X, T) + \epsilon^{3/2} \phi_2(X, T) + \dots, \quad (128)$$

where $\rho_0(X)$ is the ground state of the system determined by the Thomas–Fermi approximation $g(\rho_0) = \mu_0 - V(X)$ (with μ_0 being the chemical potential), and $T = \epsilon^{1/2}(t - \int_0^x C^{-1}(x') dx')$ is a slow time-variable (where $C = \sqrt{\dot{g}_0 \rho_0}$ is the local speed of sound and $\dot{g}_0 \equiv (dg/d\rho)|_{\rho=\rho_0}$). This way, in the lowest-order approximation in ϵ we obtain an equation for the phase,

$$\phi_1(X, T) = -\dot{g}_0(X) \int_0^T \rho_1(X, T') dT', \quad (129)$$

and derive the following KdV equation for the density ρ_1 :

$$\rho_{1X} - \frac{(3\dot{g}_0 + \rho_0\ddot{g}_0)}{2C^3}\rho_1\rho_{1T} + \frac{1}{8C^5}\rho_{1TTT} = -\frac{d}{dX}[\ln(|C|\dot{g}_0)^{1/2}]\rho_1, \quad (130)$$

where $\ddot{g}_0 \equiv (d^2g/d\rho^2)|_{\rho=\rho_0}$. Importantly, in a homogeneous gas with $\rho_0(X) = \rho_p = \text{const.}$, equation (130) is the completely integrable KdV equation; the soliton solution of the latter, which is $\sim \text{sech}^2(T)$, is in fact a density notch on the background density ρ_p (see equation (127)), with a phase jump across it (see equation (129), which implies that $\phi_1 \sim \tanh(T)$) and, thus, it represents an approximate dark soliton solution of equation (126). On the other hand, the results obtained earlier for the analysis of the KdV equation with variable coefficients [271,272] have been used to analyse shallow soliton dynamics in the BEC context. In particular, the KdV equation (130) was obtained in the framework of the cubic nonlinear version of equation (126) (with $g(\rho) \sim \rho$), and used to study the dynamics and the collisions of shallow dark solitons in BECs [260,273]. Moreover, other versions of equation (130) relevant to the Tonks gas (corresponding to $g(\rho) \sim \rho^2$) [159], as well as the BEC–Tonks crossover regime (corresponding to a generalized nonlinearity) [150] were derived and analysed as well.

Finally, it is relevant to note that there exist studies in higher-dimensional (disc-shaped) BECs, where the RPM was used to predict 2D nonlinear structures, such as ‘lumps’ described by an effective Kadomtsev–Petviashvili equation [274], and ‘dromions’ described by an effective Davey–Stewartson equation [275,276].

4.4. Methods for discrete systems

As our final class of methods, we present a series of results that are relevant to systems with periodic potentials and, in particular, with discrete lattices per the Wannier function reduction of section 3.6.2. Starting with the prototypical discrete model of the 1D DNLS equation (see, e.g., [186] for a review) of the form

$$i\dot{u}_n = -\epsilon(u_{n+1} + u_{n-1}) - |u_n|^2u_n, \quad (131)$$

we look for standing waves of the form $u_n = \exp(i\mu t)v_n$ which satisfy the steady state equation

$$(\mu - |v_n|^2)v_n = \epsilon(v_{n+1} + v_{n-1}). \quad (132)$$

One of the fundamental ideas that we exploit in this setting is the so-called anti-continuum (AC) limit of MacKay and Aubry [277] for $\epsilon = 0$, where equation (132) is completely solvable $v_n = \{0, \pm\sqrt{\mu} \exp(i\theta_n)\}$, where θ_n is a free phase parameter for each site. However, a key question is which of all these possible sequences of v_n will persist as solutions when $\epsilon \neq 0$. A simple way to see this in the 1D case of equation (131) is to multiply equation (132) by v_n^* and subtract the complex conjugate of the resulting equation, which in turn leads to

$$v_n^*v_{n+1} - v_nv_{n+1}^* = \text{const} \Rightarrow 2\arg(v_{n+1}) = 2\arg(v_n), \quad (133)$$

since we are considering solutions vanishing as $n \rightarrow \pm\infty$. Without loss of generality (using the scaling of the equation), we can scale $\mu = 1$, in which case the only states that will persist for finite ϵ are ones containing sequences with combinations of $v_n = \pm 1$ and $v_n = 0$. A systematic computational classification of the simplest of these sequences and of their bifurcations is provided in [278]. Note that we are tackling here the focusing case of $s = -1$, however, the defocusing case of $s = 1$ can also be addressed based on the same considerations and using the so-called staggering transformation $w_n = (-1)^n u_n$ (which converts the defocusing nonlinearity into a focusing one, with an appropriate frequency rescaling which can be absorbed in a gauge transformation).

We subsequently consider the issue of stability, using once again the standard symplectic formalism $J\mathcal{L}w = \lambda w$, where \mathcal{L} is given by equation (100) and J is the symplectic matrix. In this case, the L_+ and L_- operators are given by

$$(1 - 3v_n^2)a_n - \epsilon(a_{n+1} + a_{n-1}) = \mathcal{L}_+ a_n = -\lambda b_n, \quad (134)$$

$$(1 - v_n^2)b_n - \epsilon(b_{n+1} + b_{n-1}) = \mathcal{L}_- b_n = \lambda a_n. \quad (135)$$

We again use the AC limit where we assume a sequence for v_n with N ‘excited’ (i.e. $\neq 0$) sites; then, it is easy to see that for $\epsilon = 0$ these sites correspond to eigenvalues $\lambda_{L_+} = -2$ for L_+ and to eigenvalues $\lambda_{L_-} = 0$ for L_- , and they result in N eigenvalue pairs with $\lambda^2 = 0$ for the full Hamiltonian problem. Hence, these eigenvalues are potential sources of instability, since for $\epsilon \neq 0$, $N - 1$ of those will become non-zero (there is only one symmetry, namely, the $U(1)$ invariance, persisting for $\epsilon \neq 0$). The key question for stability purposes is to identify the location of these $N - 1$ small eigenvalue pairs. One can manipulate equations (134) and (135) into the form

$$\mathcal{L}_- b_n = -\lambda^2 \mathcal{L}_+^{-1} b_n \Rightarrow \lambda^2 = -\frac{(b_n, \mathcal{L}_- b_n)}{(b_n, \mathcal{L}_+^{-1} b_n)}. \quad (136)$$

Near the AC limit, the effect of L_+ is a multiplicative one (by -2). Hence

$$\lim_{\epsilon \rightarrow 0} (b_n, \mathcal{L}_+^{-1} b_n) = -\frac{1}{2} \Rightarrow \lambda^2 = 2\gamma = 2(b_n, \mathcal{L}_- b_n). \quad (137)$$

Therefore the problem reverts to the determination of the spectrum of L_- . However, using the fact that v_n is an eigenfunction of L_- with $\lambda_{L_-} = 0$ and the Sturm comparison theorem for difference operators [279], one infers that if the number of sign changes in the solution at the AC limit is m (i.e. the number of times that adjacent to a $+1$ is a -1 and next to a -1 is a $+1$), then $n(L_-) = m$ and therefore from equation (137), the number of imaginary eigenvalue pairs of \mathcal{L} is m , while that of real eigenvalue pairs is consequently $(N - 1) - m$. An immediate conclusion is that unless $m = N - 1$ or practically unless adjacent sites are out-of-phase with each other, the solution is immediately unstable for $\epsilon \neq 0$. Note that this is also consistent with the eigenvalue count of [217,222] since $n(\mathcal{L}) - n(D) = (N + m) - 1 = (N + m - 1) + 2 \times m + 2 \times 0 = k_r + 2k_i^- + 2k_c$ (it is straightforward to show by the definition of the Krein signature [280] that these m imaginary pairs have negative Krein signature).

One can also use equation (137) quantitatively to identify the relevant eigenvalues perturbatively for the full problem by considering the perturbed (originally zero when $\epsilon = 0$) eigenvalues of L_- in the form

$$\mathcal{L}_-^{(0)} b_n^{(1)} = \gamma_1 b_n^{(0)} - \mathcal{L}_-^{(1)} b_n^{(0)}, \quad (138)$$

where $\mathcal{L}_- = \mathcal{L}_-^{(0)} + \epsilon \mathcal{L}_-^{(1)} + \mathcal{O}(\epsilon^2)$ and a similar expansion has been used for the eigenvector b_n . Also $\lambda_{L_-} = \epsilon \gamma_1 + \mathcal{O}(\epsilon^2)$. Projecting the above equation to all the eigenvectors of zero eigenvalue of $L_-^{(0)}$, one can explicitly convert equation (138) into an eigenvalue problem [280] of the form $Mc = \gamma_1 c$, where the matrix M has off-diagonal entries: $M_{n,n+1} = M_{n+1,n} = -\cos(\theta_{n+1} - \theta_n)$ and diagonal entries $M_{n,n} = (\cos(\theta_{n-1} - \theta_n) + \cos(\theta_{n+1} - \theta_n))$. Then it is straightforward to compute γ_1 and subsequently from equation (137) to evaluate the corresponding $\lambda = \pm \sqrt{2\epsilon \gamma_1}$. For example, for one-dimensional configurations with two adjacent sites with phases θ_1 and θ_2 , the matrix M becomes

$$M = \begin{pmatrix} \cos(\theta_1 - \theta_2) & -\cos(\theta_1 - \theta_2) \\ -\cos(\theta_1 - \theta_2) & \cos(\theta_1 - \theta_2) \end{pmatrix}, \quad (139)$$

whose straightforward calculation of eigenvalues leads to $\lambda^2 = 0$ and $\lambda^2 = \pm 2\sqrt{\epsilon} \cos(\theta_1 - \theta_2)$. Note that this result is consonant with our qualitative theory above since

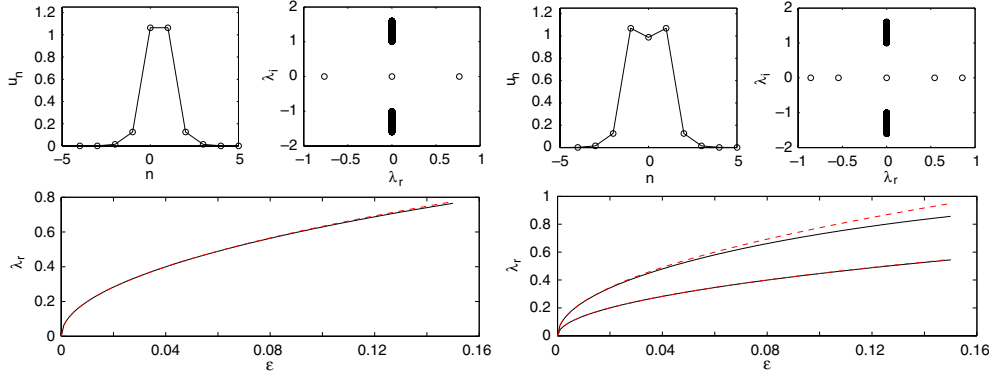


Figure 6. A typical example of a two-site configuration is shown in the left panels of the figure, and a corresponding one of a three-site configuration in the right panels. The top panels show a solution (for a particular value of ϵ) and its corresponding spectral plane (λ_r, λ_i) of eigenvalues $\lambda = \lambda_r + i\lambda_i$, while the bottom ones show the dependence of the relevant real eigenvalues as a function of the inter-site coupling ϵ obtained analytically (dashed/red lines) and numerically (solid/black lines). Reprinted from [280], Copyright (2005), with permission from Elsevier.

for same phase excitations ($\theta_1 = \theta_2$), the configuration is unstable, while the opposite is true if $\theta_1 = \theta_2 \pm \pi$. Similar calculations are possible for 3-site configurations with phases $\theta_{1,2,3}$, in which case, one of the eigenvalues of M is again 0 (as has to generically be the case, due to the $U(1)$ invariance), while the other two are given by

$$\gamma_1 = \cos(\theta_2 - \theta_1) + \cos(\theta_3 - \theta_2) \pm \sqrt{\cos^2(\theta_2 - \theta_1) - \cos(\theta_2 - \theta_1) \cos(\theta_3 - \theta_2) + \cos^2(\theta_3 - \theta_2)}. \quad (140)$$

Some of the examples of the accuracy of these theoretical predictions for some typical two-site and three-site configurations (in particular, the in-phase ones, which should have one and two real eigenvalue pairs, respectively) are shown in figure 6.

This approach can be generalized to different settings, such as in particular higher dimensions [281, 282] or multicomponent systems [283]. Perhaps the fundamental difference that arises in the higher-dimensional settings is that one can excite sites over a contour and then, for the N excited sites around the contour, the persistence (Lyapunov–Schmidt) conditions can be obtained as a generalization of equation (131) that reads [281, 284]

$$\sin(\theta_1 - \theta_2) = \sin(\theta_2 - \theta_3) = \dots = \sin(\theta_N - \theta_1), \quad (141)$$

which indicates that a key difference of higher-dimensional settings is that not only ‘solitary wave’ structures with phases $\theta \in \{0, \pi\}$ are possible, but also both symmetric and asymmetric vortex families [281, 284] may, in principle, be possible (although equation (141) provides the leading order persistence condition and one would need to also verify the corresponding conditions to higher order to confirm that such solutions persist [281]). Such vortex solutions had been predicted numerically earlier [285, 286] and have been observed experimentally in the optical setting of photorefractive crystals [287, 288]. Performing the stability analysis is possible for these higher-dimensional structures, although the relevant calculations are technically far more involved. However, the theory can be formulated in an entirely general manner: we give its outline and some prototypical examples of higher-dimensional theory–computation comparisons below.

The existence problem can be generally formulated in the multidimensional case as the vanishing of the vector field \mathbf{F}_n of the form:

$$\mathbf{F}_n(\phi, \epsilon) = \begin{bmatrix} (1 - |\phi_n|^2)\phi_n - \epsilon \Sigma \phi_n \\ (1 - |\phi_n|^2)\phi_n^* - \epsilon \Sigma \phi_n^* \end{bmatrix}. \quad (142)$$

If we then define the matrix operator:

$$\mathcal{H}_n = \begin{pmatrix} 1 - 2|\phi_n|^2 & -\phi_n^2 \\ -\bar{\phi}_n^2 & 1 - 2|\phi_n|^2 \end{pmatrix} - \epsilon(s_{+e_1} + s_{-e_1} + s_{+e_2} + s_{-e_2} + s_{+e_3} + s_{-e_3}) \begin{pmatrix} 1 & 0 \\ 0 & 1 \end{pmatrix}, \quad (143)$$

where the $s_{\pm e_i}$ denotes the shift operators along the respective directions, then the stability problem is given by $\sigma \mathcal{H} \psi = i\lambda \psi$, where the 2-block of σ is the diagonal matrix of $(1, -1)$ at each node n . Furthermore, the existence problem is connected to \mathcal{H} through: $\mathcal{H} = D_\phi \mathbf{F}(\phi, 0)$. At the AC limit of $\epsilon = 0$

$$(\mathcal{H}^{(0)})_n = \begin{bmatrix} 1 & 0 \\ 0 & 1 \end{bmatrix}, \quad n \in S^\perp, \quad (\mathcal{H}^{(0)})_n = \begin{bmatrix} -1 & -e^{2i\theta_n} \\ -e^{-2i\theta_n} & -1 \end{bmatrix}, \quad n \in S,$$

where S is the set of excited sites. Then the eigenvectors of zero eigenvalue are of the form

$$(\mathbf{e}_n)_k = i \begin{bmatrix} e^{i\theta_n} \\ -e^{-i\theta_n} \end{bmatrix} \delta_{k,n}.$$

Defining the projection operator:

$$(\mathcal{P}\mathbf{f})_n = \frac{(\mathbf{e}_n, \mathbf{f})}{(\mathbf{e}_n, \mathbf{e}_n)} = \frac{1}{2i} (e^{-i\theta_n} (\mathbf{f}_1)_n - e^{i\theta_n} (\mathbf{f}_2)_n), \quad n \in S, \quad (144)$$

and decomposing the solution as

$$\phi = \phi^{(0)}(\theta) + \varphi \in X, \quad (145)$$

one can obtain the Lyapunov–Schmidt persistence conditions as [282]

$$\mathbf{g}(\theta, \epsilon) = \mathcal{P}\mathbf{F}(\phi^{(0)}(\theta) + \varphi(\theta, \epsilon), \epsilon) = 0. \quad (146)$$

This leads to the persistence theorem [282]: The configuration $\phi^{(0)}(\theta)$ can be continued to the domain $\epsilon \in \mathcal{O}(0)$ if and only if there exists a root θ_* of the vector field $\mathbf{g}(\theta, \epsilon)$. Moreover, if the root θ_* is analytic in $\epsilon \in \mathcal{O}(0)$ and $\theta_* = \theta_0 + \mathcal{O}(\epsilon)$, the solution ϕ of the difference equation is analytic in $\epsilon \in \mathcal{O}(0)$, such that

$$\phi = \phi^{(0)}(\theta_*) + \varphi(\theta_*, \epsilon) = \phi^{(0)}(\theta_0) + \sum_{k=1}^{\infty} \epsilon^k \phi^{(k)}(\theta_0). \quad (147)$$

One can also formulate on the same footing a general stability theory. More specifically, let the solution of interest persist for $\epsilon \neq 0$. If the operator \mathcal{H} has a small eigenvalue μ of multiplicity d , such that $\mu = \epsilon^k \mu_k + \mathcal{O}(\epsilon^{k+1})$, then the full Hamiltonian eigenvalue problem admits $(2D)$ small eigenvalues λ . These are such that $\lambda = \epsilon^{k/2} \lambda_{k/2} + \mathcal{O}(\epsilon^{k/2+1})$, where non-zero values $\lambda_{k/2}$ are found from

$$\text{odd } k: \quad \mathcal{M}^{(k)} \alpha = \frac{1}{2} \lambda_{k/2}^2 \alpha, \quad (148)$$

$$\text{even } k: \quad \mathcal{M}^{(k)} \alpha + \frac{1}{2} \lambda_{k/2} \mathcal{L}^{(k)} \alpha = \frac{1}{2} \lambda_{k/2}^2 \alpha, \quad (149)$$

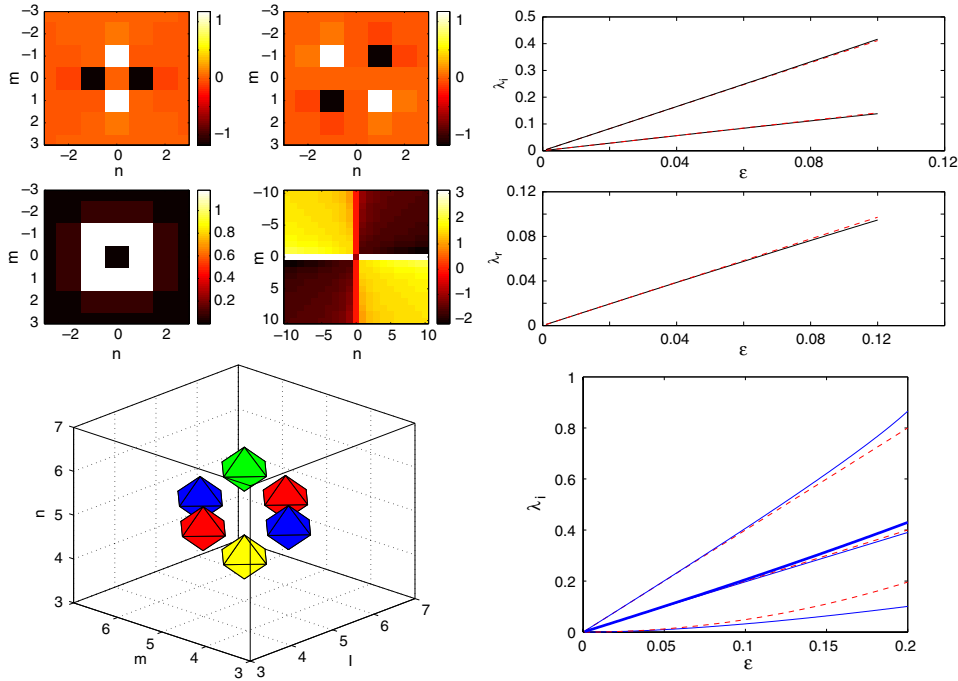


Figure 7. The array of the four panels on the top-left shows a 2D $S = 2$ vortex configuration (the top panels show its real (left) and imaginary (right) parts, while the bottom panels show its amplitude (left) and phase (right)). The two panels to the right of this quadrant, show the imaginary (top) and real (bottom) linear stability eigenvalues of this configuration. The bottom-left and bottom-right panels are similar to the above, but are for a 3D diamond configuration (see the explanation of its phases in the text). The diamond configuration is shown using iso-level contours of different hues: dark grey/grey (blue/red in the colour version) are positive/negative real iso-contours while the light grey/very light grey (green/yellow in the colour version) correspond to positive/negative imaginary iso-contours. The theoretical predictions for the eigenvalues as a function of the coupling are shown by dashed lines, while the full numerical results by solid ones. Partially reprinted from [281], Copyright (2005), and [282], Copyright (2008), with permission from Elsevier.

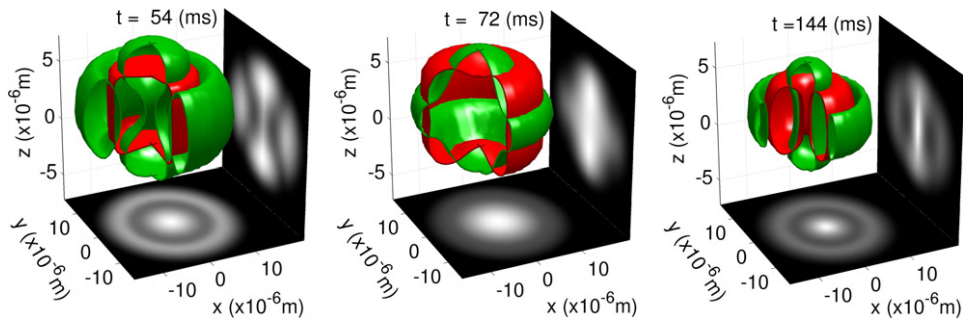


Figure 8. Nonlinear dynamics of a binary 50 : 50 mixture of two spin states ($|1, -1\rangle$ and $|2, 1\rangle$) of $N = 375\,000$ Rb atoms. Each component is depicted by a contour slice at half of its corresponding maximal density. The horizontal (vertical) projection corresponds to the z - (x -) integrated density for the $|1, -1\rangle$ component as observed in laboratory experiments [322]. Please visit: <http://www.rohan.sdsu.edu/~rcarrete/> (Publications) to view movies showing the interpenetrating time evolution between the two components over a span of 220 ms. Adapted from [322] with permission.

where

$$\begin{aligned}\mathcal{M}^{(k)} &= D_{\theta} \mathbf{g}^{(k)}(\theta_0), \\ \mathcal{L}^{(k)} &= \mathcal{P}[\mathcal{H}^{(1)} \Phi^{(k')}(\theta_0) + \dots + \mathcal{H}^{(k'+1)} \Phi^{(0)}(\theta_0)],\end{aligned}$$

and $k' = (k - 1)/2$. For more details, we refer the interested reader to [282].

In figure 7 we show typical examples of 2D and 3D configurations that satisfy the persistence conditions formulated above. The former configuration is a vortex of topological charge $S = 2$ (i.e. its phase changes uniformly by $\pi/2$ from each site to the next so that it changes from 0 to 4π around the discrete contour of the solution). This structure is unstable due to a real eigenvalue pair that is theoretically predicted from equations (148) and (149) to be $\lambda = \pm\sqrt{\sqrt{80} - 8\epsilon}$ (while it also has a pair of simple eigenvalues $\lambda = \pm i\epsilon\sqrt{\sqrt{80} + 8}$, a quadruple eigenvalue $\lambda = \pm i\epsilon\sqrt{2}$ and a single eigenvalue of higher order). The latter configuration is a three-dimensional diamond configuration (a quadrupole in the plane with phases 0, π , 0, π and two out-of-plane sites with phases $\pi/2$ and $3\pi/2$). This is a stable 3D structure with a single eigenvalue $\lambda = \pm 4i\epsilon$, a triple eigenvalue $\lambda = \pm 2i\epsilon$ and an eigenvalue of higher order according to equations (148) and (149). Note in both cases the remarkable agreement between the theoretical prediction for the eigenvalues (dashed lines) and the full numerical results (solid lines).

5. Special topics of recent physical interest

In this section we give a very brief overview of some of the more recent themes of interest in the nonlinear phenomenology emerging in the realm of Bose–Einstein condensation. We pay special attention to the physical motivation of the different topics. Note that an in-depth treatment of the emergent nonlinear behaviour displayed by BECs and the synergy between experiments and theory can be found in the recent review [55].

5.1. Spinor/multicomponent condensates

Advances in trapping techniques for BECs have opened the possibility to simultaneously confine atomic clouds in different hyperfine spin states. The first such experiment, the so-called *pseudospinor* condensate, was achieved in mixtures of two magnetically trapped hyperfine states of ^{87}Rb [289]. Subsequently, experiments in optically trapped ^{23}Na [290] were able to produce multicomponent condensates for different Zeeman sub-levels of the same hyperfine level, the so-called *spinor* condensates. In addition to these two classes of experiments, mixtures of two different species of condensates have been created by sympathetic cooling (i.e. condensing one species and allowing the other one to condense by taking advantage of the coupling with the first species) where ^{41}K atoms were sympathetically cooled by ^{87}Rb atoms [291]. More exotic mixtures are also currently being explored in degenerate fermion–boson mixtures in ^{40}K – ^{87}Rb [292] and pure degenerate fermion mixtures in ^{40}K – ^6Li [293–295].

The mean-field dynamics of such multicomponent condensates is described by a system of coupled GP equations analogous to equation (43), which for mixtures of \mathcal{N} bosonic components reads

$$i \frac{\partial \psi_n}{\partial t} = -\frac{1}{2} \Delta \psi_n + V_n(\mathbf{r}) \psi_n + \sum_{k=1}^{\mathcal{N}} [g_{n,k} |\psi_k|^2 \psi_n - \kappa_{n,k} \psi_k + \Delta \mu_k \psi_n] - i\sigma_n \psi_n, \quad (150)$$

where ψ_n is the wavefunction of the n th component ($n = 1, \dots, \mathcal{N}$), $V_n(\mathbf{r})$ is the potential confining the n th component, $\Delta \mu_{n,k}$ is the chemical potential difference between components

n and k , and σ_n describes the losses of the n th component. The components n and k are coupled via (i) nonlinear coupling with coefficients $g_{n,k}$ and (ii) linear coupling with coefficients $\kappa_{n,k}$; where, by symmetry, $g_{n,k} = g_{k,n}$ and $\kappa_{n,k} = \kappa_{k,n}$. The nonlinear coupling results from interatomic collisions while the linear coupling accounts for spin state interconversion usually induced by a spin-flipping resonant electromagnetic wave [296]. In the case of fermionic mixtures one needs to replace the self-interacting nonlinear terms by $g_{n,n}|\psi_n|^{4/3}\psi_n$ [297–299]. In the absence of losses ($\sigma_n = 0$), the total number of atoms is conserved:

$$N \equiv \sum_{k=1}^{\mathcal{N}} N_k = \sum_{k=1}^{\mathcal{N}} \int |\psi_k|^2 d\mathbf{r}. \quad (151)$$

In fact, in the further absence of linear interconversions ($\kappa_{n,k} = 0$), each norm N_k is conserved separately.

The simplest case of two species ($\mathcal{N} = 2$) has been studied extensively. In particular, if one considers the trapless system ($V_n = 0$) in the absence of linear interconversion, losses, and chemical potential differences, the two components tend to segregate if the immiscibility condition

$$\Delta \equiv (g_{12}g_{21} - g_{11}g_{22})/g_{11}^2 > 0 \quad (152)$$

is satisfied [300]. This condition can be interpreted as if the mutual repulsion between species is stronger than the combined self-repulsions. In typical experiments, the miscibility parameter (an adimensional quantity) is rather small: $\Delta \approx 9 \times 10^{-4}$ for ^{87}Rb [289, 301] and $\Delta \approx 0.036$ for ^{23}Na [66]. Depending on the various nonlinear coefficients, a vast array of solutions can be supported by a binary condensate. These include, ground state solutions [302–304], small-amplitude excitations [305–308], bound states of dark–bright [309] and dark–dark [310], dark–grey, bright–grey, bright–antidark and dark–antidark [311] complexes of solitary waves, vector solitons with embedded domain-walls (DWs) [312], spatially periodic states [313] and modulated amplitude waves [314]. Extensions of some of these patterns in two dimensions, namely, DWs, have been investigated in [303, 304, 315–321]. The non-equilibrium dynamics of a binary condensate has been shown to support (experimentally and theoretically) long lived ring excitations whereby each component inter-penetrates the other one repeatedly [322] (see figure 8). The effects of adding the linear inter-species coupling between the components has also been studied in some detail [313, 323–333]. One of the salient features of adding the linear inter-species coupling is the suppression or promotion of the transition to miscibility (cf [334] and chapter 15 in [55]). Spinor condensates with three species have also drawn considerable attention since their experimental creation [66, 335]. Such systems give rise to spin domains [290], polarized states [336], spin textures [337] and multicomponent (vectorial) solitons of bright [338–341], dark [342], gap [343] and bright–dark [344] types.

5.2. Vortices and vortex lattices

Arguably, one of the most striking nonlinear matter-wave manifestations in BECs is the possibility of supporting vortices [345, 346]. Vortices are characterized by their non-zero topological charge S whereby the phase of the wavefunction has a phase jump of $2\pi S$ along a closed contour surrounding the core of the vortex (cf phase profile for a singly charged vortex, $S = +1$, in the right panel of figure 9). Historically, the first observation of vortices in BECs was achieved [28] by phase imprinting between two hyperfine spin states of Rb [347]. Nowadays, the standard technique to nucleate vortices in BECs is based on stirring [35] the condensate cloud above a certain critical angular speed [348–350]. This technique has proven

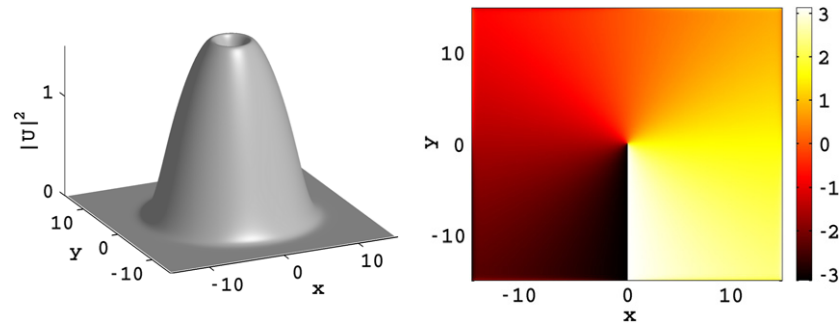


Figure 9. Two-dimensional, singly charged ($S = 1$), vortex inside a parabolic magnetic trap $V(z) = \frac{1}{2}\Omega^2(x^2 + y^2)$ with $\Omega = 0.2$. Depicted are the density (left) and the phase profile (right) for a chemical potential $\mu = 2$.

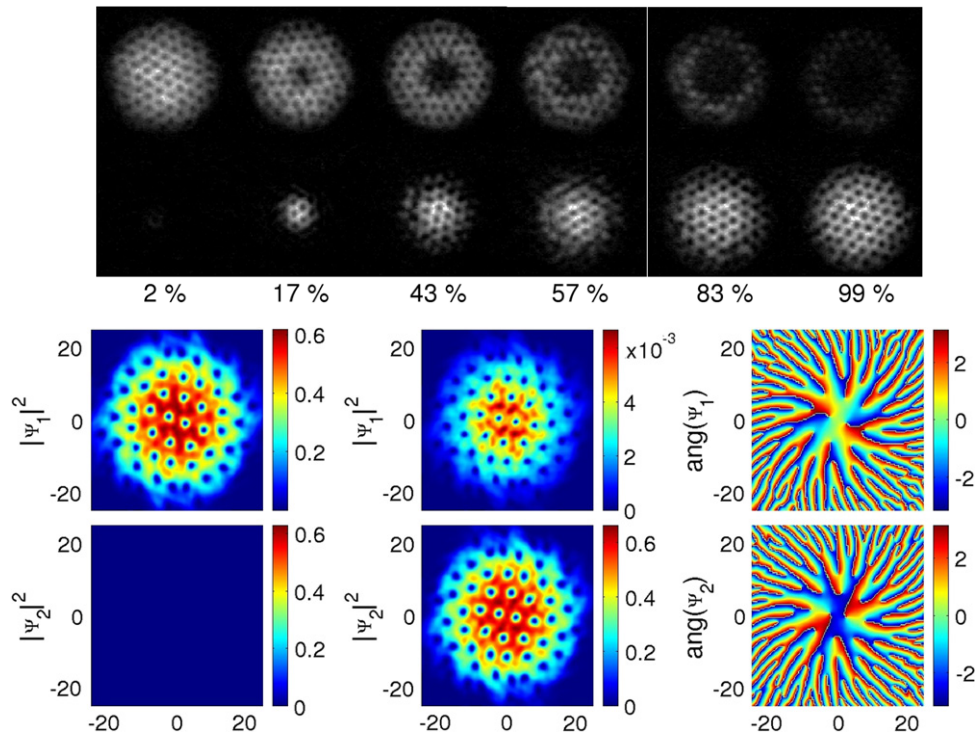


Figure 10. (Top) Experimental look at component separation in a rotating BEC of Rb atoms (image provided by D S Hall) after 30 ms evolution, release and 20 ms free expansion from a relatively tight trapping potential. The percentages quoted are the fraction of atoms transferred from the $|1, -1\rangle$ state (top row) to the $|2, 1\rangle$ state (bottom row). (Bottom) Numerical vortex lattice (VL) transfer by linear coupling from the first (top row) to the second component (bottom row). The initial VL (left column) is successfully transferred between components (see middle column where the scale in the top panel clearly indicates that the first component is almost depleted of atoms after transfer). More importantly, note that the phase distribution is also transferred between components (right column).

to be extremely efficient, not only in creating single vortices but also, from a few vortices [350], to vortex lattices [351]. It is also possible to nucleate vortices by dragging a moving impurity through the condensate for speeds above a critical velocity (depending on the local density and also the shape of the impurity) [352–359]. Yet another possibility to nucleate vortices can be achieved by separating the condensate into different fragments and allowing them to collide [360–362].

The profile of a vortex in a two-dimensional setting (see left panel of figure 9) can be obtained by solving for the density $U(r)$ when considering a wave function of the form $\psi(r, \theta) = U(r) \exp(iS\theta - i\mu t)$ that satisfies the 2D GP equation with repulsive nonlinearity ($g = +1$), where (r, θ) are the polar coordinates and μ is the chemical potential. The equation for U takes the form

$$\frac{d^2U}{dr^2} + \frac{1}{r} \frac{dU}{dr} - \frac{S^2}{r^2} U + (\mu - V(r) - U^2) U = 0, \quad (153)$$

with boundary conditions $U(0) = 0$ and $U(+\infty) = \sqrt{\mu}$ for a confining potential $V(r = +\infty) = +\infty$. Unfortunately, the ensuing equation for the vortex profile cannot be solved exactly (even in the simplest homogeneous case with $V(r) \equiv 0$) and one has to resort to numerical or approximate methods [363]. The asymptotic behaviour of the vortex profile $U(r)$ can be found from equation (153), i.e. $U(r) \sim r^{|S|}$ as $r \rightarrow 0$, and $U(r) \sim \sqrt{\mu} - S^2/(2r^2)$ as $r \rightarrow +\infty$. Note that the width of singly charged vortices in BECs is $\mathcal{O}(\xi)$ (where ξ is the healing length given in equation (19)), while higher-charge vortices ($|S| > 1$) have cores wider than the healing length and are unstable in the homogeneous background case ($V(r) \equiv 0$) but might be rendered stable by external impurities [364] or by external potentials [365–368]. When unstable, higher order charge vortices typically split into multiple single charge vortices.

Single charge vortices are extremely robust due to their inherent topological charge since continuous transformations/deformations of the vortex profile cannot eliminate the $2\pi S$ phase jump—unless the density is close to zero (this is the reason why, in the stirring experiments, vortices are nucleated at the periphery of the condensate cloud where the density tends to zero for confining potentials [369–372]). Vortices are prone to motion induced by gradients in both density and phase of the background [373]. These gradients can be induced by an external potential or the presence of another vortex. The effect of vortex precession induced by the external trap has been extensively studied [374–381]. The motion induced on a vortex by another vortex is equivalent to the one observed in fluid vortices whereby vortices with the same charge travel parallel to each other at constant speed, while vortices of opposite charges rotate about each other at constant angular speed.

Another topic that has attracted an enormous amount of attention in recent years is the ubiquitous existence of robust vortex lattices in rapidly rotating condensates consisting of ordered lattices of vortices arranged in triangular configurations (the so-called Abrikosov lattices [382]). The first experimental observation of vortex lattices consisted of just a few (< 15) vortices [351] but soon experiments were able to maintain vortex lattices with some 100 vortices [383]. Alternative methods to describe vortex lattice configurations have been given in terms of Kelvin’s variational principle [384] and through a linear algebra formulation [385]. Another approach is to treat each vortex as a quasi-particle and apply ideas borrowed from molecular dynamics to find the most energetically favorable configurations [386]. Some other interesting phenomenology of vortex lattices includes the excitation of Tkachenko modes [387] via the annihilation of a central chunk of vortex lattice matter through localized laser heating [388].

Yet another promising avenue of research that is currently being explored is the topic of vortex lattices in multicomponent condensates. For example, starting with a two-component

BEC mixture with only one atomic species containing a vortex lattice, and subsequently ‘activating’ the linear coupling, it is possible to *entirely transfer* the vortex lattice to the second component (cf results in figure 10). This ‘Rabi oscillation’ between atomic species [389, 313] is an extremely useful tool for controlling the transfer of desirable fractions of atoms from one state to another and can be extended to multicomponent condensates [390, 391]. Furthermore, it is important to note that the interaction of vortex lattices in a multicomponent BEC can result in structural changes in the configurations of the vortex lattices, i.e. resulting in lattices with different symmetry [392, 393].

5.3. Shock waves

One of the classical types of nonlinear waves appearing in the context of BECs is shock waves. Shock waves were first observed in the experiments reported in [31], where a slow-light technique was used to produce density depressions in a sodium BEC. More recently, they were observed in rapidly rotating ^{87}Rb BECs triggered by repulsive laser pulses [394], while their formation was discussed in an experiment involving the growth dynamics of a 1D sodium quasi-condensate in a dimple microtrap created on top of the harmonic confinement of an atom chip [395]. Finally, shock waves were studied experimentally and theoretically in [396]; in the experiments reported in this work, repulsive laser beams were used (as in [394], but with a non-rotating condensate) to push atoms from the BEC centre, thus forming ‘blast-wave’ patterns.

On the theoretical side, shock waves in repulsive BECs were mainly studied in the framework of mean-field theory and the GP equation for weakly interacting Bose gases [396–404], but also for strongly interacting ones [405] and in the BEC–Tonks crossover [406]; additionally, the effect of temperature (see section 5.7) on shock wave formation and dynamics and the effect of depleted atoms were, respectively, discussed in [395, 406]. Many of the above mentioned theoretical studies rely on the hydrodynamic equations that can be obtained from the GP equation via the Madelung transformation $\psi = \sqrt{\rho} \exp(i\phi)$ (with ρ and ϕ being the condensate’s density and phase, respectively, see also section 4.3.3). These hydrodynamic equations are then treated in the long-wavelength limit (or, equivalently, in the weakly dispersive regime) where the so-called quantum pressure term, $\sim(\nabla^2 \sqrt{\rho})/\sqrt{\rho}$, is negligible. Qualitatively speaking, one may ignore this term if the so-called ‘quantum Reynolds number’ [398, 399] (see also the discussion in [397, 401]) satisfies $R \equiv an_0 L_0^2 \gg 1$, where a is the scattering length, n_0 the peak density of the BEC and L_0 a minimal scale among all the characteristic spatial scales of the condensate wavefunction. In fact, a more rigorous treatment relies on the assumption that the quantum pressure term is small, as in the case of the theoretical analysis (and the pertinent experimental results) of [396]. In any case, since the quantum pressure is reminiscent of viscosity in classical fluid mechanics, this weakly dispersive regime suggests the possibility of ‘dissipationless shock waves’ in BECs (according to the nomenclature of [402]).

The above mentioned hydrodynamic equations were treated in the limiting case of zero quantum pressure in [397–400]. In this case, the hydrodynamic equations resulting from the GP equation are reduced to a hyperbolic system of conservation laws of classical gas dynamics, namely, an Euler and a continuity equation (see, e.g., [407]). In this gas dynamics picture, the above hyperbolic system is characterized by two real eigenspeeds (i.e. characteristic speeds of propagation of weak discontinuities) $v^\pm = v \pm c$, where v is the velocity of the gas and c is the speed of sound. Since the latter depends on the condensate density ρ (see equation (18)), it is clear that higher values of ρ propagate faster than lower ones and, as a result, any compressive part of the wave ultimately breaks to give a triple-valued solution

for ρ ; this is a signature of the formation of a shock wave. In this system, a Gaussian input produces two symmetric shocks at finite time, as was shown, e.g., in [400,406] (see also [408] for a rigorous discussion). Importantly, the trailing edge of the shock wave as observed in the simulations and the experiments (see, e.g., [31,395,396,400,406]) can be considered as a modulated train of dark solitons [396,402].

In the work [401], a more careful investigation of the regimes of validity of the condition $R \gg 1$ (which may fail, e.g., in the case of expanding BECs) led to an experimentally relevant protocol to produce shock waves in BECs. This protocol is based on the use of Feshbach resonance to control the scattering length a , namely, to make a an increasing function of time (by a proper ramp-up procedure), so as to increase the time domain in which the quantum pressure is negligible. This way, this ‘Feshbach resonance management’ technique¹¹ was shown to produce multidimensional shock waves. On the other hand, in [402] the Whitham averaging method [412] was used in the weakly dispersive regime to show that dissipationless shock waves are emanating from density humps in repulsive BECs. Moreover, the formation of shock waves in BECs confined in optical lattices was discussed in [403], while in [396] an in-depth analysis of the shock waves appearing in BECs and in gas dynamics (also in connection to relevant experiments of the JILA group) was presented. Finally, it should also be mentioned that the above mentioned works chiefly refer to repulsive BECs; an analysis of the shock wave formation in attractive BECs can be found in [91].

5.4. Multidimensional solitons and collapse

As was highlighted in section 3, a strong transverse confinement may effectively render the BEC quasi-1D, in which case the 1D soliton solutions are physically relevant and are stable. In contrast, in the absence of a tight transversal trapping, higher-dimensional extensions of 1D solitons are generally unstable [12]. However, by restricting the transverse direction(s) of the condensate, it is possible to obtain higher-dimensional soliton solutions that are stabilized for times longer than the lifespan of the experiments [413–415].

Let us now showcase some of the possible higher-dimensional soliton solutions displayed by the GP model. In this section we focus on higher-dimensional extensions of 1D bright and dark solitons. More complex higher-dimensional coherent structures (i.e. solutions that do not have a 1D equivalent) include 2D vortices (see previous section), 3D vortex lines [11,416–419], vortex rings [33,420,421] or more complicated topologically charged structures such as skyrmions [422–427].

5.4.1. Dark solitons. The trademark of a dark soliton is its phase jump along its centre separating two repelling phases. In a 2D geometry a dark soliton corresponds to a nodal line separating the two phases while in 3D it corresponds to a nodal plane. Both the 2D and 3D dark solitons, respectively, called band (or stripe) and planar dark solitons, are prone to the snaking instability along their nodal extent [428,429]. These instabilities result in the nucleation of vortex pairs in 2D [430,431] and pairs of vortex lines and/or vortex rings in 3D. When the dark soliton is set into motion inside a confining trap, it suffers bending resulting from the different speeds of sounds at the edge of the cloud (low density and thus slower speeds compared with the speed at the centre of the cloud) accelerating the formation of vortices at the trailing edges [30]. It is also possible to create dark soliton structures whose nodal sets, instead of extending linearly, can be wrapped around. It is therefore possible to create in

¹¹ This technique was suggested in earlier works in various important applications, as e.g. a means to prevent collapse of higher-dimensional attractive BECs [193,203,409] to produce periodic waves [107] and robust matter-wave breathers [241,242,410,411].

2D ring dark solitons and in 3D spherical shell dark solitons, such as the ones discussed in section 4.3.2. Such structures can be described by nonlinear Bessel functions (cf [432] and chapter 7 in [55]) and are also prone to the snaking instability. It is worth mentioning that the above-mentioned instabilities can be weak (slow) enough so that these solitons can be observed in the experiments [31, 33, 433].

5.4.2. Bright solitons and collapse. Bright solitons in higher dimensions are prone to a different type of instability due to the intrinsic collapse of solutions of the NLS equation [12]. The first experiments with attractive condensates suffered from this collapse instability [81, 82, 434, 435] while the more recent experiments were able to focus on stable regimes and demonstrate bright soliton formation [40–42]. In fact, the key feature of these experiments was the quasi-1D nature of the attractive BEC realized in anisotropic traps as discussed in section 3. Thus, the observed bright solitons were found to be robust, which would not be the case in a higher-dimensional system, as they should either collapse or expand indefinitely depending on the number of atoms and the density profile. The solution that constitutes the unstable separatrix between expansion and collapse is the well-known Townes soliton [436, 437].

In this connection, it is important to mention that even though the experimental condensates are never truly 1D, fortunately, the tight trapping in the transverse direction(s) is able to slow collapse to times much longer than the duration of the experiments. Nonetheless, interactions of bright solitons in higher dimensions, in contrast to their 1D counterparts, may be inelastic [89, 117, 438], and, furthermore, when two (or more) solitons overlap their combined number of atoms can exceed the critical threshold and initiate collapse. The overlap of higher-dimensional solitons, even when the critical number of atoms is exceeded, might not result in collapse since one has to take into account the time of the interaction (depending on the velocities of the solitons and their relative phases, cf chapter 7 in [55] and references therein).

Finally, we note that stabilization of higher-dimensional bright solitons by means of lower-dimensional optical lattices has been proposed in [192, 411, 439]. Moreover, stable bright ring solitons carrying topological charge have been theoretically predicted to exist [83, 366, 440–442] but no experiment has yet corroborated these results.

5.5. Manipulation of matter waves

As discussed in section 3, one of the most appealing features in BECs is the level of control over the different contributions on the GP equation. This includes the possibility to craft almost any desired external potential (by the appropriate superposition of multiple laser beams), and to change the strength and sign of the nonlinearity via the Feshbach resonance mechanism. This is to be contrasted with other contexts where the NLS equation is also a relevant model, as, e.g., in nonlinear optics [17], where it is extremely difficult and often impossible to demonstrate such control. In the BEC context, particularly appealing is the fact that the external potential and/or nonlinearity can be made to follow in time any desired evolution. In this section we focus on the use of appropriately crafted time-dependent external potentials to manipulate matter-waves in BECs. In this section we only consider matter-wave manipulation by two main types of external potentials: localized and periodic potentials. These potentials are experimentally generated by laser beams as explained in section 2.4. Here, it would be useful to recall that the sign of the external optical potential is positive (negative) for blue- (red-) detuned laser beams.

5.5.1. Localized potentials. The interaction of solitons with localized impurities has attracted much attention in the theory of nonlinear waves [253, 254, 443] and solid state physics [444, 445]. In 1D BECs confined by a harmonic trap, bright and dark solitons perform

harmonic oscillations as discussed in section 4 as a consequence of the Kohn theorem (the ‘nonlinear analogue’ of the Ehrenfest theorem) [198, 446], which states that the motion of the centre of mass of a cloud of particles trapped in a parabolic potential decouples from the internal excitations. The existence, stability and dynamics of bright solitons in the presence of the external potential can be analysed using perturbation techniques expounded in section 4. In fact, the combined effects of the harmonic trap $V_{\text{HT}}(x) = \Omega^2 x^2/2$ and an infinitely localized delta impurity, located at x_i , namely, $V_{\text{imp}}(x) = V_{\text{imp}}^{(0)} \delta(x - x_i)$, yield the following effective force on a bright soliton [447],

$$F_{\text{eff}} = F_{\text{HT}} + F_{\text{imp}} = -2\Omega^2 \eta \zeta - 2\eta^3 V_{\text{imp}}^{(0)} \tanh(\eta(x_i - \zeta)) \operatorname{sech}^2(\eta(x_i - \zeta)), \quad (154)$$

where ζ and η are, respectively, the centre and height of the bright soliton, while the first (second) term on the right-hand side corresponds to the harmonic trapping (localized impurity) potential. This effective force induces a Newton-type dynamics for the centre ζ of the bright soliton, as discussed previously. Note that the force induced by the harmonic trap always points towards its centre, while the direction of the force induced by the impurity depends on the sign of $V_{\text{imp}}^{(0)}$. In the case of an attractive impurity it is possible to not only pin the bright soliton away from the centre of the harmonic trap but also to adiabatically drag it and reposition it at, almost, any desired location by slowly moving the impurity [447]. The success in dragging the soliton not only depends on the profiles of the soliton and the impurity, but more crucially, on the degree of adiabaticity when displacing the impurity.

A similar study can also be performed in the case of dark solitons. The interactions of dark solitons with localized impurities were analysed in [448], by using the so-called direct perturbation theory for dark solitons [449], and later in the BEC context in [258], by using the adiabatic perturbation theory for dark solitons [114]. Following the analysis of [258], it is possible to show that the centre ζ of a dark matter-wave soliton obeys a Newton-type equation of motion with an effective potential given by

$$V_{\text{eff}}(\zeta) = V_{\text{HT}}^{\text{eff}}(\zeta) + V_{\text{imp}}^{\text{eff}}(\zeta) = \frac{1}{2} V_{\text{HT}}(\zeta) + \frac{1}{4} V_{\text{imp}}^{(0)} \operatorname{sech}^2(\zeta). \quad (155)$$

Thus, similarly to the bright soliton case, one can use the above pinning of the dark soliton to drag it by adiabatically moving the impurity [258].

Finally, it is also possible to pin and drag vortices with a localized impurity (see chapter 17 in [55] for more details). As discussed above, the presence of the harmonic trap induces vortex precession [374–381]. Therefore, in order to pin/drag the vortex at an off-centre position, the pinning force exerted by the impurity has to be stronger than the vortex precession force induced by the harmonic trap and the impurity has to be deep enough to avoid emission of sound waves [450]. An interesting twist to this manipulation problem is the possibility to snare a moving vortex by an appropriately located/designed impurity.

5.5.2. Periodic potentials. A similar approach to the one described in the previous section can be devised by using periodic potentials. This method relies, as in the case of localized impurities, on the pinning properties of properly crafted periodic potentials. Specifically, a periodic potential with a wavelength longer than the width of the soliton width induces a periodic series of effective potential minima that help to pin the soliton. For instance, in a 1D BEC, a bright soliton subject to a periodic potential generated by an optical lattice of the form

$$V_{\text{OL}}(x) = V_{\text{OL}}^{(0)} \sin^2(kx), \quad (156)$$

behaves (in appropriate parameter ranges) as a quasi-particle inside the effective potential [257]:

$$V_{\text{eff}}(\zeta) = \eta \Omega^2 \zeta^2 - \pi V_{\text{OL}}^{(0)} k \operatorname{csch}(k\pi/\eta) \cos(2k\zeta). \quad (157)$$

This effective potential possesses minima that, as indicated above, can be rigorously shown to correspond to stable positions for the solitons [217–222, 451, 452]. This in turn can be used, in the same manner as above for the localized impurities, to successfully pin, drag and capture bright solitons [257].

The case of manipulation of dark solitons by periodic potentials is more subtle because dark solitons subject to tight confinements are prone to weak radiation loss, as shown numerically in [453–456] and analytically in [263]. Since a dark soliton is an effectively negative mass (density void) structure, radiation loss implies that the soliton travels faster and eventually escapes the local minimum in the effective potential landscape. The motion of a dark soliton subject to an external potential has been treated in detail before [258–263, 457]. In the presence of both the magnetic trap and the optical lattice of equation (156), the motion of the dark soliton depends on the period of the optical lattice when compared with the soliton's width [458]. The case of an optical lattice with long period can be treated as a perturbation (see section 4.3.2), and the dynamics of the dark soliton can adjust itself to the smooth potential. The short period optical lattice case can be treated by multiple-scale expansion [458] and it is equivalent to the motion of a dark soliton inside a renormalized magnetic trap (with no optical lattice) [458]. For intermediate periods, the optical lattice has the ability to drag/manipulate the dark soliton as shown in [458, 459]. However, the effects of radiation loss described above eventually drive the dark soliton into large-amplitude oscillations inside the local effective potential minima leading, eventually, to its expulsion.

Finally, we briefly discuss vortices under the presence of periodic potentials. Their stability and dynamics has been studied in [460, 461], while the existence of gap vortices in the gaps of the band-gap spectrum due to Bragg scattering were considered in [177]. Also, in the presence of deep periodic lattices, where the discrete version of the GP equation (namely the DNLS equation, see, e.g., section 3.6.2) becomes relevant, purely 3D discrete vortices can be constructed [462–464]. An interesting twist of the pinning of vortices (which has been observed experimentally [465]) is the case when a vortex lattice is induced to transition from a triangular Abrikosov vortex lattice to a square lattice by an optical lattice [466, 467]. Another type of vortex lattice manipulation is the use of large-amplitude oscillations to induce structural phase transitions (e.g. from triangular to orthorhombic) [39].

5.6. Matter waves in disordered potentials

Recently, there has been much attention focused on the dynamics of matter waves in disordered potentials. Generally speaking, disorder in quantum systems has been a subject of intense theoretical and experimental studies. In the context of ultracold atomic gases, disorder may result from the roughness of a magnetic trap [468] or a magnetic microtrap [469]. However, it is important to note that *controlled* disorder (or quasi-disorder) may also be created by means of different techniques. These include the use of two-colour superlattice potentials [470–472], the employment of so-called quasi-crystal (i.e. quasi-periodic) optical lattices in 2D or 3D [473–475], the use of impurity atoms trapped at random positions in the nodes of a periodic optical lattice [476], random phase masks [477] or optical speckle patterns [478–480]. The latter is a random intensity pattern which is produced by the scattering of a coherent laser beam from a rough surface (see, e.g., [481] for a detailed discussion).

The theoretical and experimental investigations of ultracold atomic gases confined in disordered potentials pave the way for the study of fundamental effects in quantum systems. Among them, the most famous phenomenon is Anderson localization, i.e. localization and absence of diffusion of non-interacting quantum particles, which was originally predicted to occur in the context of electronic transport [482]. Other important effects include the realization

of Bose [483,484] or Fermi [485,486] glasses, quantum spin glasses [487], the Anderson–Bose glass and crossover between Anderson-glass to Bose-glass localization, and so on (see also the recent review [488]). Importantly, as we discuss below, there exist very recent relevant experimental results (and theoretical predictions) in these interesting directions.

The first experimental results concerning BECs confined in disordered potentials were reported almost simultaneously in 2005 [477–480]. In the first of these experiments [478], static and dynamic properties of a rubidium BEC were studied and it was found that both dipole and quadrupole oscillations are damped (the damping was found to be stronger as the speckle height was increased). The suppression of transport of the condensate in the presence of a random potential was also reported in [479,480]. In these works, a strong reduction of the mobility of atoms was demonstrated, as the 1D expansion of the elongated condensate along a magnetic [479] or an optical [480] guide was found to be strongly inhibited in the presence of the speckle potential. On the other hand, in [477] a speckle pattern was superimposed onto a regular 1D optical lattice and, thus, a genuine random potential was created. In this setting the possibility of observation of Anderson localization was analysed in detail, and the crossover from Anderson localization in the absence of interactions to the ‘screening regime’ (where nonlinear interactions suppress Anderson localization in the random potential) was investigated.

Although the above mentioned results underscore a disorder-induced trapping of the condensate, this effect does not correspond to a genuine Anderson localization: for the latter, the correlation length of the disorder has to be smaller than the size of the system (see discussion in [488]). Nevertheless, a detailed study [489] has shown that expansion of a quasi-2D cloud may lead to weak and even strong localization using currently available speckle patterns. Other works have revealed that Anderson localization may occur during transport processes in repulsive BECs [490–492]. In this case, however, and for condensates at equilibrium, the interaction-induced delocalization dominates disorder-induced localization, except for the case of weak interactions [493] (see also earlier work in [494]). Another possibility is Anderson localization of elementary excitations in interacting BECs, as analysed in the recent works [495,496]. Finally, it is worth also mentioning in passing parallel developments in this area, within the mathematically similar setting of photonic lattices, where Anderson localization and transition from ballistic to diffusive transport were recently observed in the presence of random fluctuations [497].

In any case, the above discussion shows that there exists an intense theoretical and experimental effort concerning this hot topic of BECs in disordered potentials. Although it seems that relevant experiments have just started, the perspectives are very promising: they include not only the possibility of the detection of Anderson localization but also other relevant effects, such as the observation of a Bose-glass phase [498] and the possibility of the appearance of a novel Lifshits-glass phase [499].

5.7. Beyond mean-field description

The GP equation has been extremely successful in describing a wide range of mean-field phenomena in Bose–Einstein condensation. By construction, as explained in detail in section 2, the GP equation is the mean-field description of the multibody quantum Hamiltonian describing the interaction of a dilute gas of bosonic atoms and it relies on two main assumptions: (a) collisions between atoms are approximated by hard sphere collisions with a Dirac delta interatomic potential, and (b) the gas is at absolute zero temperature where thermal effects are not present. Nonetheless, in many BEC settings, finite temperature effects and quantum fluctuations may play an important role. The main effect of finite temperature is due to the fact

that a part of the atomic cloud is not condensed (the so-called thermal cloud) and couples to the condensed cloud. A microscopic derivation of the mean-field operator for the gas of bosonic particles reveals that the (standard) condensate mean field is coupled to higher order mean fields (cf the insightful review in chapter 18 of [55] and references therein for more details). Neglecting the exchange of particles between condensed and non-condensed atoms and taking into account the three lowest mean-field orders, the so-called Hartree–Fock–Bogoliubov (HFB) theory, leads to the generalized GP equation for the condensate wavefunction $\psi(\mathbf{r}, t)$ [500–503]

$$i\hbar \frac{\partial}{\partial t} \psi(\mathbf{r}, t) = [H_{\text{GP}} + g [2n'(\mathbf{r}, t)]] \psi(\mathbf{r}, t) + \tilde{m}_0(\mathbf{r}, t) \psi^*(\mathbf{r}, t), \quad (158)$$

where $H_{\text{GP}} = -(1/2)\nabla^2 + V_{\text{ext}}(\mathbf{r}, t) + g|\psi|^2$ accounts for the ‘classical’ GP terms in non-dimensional units, $n'(\mathbf{r}, t)$ denotes the non-condensate density and $\tilde{m}_0(\mathbf{r}, t)$ the anomalous mean-field average [504–507]. Furthermore, taking into account that atomic collisions happen within the gas (and not in vacuum), one has to modify the interatomic interactions by a contact potential with a position-dependent amplitude: $g \rightarrow g[1 + \tilde{m}_0(\mathbf{r})/\psi^2(\mathbf{r})]$ [508–510].

A similar approach to the above is to consider the coupling with the thermal cloud by ignoring the anomalous average and including a local energy and momentum conservation [511, 512] that yields

$$i\hbar \frac{\partial}{\partial t} \psi(\mathbf{r}, t) = [H_{\text{GP}} + g [2n'(\mathbf{r}, t)] - iR(\mathbf{r}, t)] \psi(\mathbf{r}, t), \quad (159)$$

where the non-condensate density $n'(\mathbf{r}, t)$ is described in terms of a Wigner phase-space representation and a generalized Boltzmann quantum-hydrodynamical equation (see chapter 18 of [55]). This term includes collisions between non-condensed atoms and transfer to and from the condensed cloud. In equation (159), $R(\mathbf{r}, t)$ accounts for triplet correlations.

Other approaches to incorporate the thermal cloud include Stoof’s non-equilibrium theory based on quantum kinetic theory [513–516] and Gardiner–Zoller’s quantum kinetic master equation using techniques borrowed from quantum optics [517–523]. Also, efforts to include stochastic effects have been considered in [524] by considering the thermal cloud to be close enough to equilibrium that it can be described by a Bose cloud with chemical potential μ_T at temperature T . In fact, this approach leads, after neglecting noise terms, to the phenomenological damping included in the GP equation through the damped GP equation

$$i\hbar \frac{\partial}{\partial t} \psi(\mathbf{r}, t) = (1 - i\gamma) (H_{\text{GP}} - \mu_T) \psi(\mathbf{r}, t), \quad (160)$$

with damping rate $\gamma > 0$. This approach was originally proposed by Pitaevskii [525] and applied with a position-dependent loss rate in [526]. A similar phenomenological damping term (but on the left-hand side) has been used in [370, 371] to remove the excess energy to dynamically simulate the crystallization of vortex lattices in rapidly rotating BECs.

It is important to note that recently there has been a lot of activity on the study of formation, stability and dynamics of matter-wave solitons beyond the mean-field theory. In particular, in the case of attractive BECs, the velocity- and temperature-dependent frictional force and diffusion coefficient of a matter-wave bright soliton immersed in a thermal cloud was calculated in [116]. Moreover, the full set of time-dependent HFB equations was used in [527] to show that the matter flux from the condensate to the thermal cloud may cause the bright matter-wave solitons to split into two solitonic fragments (each of them is a mixture of the condensed and non-condensed particles); these may be viewed as partially *incoherent solitons*, similar to the ones known in the context of nonlinear optics [528, 529]. Partially incoherent *lattice solitons* at a finite temperature T were also predicted to exist in [530]; there, a numerical integration of the GP equation, starting with a random Bose distribution at finite T , revealed the generation of lattice solitons upon gradual switch-on of an optical lattice potential. In a more recent

study [531], the time-dependent HFB theory was used to find inter-gap and intra-gap partially incoherent solitons (composed, as in [527], by a condensed and a non-condensed part). On the other hand, in [532, 533], the so-called Zaremba–Nikuni–Griffin formalism [511] was used to analyse the dissipative dynamics of dark solitons in the presence of the thermal cloud, as observed in the Hannover experiment [32]. Finally, other quantum effects associated with matter-wave solitons have been considered as well; these include quantum depletion of dark solitons [534–537] (see also [115]), formation of a broken-symmetry bright matter-wave soliton by superpositions of quasi-degenerate many-body states [538], quantum-noise squeezing and quantum correlations of gap solitons [539], and so on.

Note added in proof:

A considerable volume of work in many of the directions mentioned in this review has continued to emerge both in preprint and in published form. As two examples thereof, we mention the work of [540–542] on various higher dimensional aspects of BECs in random potentials and transitions associated with Anderson localization (we thank Dr B Shapiro for bringing these works to our attention) and the intense experimental activity on the oscillations and interactions of dark and dark-bright solitons in [543, 544].

Acknowledgments

This review would simply not have existed without the invaluable contribution of our collaborators in many of the topics discussed here: Egor Alfimov, Brian Anderson, Alan Bishop, Lincoln Carr, Zhigang Chen, Fotis Diakonou, Peter Engels, David Hall, Todd Kapitula, Yannis Kevrekidis, Yuri Kivshar, Volodya Konotop, Boris Malomed, Kevin Mertes, Alex Nicolin, Hector Nistazakis, Markus Oberthaler, Dmitry Pelinovsky, Mason Porter, Nick Proukakis, Mario Salerno, Peter Schmelcher, Augusto Smerzi, Giorgos Theocharis and Andrea Trombettoni are greatly thanked. RCG and PGK both acknowledge support from NSF-DMS-0505663. PGK is also grateful to the NSF for support through the grants NSF-DMS-0619492 and NSF-CAREER. The work of DJF is partially supported by the Special Research Account of the University of Athens.

References

- [1] Bose S N 1924 *Z. Phys.* **26** 178
- [2] Einstein A 1924 *Sitzungsber. K. Preuss. Akad. Wiss., Phys. Math. Kl.* **261**
- [3] Einstein A 1925 *Sitzungsber. K. Preuss. Akad. Wiss., Phys. Math. Kl.* **3**
- [4] Griffin A, Snoke D W and Stringari S (ed) 1995 *Bose–Einstein Condensation* (Cambridge: Cambridge University Press)
- [5] Anderson M H J, Ensher J R, Matthews M R and Wieman C E 1995 *Science* **269** 198
- [6] Davis K B, Mewes M-O, Andrews M R, van Druten N J, Durfee D S, Kurn D M and Ketterle W 1995 *Phys. Rev. Lett.* **75** 3969
- [7] Bradley C C, Sackett C A, Tollett J J and Hulet R G 1995 *Phys. Rev. Lett.* **75** 1687
For a more systematic confirmation of Bose–Einstein condensation in lithium see also Bradley C C, Sackett C A, Tollett J J and Hulet R G 1997 *Phys. Rev. Lett.* **79** 1170 and references therein
- [8] Cornell E A and Wieman C E 2002 *Rev. Mod. Phys.* **74** 875
- [9] Ketterle W 2002 *Rev. Mod. Phys.* **74** 1131
- [10] Gross E P 1963 *J. Math. Phys.* **4** 195
- [11] Pitaevskii L P 1961 *Sov. Phys. JETP* **13** 451
- [12] Sulem C and Sulem P L 1999 *The Nonlinear Schrödinger Equation* (New York: Springer)
- [13] Dodd R K, Eilbeck J C, Gibbon J D and Morris H C 1983 *Solitons and Nonlinear Wave Equations* (New York: Academic)

- [14] Hasegawa A 1990 *Optical Solitons in Fibers* (Heidelberg: Springer)
- [15] Abdullaev F Kh, Darmanyan S A and Khabibullaev P K 1993 *Optical Solitons* (Heidelberg: Springer)
- [16] Hasegawa A and Kodama Y 1995 *Solitons in Optical Communications* (Oxford: Clarendon)
- [17] Kivshar Yu S and Agrawal G P 2003 *Optical Solitons: From Fibers to Photonic Crystals* (New York: Academic)
- [18] Infeld E and Rowlands G 1990 *Nonlinear Waves, Solitons and Chaos* (Cambridge: Cambridge University Press)
- [19] Ablowitz M J, Prinari B and Trubatch A D 2004 *Discrete and Continuous Nonlinear Schrödinger Systems* (Cambridge: Cambridge University Press)
- [20] Bourgain J 1999 *Global Solutions of Nonlinear Schrödinger Equations* (Providence, RI: American Mathematical Society)
- [21] Ablowitz M J and Segur H 1981 *Solitons and the Inverse Scattering Transform* (Philadelphia: SIAM)
- [22] Zakharov V E, Manakov S V, Nonikov S P and Pitaevskii L P 1984 *Theory of Solitons* (New York: Consultants Bureau)
- [23] Newell A C 1985 *Solitons in Mathematics and Physics* (Philadelphia, PA: SIAM)
- [24] van Saarloos W and Hohenberg P C 1992 *Physica D* **56** 303
- [25] Aranson I S and Kramer L 2002 *Rev. Mod. Phys.* **74** 99
- [26] Cross M C and Hohenberg P C 1993 *Rev. Mod. Phys.* **65** 851
- [27] Scott A 2003 *Nonlinear Science. Emergence and Dynamics of Coherent Structures* 2nd edn (Oxford: Oxford University Press)
- [28] Matthews M R, Anderson B P, Haljan P C, Hall D S, Wieman C E and Cornell E A 1999 *Phys. Rev. Lett.* **83** 2498
- [29] Williams J E and Holland M J 1999 *Nature* **568** 401
- [30] Denschlag J *et al* 2000 *Science* **287** 97
- [31] Dutton Z, Budde M, Slowe C and Hau L V 2001 *Science* **293** 663
- [32] Burger S, Bongs K, Dettmer S, Ertmer W, Sengstock K, Sanpera A, Shlyapnikov G V and Lewenstein M 1999 *Phys. Rev. Lett.* **83** 5198
- [33] Anderson B P, Haljan P C, Regal C A, Feder D L, Collins L A, Clark C W and Cornell E A 2001 *Phys. Rev. Lett.* **86** 2926
- [34] Engels P and Atherton C 2007 *Phys. Rev. Lett.* **99** 160405
- [35] Madison K W, Chevy F, Wohlleben W and Dalibard J 1999 *Phys. Rev. Lett.* **84** 806
- [36] Inouye S, Gupta S, Rosenband T, Chikkatur A P, Görlitz A, Gustavson T L, Leanhardt A E, Pritchard D E and Ketterle W 2001 *Phys. Rev. Lett.* **87** 080402
- [37] Abo-Shaer J R, Raman C, Vogels J M and Ketterle W 2001 *Science* **292** 476
- [38] Abo-Shaer J R, Raman C and Ketterle W 2002 *Phys. Rev. Lett.* **88** 070409
- [39] Engels P, Coddington I, Haljan P C and Cornell E A 2002 *Phys. Rev. Lett.* **89** 100403
- [40] Strecker K E, Partridge G B, Truscott A G and Hulet R G 2002 *Nature* **417** 150
- [41] Khaykovich L, Schreck F, Ferrari G, Bourdel T, Cubizolles J, Carr L D, Castin Y and Salomon C 2002 *Science* **296** 1290
- [42] Cornish S L, Thompson S T and Wieman C E 2006 *Phys. Rev. Lett.* **96** 170401
- [43] Strecker K E, Partridge G B, Truscott A G and Hulet R G 2003 *New J. Phys.* **5** 73
- [44] Eiermann B, Anker Th, Albiez M, Taglieber M, Treutlein P, Marzlin K P and Oberthaler M K 2004 *Phys. Rev. Lett.* **92** 230401
- [45] Parkins A S and Walls D F 1998 *Phys. Rep.* **303** 1
- [46] Dalfovo F, Giorgini S, Pitaevskii L P and Stringari S 1999 *Rev. Mod. Phys.* **71** 463
- [47] Leggett A J 2001 *Rev. Mod. Phys.* **73** 307
- [48] Fetter A L 2002 *J. Low Temp. Phys.* **129** 263
- [49] Andersen J O 2004 *Rev. Mod. Phys.* **76** 599
- [50] Bongs K and Sengstock K 2004 *Rep. Prog. Phys.* **67** 907
- [51] Lieb E H, Seiringer R, Solovej J P and Yngvason J 2005 *The Mathematics of the Bose Gas and its Condensation (Oberwolfach Seminar Series vol 34)* (Basle: Birkhaeuser) (Preprint arXiv:cond-mat/0610117)
- [52] Pethick C J and Smith H 2002 *Bose–Einstein Condensation in Dilute Gases* (Cambridge: Cambridge University Press)
- [53] Pitaevskii L P and Stringari S 2003 *Bose–Einstein Condensation* (Oxford: Oxford University Press)
- [54] Martellucci S, Chester A N and Aspect A 2000 *Bose–Einstein Condensates and Atom Lasers* (New York: Plenum)
- [55] Kevrekidis P G, Frantzeskakis D J and Carretero-González R (eds) 2007 *Emergent Nonlinear Phenomena in Bose–Einstein Condensates: Theory and Experiment (Springer Series on Atomic, Optical, and Plasma Physics vol 45)*

- [56] Bogoliubov N N 1947 *J. Phys. (Moscow)* **11** 23
- [57] Lieb E H, Seiringer R and Yngvason J 2000 *Phys. Rev. A* **61** 043602
- [58] Elgart A, Erdős L, Schlein B and Yau H T 2006 *Arch. Ration. Mech. Anal.* **179** 265
- [59] Weiner J 2003 *Cold and Ultracold Collisions in Quantum Microscopic and Mesoscopic Systems* (Cambridge: Cambridge University Press)
- [60] Moerdijk A J, Verhaar B J and Axelsson A 1995 *Phys. Rev. A* **51** 4852
- [61] Roberts J L, Claussen N R, Cornish S L and Wieman C E 2000 *Phys. Rev. Lett.* **85** 728
- [62] Inouye S, Andrews M R, Stenger J, Miesner H J, Stamper-Kurn D M and Ketterle W 1998 *Nature* **392** 151
- [63] Stenger J, Inouye S, Andrews M R, Miesner H-J, Stamper-Kurn D M and Ketterle W 1999 *Phys. Rev. Lett.* **82** 2422
- [64] Roberts J L, Claussen N R, Burke J P Jr, Greene C H, Cornell E A and Wieman C E 1998 *Phys. Rev. Lett.* **81** 5109
- [65] Cornish S L, Claussen N R, Roberts J L, Cornell E A and Wieman C E 2000 *Phys. Rev. Lett.* **85** 1795
- [66] Stamper-Kurn D M, Andrews M R, Chikkatur A P, Inouye S, Miesner H J, Stenger J and Ketterle W 1998 *Phys. Rev. Lett.* **80** 2027
- [67] Barrett M D, Sauer J A and Chapman M S 2001 *Phys. Rev. Lett.* **87** 010404
- [68] Weiner J, Bagnato V S, Zilio S and Julienne P S 1999 *Rev. Mod. Phys.* **71** 1
- [69] Grimm R, Weidemüller M and Ovchinnikov Y B 2000 *Adv. At. Mol. Opt. Phys.* **42** 95
- [70] Morsch O and Arimondo E 2002 *Dynamics and Thermodynamics of Systems with Long-Range Interactions* ed T Dauxois *et al* (Berlin: Springer) p 312
- [71] Bloch I 2005 *J. Phys. B: At. Mol. Opt. Phys.* **38** S629
Bloch I 2005 *Nature Phys.* **1** 23
- [72] Morsch O and Oberthaler M K 2006 *Rev. Mod. Phys.* **78** 179
- [73] Peil S, Porto J V, Tolra B L, Obrecht J M, King B E, Subbotin M, Rolston S L and Phillips W D 2003 *Phys. Rev. A* **67** 051603(R)
- [74] Andrews M R, Townsend C G, Miesner H-J, Durfee D S, Kurn D M and Ketterle W 1999 *Science* **275** 637
- [75] Albiez M, Gati R, Fölling J, Hunsmann S, Cristiani M and Oberthaler M K 2005 *Phys. Rev. Lett.* **95** 010402
- [76] Anderson B P and Kasevich M A 1998 *Science* **282** 1686
- [77] Folman R and Schmiedmayer J 2001 *Nature* **413** 466
- [78] Hänsel W, Hommelhoff P, Hänsch T W and Reichel J 2001 *Nature (London)* **413** 501
- [79] Ott H, Fortagh J, Schlotterbeck G, Grossmann A and Zimmermann C 2001 *Phys. Rev. Lett.* **87** 230401
- [80] Folman R, Krueger P, Schmiedmayer J, Denschlag J and Henkel C 2002 *Adv. At. Mol. Opt. Phys.* **48** 263
- [81] Gerton J M, Strelakov D, Prodan I and Hulet R G 2000 *Nature* **408** 692
- [82] Donley E A, Claussen N R, Cornish S L, Roberts J L, Cornell E A and Wieman C E 2001 *Nature* **412** 295
- [83] Ruprecht P A, Holland M J, Burnett K and Clark C W 1995 *Phys. Rev. A* **51** 4704
- [84] Pérez-García V M, Michinel H and Herrero H 1998 *Phys. Rev. A* **57** 3837
- [85] Gammal A, Frederico T and Tomio L 2001 *Phys. Rev. A* **64** 055602
- [86] Gammal A, Frederico T and Tomio L 2002 *Phys. Rev. A* **66** 043619
- [87] Theocharis G, Rapti Z, Kevrekidis P G, Frantzeskakis D J and Konotop V V 2003 *Phys. Rev. A* **67** 063610
- [88] Salasnich L, Parola A and Reatto L 2003 *Phys. Rev. Lett.* **91** 080405
- [89] Carr L D and Brand J 2004 *Phys. Rev. A* **70** 033607
- [90] Kevrekidis P G and Frantzeskakis D J 2004 *Mod. Phys. Lett. B* **18** 173
- [91] Abdullaev F Kh, Gammal A, Kamchatnov A M and Tomio L 2005 *Int. J. Mod. Phys. B* **19** 3415
- [92] Petrov D S, Shlyapnikov G V and Walraven J T M 2000 *Phys. Rev. Lett.* **85** 3745
- [93] Petrov D S, Shlyapnikov G V and Walraven J T M 2001 *Phys. Rev. Lett.* **87** 050404
- [94] Andersen J O, Al Khawaja U and Stoof H T C 2002 *Phys. Rev. Lett.* **88** 070407
- [95] Al Khawaja U, Andersen J O, Proukakis N P and Stoof H T C 2002 *Phys. Rev. A* **66** 013615
- [96] Luxat D L and Griffin A 2003 *Phys. Rev. A* **67** 043603
- [97] Al Khawaja U, Proukakis N P, Andersen J O, Romans M W J and Stoof H T C 2003 *Phys. Rev. A* **68** 043603
- [98] Mora C and Castin Y 2003 *Phys. Rev. A* **67** 053615
- [99] Görlitz A *et al* 2001 *Phys. Rev. Lett.* **87** 130402
- [100] Greiner M, Bloch I, Mandel O, Hänsch T W and Esslinger T 2001 *Phys. Rev. Lett.* **87** 160405
- [101] Burger S, Cataliotti F S, Fort C, Maddaloni P, Minardi F and Inguscio M 2002 *Europhys. Lett.* **57** 1
- [102] Cataliotti F S, Burger S, Fort C, Maddaloni P, Minardi F, Trombettoni A, Smerzi A and Inguscio M 2001 *Science* **293** 843
- [103] Denschlag J H, Simsarian J E, Haffner H, McKenzie C, Browaeys A, Cho D, Helmerson K, Rolston S L and Phillips W D 2002 *J. Phys. B: At. Mol. Opt. Phys.* **35** 3095
- [104] Jackson A D, Kavoulakis G M and Pethick C J 1998 *Phys. Rev. A* **58** 2417

- [105] Kivshar Yu S, Alexander T J and Turitsyn S K 2001 *Phys. Lett. A* **278** 225
- [106] Konotop V V and Salerno M 2002 *Phys. Rev. A* **65** 021602
- [107] Abdullaev F Kh, Kamchatnov A M, Konotop V V and Brazhnyi V A 2003 *Phys. Rev. Lett.* **90** 230402
- [108] Abdallah N B, Méhats F, Schmeiser C and Weishäupl R M 2005 *SIAM J. Math. Anal.* **37** 189
- [109] Zakharov V E and Shabat A B 1971 *Zh. Eksp. Teor. Fiz.* **61** 118
Zakharov V E and Shabat A B 1971 *Sov. Phys. JETP* **34** 62
- [110] Kaup D J 1976 *J. Math. Phys.* **16** 2036
- [111] Zakharov E V and Shabat A B 1973 *Zh. Eksp. Teor. Fiz.* **64** 1627
Zakharov E V and Shabat A B 1973 *Sov. Phys. JETP* **37** 823
- [112] Uzunov I M and Gerdjikov V S 1993 *Phys. Rev. A* **47** 1582
- [113] Barashenkov I V and Panova E Y 1993 *Physica D* **69** 114
- [114] Kivshar Yu S and Yang X 1994 *Phys. Rev. E* **49** 1657
- [115] Muryshev A E, Shlyapnikov G V, Ertmer W, Sengstock K and Lewenstein M 2002 *Phys. Rev. Lett.* **89** 110401
- [116] Sinha S, Cherny A Y, Kovrizhin D and Brand J 2006 *Phys. Rev. Lett.* **96** 030406
- [117] Khaykovich L and Malomed B A 2006 *Phys. Rev. A* **74** 023607
- [118] Muñoz Mateo A and Delgado V 2007 *Phys. Rev. A* **75** 063610
- [119] Muñoz Mateo A and Delgado V 2008 *Phys. Rev. A* **77** 013617
- [120] Gerbier F 2004 *Europhys. Lett.* **66** 771
- [121] Salasnich L, Parola A and Reatto L 2002 *Phys. Rev. A* **65** 043614
- [122] Band Y B, Towers I and Malomed B A 2003 *Phys. Rev. A* **67** 023602
- [123] Kamchatnov A M and Shchesnovich V 2004 *Phys. Rev. A* **70** 023604
- [124] Massignan P and Modugno M 2003 *Phys. Rev. A* **67** 023614
- [125] Zhang W and You L 2005 *Phys. Rev. A* **71** 025603
- [126] Salasnich L, Parola A and Reatto L 2004 *Phys. Rev. A* **69** 045601
- [127] Nicolin A I, Carretero-González R and Kevrekidis P G 2007 *Phys. Rev. A* **76** 063609
- [128] Moerdijk A J, Boesten H M J M and Verhaar B J 1996 *Phys. Rev. A* **53** 916
- [129] Köhler T 2002 *Phys. Rev. Lett.* **89** 210404
- [130] Abdullaev F Kh, Gammal A, Tomio L and Frederico T 2001 *Phys. Rev. A* **63** 043604
- [131] Kagan Yu, Muryshev A E and Shlyapnikov G V 1988 *Phys. Rev. Lett.* **81** 933
- [132] Saito H and Ueda M 2001 *Phys. Rev. Lett.* **86** 1406
- [133] Leung V Y F, Truscott A G and Baldwin K G H 2002 *Phys. Rev. A* **66** 061602
- [134] Zhang W, Wright E M, Pu H and Meystre P 2003 *Phys. Rev. A* **68** 023605
- [135] Abdullaev F Kh and Salerno M 2005 *Phys. Rev. A* **72** 033617
- [136] Zhang A X and Xue J K 2007 *Phys. Rev. A* **75** 013624
- [137] Abdullaev F Kh, Bouketir A, Messikh A and Umarov B A 2007 *Physica D* **232** 54
- [138] Rapti Z, Kevrekidis P G, Frantzeskakis D J and Malomed B A 2004 *Phys. Scripta* **T113** 74
- [139] Dunjko V, Lorent V and Olshanii M 2001 *Phys. Rev. Lett.* **86** 5413
- [140] Tonks L 1936 *Phys. Rev.* **50** 955
- [141] Girardeau M 1960 *J. Math. Phys.* **1** 516
- [142] Paredes B, Widera A, Murg V, Mandel O, Fölling S, Cirac I, Shlyapnikov G V, Hänsch T W and Bloch I 2004 *Nature* **429** 277
- [143] Kinoshita T, Wenger T and Weiss D S 2004 *Science* **305** 1125
- [144] Moritz H, Stöferle T, Köhl M and Esslinger T 2003 *Phys. Rev. Lett.* **91** 250402
- [145] Laburthe B Tolra, O'Hara K M, Huckans J H, Phillips W D, Rolston S L and Porto J V 2004 *Phys. Rev. Lett.* **92** 190401
- [146] Lieb E H and Liniger W 1963 *Phys. Rev.* **130** 1605
- [147] Öhberg P and Santos L 2002 *Phys. Rev. Lett.* **89** 240402
- [148] Brand J 2004 *J. Phys. B: At. Mol. Opt. Phys.* **37** S287
- [149] Salasnich L, Parola A and Reatto L 2005 *Phys. Rev. A* **72** 025602
- [150] Frantzeskakis D J, Kevrekidis P G and Proukakis N P 2007 *Phys. Lett. A* **364** 129
- [151] Kolomeisky E B, Newman T J, Straley J P and Qi X 2000 *Phys. Rev. Lett.* **85** 1146
- [152] Kolomeisky E B and Straley J P 1992 *Phys. Rev. B* **46** 11749
- [153] Tanatar B 2000 *Europhys. Lett.* **51** 261
- [154] Lee M D, Morgan S A, Davis M J and Burnett K 2002 *Phys. Rev. A* **65** 043617
- [155] Kim Y E and Zubarev A L 2003 *Phys. Rev. A* **67** 015602
- [156] Lieb E H, Seiringer R and Yngvason J 2003 *Phys. Rev. Lett.* **91** 150401
- [157] Girardeau M D and Wright E M 2000 *Phys. Rev. Lett.* **84** 5691
- [158] Minguzzi A, Vignolo P, Chiofalo M L and Tosi M P 2001 *Phys. Rev. A* **64** 033605

- [159] Frantzeskakis D J, Proukakis N P and Kevrekidis P G 2004 *Phys. Rev. A* **70** 015601
- [160] Ögren M, Kavoulakis G M and Jackson A D 2005 *Phys. Rev. A* **72** 021603(R)
- [161] Brazhnyi V A, Konotop V V and Pitaevskii L P 2006 *Phys. Rev. A* **73** 053601
- [162] Jordan D W and Smith P 1977 *Nonlinear Ordinary Differential Equations* (Oxford: Clarendon)
- [163] Wu B and Niu Q 2000 *Phys. Rev. A* **61** 023402
- [164] Bronski J C, Carr L D, Deconinck B and Kutz J N 2001 *Phys. Rev. Lett.* **86** 1402
- [165] Wu B, Diener R B and Niu Q 2002 *Phys. Rev. A* **65** 025601
- [166] Diakonov D, Jensen L M, Pethick C J and Smith H 2002 *Phys. Rev. A* **66** 013604
- [167] Machholm M, Pethick C J and Smith H 2002 *Phys. Rev. A* **67** 053613
- [168] Louis P J Y, Ostrovskaya E A, Savage C M and Kivshar Y S 2003 *Phys. Rev. A* **67** 013602
- [169] Machholm M, Nicolin A, Pethick C J and Smith H 2004 *Phys. Rev. A* **69** 043604
- [170] Seaman B T, Carr L D and Holland M J 2005 *Phys. Rev. A* **72** 033602
- [171] de Sterke C M and Sipe J E 1988 *Phys. Rev. A* **38** 5149
- [172] Steel M and Zhang W 1998 *Preprint cond-mat/9810284*
- [173] Baizakov B B, Konotop V V and Salerno M 2002 *J. Phys. B: At. Mol. Opt. Phys.* **35** 5105
- [174] Sakaguchi H and Malomed B A 2005 *Math. Comput. Simul.* **69** 492
- [175] Brazhnyi V A and Konotop V V 2004 *Mod. Phys. Lett. B* **18** 627
- [176] Pu H, Baksmaty L O, Zhang W, Bigelow N P and Meystre P 2003 *Phys. Rev. A* **67** 043605
- [177] Ostrovskaya E A and Kivshar Yu S 2004 *Phys. Rev. Lett.* **93** 160405
- [178] Ostrovskaya E A, Alexander T J and Kivshar Yu S 2006 *Phys. Rev. A* **74** 023605
- [179] Christodoulides D N and Joseph R I 1989 *Phys. Rev. Lett.* **62** 1746
- [180] Zobay O, Pötting S, Meystre P and Wright E M 1999 *Phys. Rev. A* **59** 643
- [181] Efremidis N K and Christodoulides D N 2003 *Phys. Rev. A* **67** 063608
- [182] Yulin A V and Skryabin D V 2003 *Phys. Rev. A* **67** 023611
- [183] Porter M A, Chugunova M and Pelinovsky D E 2006 *Phys. Rev. E* **74** 036610
- [184] Abdullaev F Kh, Abdumalikov A and Galimzyanov R 2007 *Phys. Lett. A* **367** 149
- [185] Agueev D and Pelinovsky D E 2005 *SIAM J. Appl. Math.* **65** 1101
- [186] Kevrekidis P G, Rasmussen K Ø and Bishop A R 2001 *Int. J. Mod. Phys. B* **15** 2833
- [187] Trombettoni A and Smerzi A 2001 *Phys. Rev. Lett.* **86** 2353
- [188] Abdullaev F Kh, Baizakov B B, Darmanyany S A, Konotop V V and Salerno M 2001 *Phys. Rev. A* **64** 043606
- [189] Alfimov E G, Kevrekidis P G, Konotop V V and Salerno M 2002 *Phys. Rev. E* **66** 046608
- [190] Malomed B A 2002 *Progress in Optics* vol 43 ed E Wolf (Amsterdam: North-Holland) p 71
- [191] Pérez-García V M, Michinel H, Cirac J I, Lewenstein M and Zoller P 1996 *Phys. Rev. Lett.* **77** 5320
- [192] Baizakov B B, Malomed B A and Salerno M 2003 *Europhys. Lett.* **63** 642
- [193] Saito H and Ueda M 2003 *Phys. Rev. Lett.* **90** 040403
- [194] Malomed B A 2006 *Soliton Management in Periodic Systems* (New York: Springer)
- [195] Kaup D J and Lakoba T I 1996 *J. Math. Phys.* **37** 3442
- [196] Kaup D J and Vogel T K 2007 *Phys. Lett. A* **362** 289
- [197] Pérez-García V M, Montesinos G D and Torres P 2007 *SIAM J. Appl. Math.* **67** 990
- [198] Kohn W 1961 *Phys. Rev.* **123** 1242
- [199] García-Ripoll J J and Pérez-García V M 1999 *Phys. Rev. A* **59** 2220
- [200] Espinoza P B 2000 *Preprint math-ph/0002005*
- [201] García-Ripoll J J, Pérez-García V M and Torres P 1999 *Phys. Rev. Lett.* **83** 1715
- [202] Kevrekidis P G, Bishop A R and Rasmussen K Ø 2000 *J. Low Temp. Phys.* **120** 205
- [203] Montesinos G D, Pérez-García V M and Torres P J 2004 *Physica D* **191** 193
- [204] Herring G, Kevrekidis P G, Williams F, Christodoulakis T and Frantzeskakis D J 2007 *Phys. Lett. A* **367** 140
- [205] Frölich J, Fustafson S, Jonsson B L G and Sigal I M 2004 *Commun. Math. Phys.* **250** 613
- [206] Abdullaev F 1994 *Theory of Solitons in Inhomogeneous Media* (Chichester: Wiley)
- [207] Gorshkov K A and Ostrovsky L A 1981 *Physica D* **3** 428
- [208] Pérez-García V M, Torres P J and Konotop V V 2006 *Physica D* **221** 31
- [209] Ghosh P K 2003 *Phys. Lett. A* **308** 411
- [210] Rybin A V, Varzugin G G, Lindberg M, Timonen J and Bullough R K 2000 *Phys. Rev. E* **62** 6224
- [211] Belmonte-Beitia J, Pérez-García V M, Vekslerchik V and Torres P J 2007 *Phys. Rev. Lett.* **98** 064102
- [212] Golubitsky M and Schaeffer D G 1985 *Singularities and Groups in Bifurcation Theory* (New York: Springer)
- [213] Kapitula T and Kevrekidis P G 2005 *Chaos* **15** 037114
- [214] Kevrekidis P G, Konotop V V, Rodrigues A and Frantzeskakis D J 2005 *J. Phys. B: At. Mol. Opt. Phys.* **38** 1173
- [215] Alfimov G L and Zezyulin D A 2007 *Nonlinearity* **20** 2075–92

- [216] Kivshar Yu S and Alexander T J 1999 *Proc. APCTP-Nankai Symp. on Yang–Baxter Systems, Nonlinear Models and Their Applications* ed Q-Han Park *et al* (Singapore: World Scientific)
- [217] Kapitula T, Kevrekidis P G and Sandstede B 2004 *Physica D* **195** 263
see also addendum Kapitula T, Kevrekidis P G and Sandstede B 2005 *Physica D* **201** 199
- [218] Grillakis M 1988 *Commun. Pure Appl. Math.* **41** 745
- [219] Grillakis M 1990 *Commun. Pure Appl. Math.* **43** 299
- [220] Grillakis M, Shatah J and Strauss W 1987 *J. Funct. Anal.* **74** 160
- [221] Grillakis M, Shatah J and Strauss W 1990 *J. Funct. Anal.* **94** 308
- [222] Pelinovsky D E 2005 *Proc. R. Soc. Lond A* **461** 783
- [223] Kapitula T and Kevrekidis P G 2005 *Nonlinearity* **18** 2491
- [224] Theocharis G, Kevrekidis P G, Frantzeskakis D J and Schmelcher P 2006 *Phys. Rev. E* **74** 056608
- [225] Kirr E W, Kevrekidis P G, Shlizerman E and Weinstein M I 2008 *SIAM J. Math. Anal.* at press (*Preprint nlin.PS/0702038*)
- [226] Kevrekidis P G, Chen Z, Malomed B A, Frantzeskakis D J and Weinstein M I 2005 *Phys. Lett. A* **340** 275
- [227] Raghavan S, Smerzi A, Fantoni S and Shenoy S R 1999 *Phys. Rev. A* **59** 620
- [228] Ostrovskaya E A, Kivshar Y S, Lisak M, Hall B, Cattani F and Anderson D 2000 *Phys. Rev. A* **61** 031601(R)
- [229] Ananikian D and Bergeman T 2006 *Phys. Rev. A* **73** 013604
- [230] Kapitula T, Kevrekidis P G and Chen Z 2006 *SIAM J. Appl. Dyn. Sys.* **5** 598
- [231] Pelinovsky D E and Kevrekidis P G 2007 *Preprint* 0705.1016 [cond-mat]
- [232] Kapitula T, Kevrekidis P G and Carretero-González R 2007 *Physica D* **233** 112
- [233] Kapitula T and Kevrekidis P G 2004 *J. Phys. A: Math. Gen.* **37** 7509
- [234] Kapitula T 2001 *Physica D* **156** 186
- [235] Rapti Z, Kevrekidis P G, Konotop V V, Jones C K R T 2007 *J. Phys. A: Math. Theor.* **40** 14151
- [236] Porter M A and Kevrekidis P G 2005 *SIAM J. Appl. Dyn. Sys.* **4** 783
- [237] Niarchou P, Theocharis G, Kevrekidis P G, Schmelcher P and Frantzeskakis D J 2007 *Phys. Rev. A* **76** 023615
- [238] Fibich G, Sivan Y and Weinstein M I 2006 *Physica D* **217** 31
- [239] Sivan Y, Fibich G and Weinstein M I 2006 *Phys. Rev. Lett.* **97** 193902
- [240] Fibich G and Wang X 2003 *Physica D* **175** 96
- [241] Pelinovsky D E, Kevrekidis P G and Frantzeskakis D J 2003 *Phys. Rev. Lett.* **91** 240201
- [242] Pelinovsky D E, Kevrekidis P G, Frantzeskakis D J and Zharnitsky V 2004 *Phys. Rev. E* **70** 047604
- [243] Zharnitsky V and Pelinovsky D 2005 *Chaos* **15** 037105
- [244] Kevrekidis P G, Pelinovsky D E and Stefanov A 2006 *J. Phys. A: Math. Gen.* **39** 479
- [245] Di Menza L and Gallo C 2007 *Nonlinearity* **20** 461
- [246] Pelinovsky D E and Kevrekidis P G 2006 *Preprint* cond-mat/0610881
- [247] Barashenkov I V 1996 *Phys. Rev. Lett.* **77** 1193
- [248] de Bouard A 1995 *SIAM J. Math. Anal.* **26** 566
- [249] Karpman V I and Maslov E M 1978 *Zh. Eksp. Teor. Fiz.* **75** 504
Karpman V I and Maslov E M 1978 *Sov. Phys. JETP* **48** 252
- [250] Karpman V I 1979 *Phys. Scr.* **20** 462
- [251] Kaup D J and Newell A C 1978 *Proc. R. Soc. Lond. A* **361** 413
- [252] Kodama Y and Ablowitz M J 1981 *Stud. Appl. Math.* **24** 225
- [253] Kivshar Yu S and Malomed B A 1989 *Rev. Mod. Phys.* **61** 763
- [254] Kosevich A M 1981 *Physica D* **41** 253
- [255] Scharf R and Bishop A R 1993 *Phys. Rev. E* **47** 1375
- [256] Al Khawaja U, Stoof H T C, Hulet R G, Strecker K E and Partridge G B 2002 *Phys. Rev. Lett.* **89** 200404
- [257] Kevrekidis P G, Frantzeskakis D J, Carretero-González R, Malomed B A, Herring G and Bishop A R 2005 *Phys. Rev. A* **71** 023614
- [258] Frantzeskakis D J, Theocharis G, Diakonou F K, Schmelcher P and Kivshar Yu S 2002 *Phys. Rev. A* **66** 053608
- [259] Busch Th and Anglin J R 2000 *Phys. Rev. Lett.* **84** 2298
- [260] Huang G, Szeftel J and Zhu S 2002 *Phys. Rev. A* **65** 053605
- [261] Konotop V V and Pitaevskii L 2003 *Phys. Rev. Lett.* **93** 240403
- [262] Theocharis G, Schmelcher P, Oberthaler M K, Kevrekidis P G and Frantzeskakis D J 2005 *Phys. Rev. A* **72** 023609
- [263] Pelinovsky D E, Frantzeskakis D J and Kevrekidis P G 2005 *Phys. Rev. E* **72** 016615
- [264] Theocharis G, Frantzeskakis D J, Kevrekidis P G, Malomed B A and Kivshar Yu S 2003 *Phys. Rev. Lett.* **90** 120403
- [265] Jeffrey A and Kawahara T 1982 *Asymptotic Methods in Nonlinear Wave Theory* (Boston, MA: Pitman)
- [266] Zakharov V E and Kuznetsov E A 1986 *Physica D* **18** 445

- [267] Kivshar Yu S and Afanasjev V V 1991 *Phys. Rev. A* **44** R1446
- [268] Bass F G, Konotop V V and Puzenko S A 1992 *Phys. Rev. A* **46** 4185
- [269] Frantzeskakis D J 1996 *J. Phys. A: Math. Gen.* **29** 3631
- [270] Asano N 1974 *Prog. Theor. Phys. Suppl.* **55** 52
- [271] Ko K and Kuehl H H 1978 *Phys. Rev. Lett.* **40** 233
- [272] Karpman I V and Maslov E M 1982 *Phys. Fluids* **25** 1686
- [273] Huang G, Velarde M G and Makarov V A 2001 *Phys. Rev. A* **64** 013617
- [274] Huang G, Makarov V A and Velarde M G 2003 *Phys. Rev. A* **67** 023604
- [275] Huang G, Deng L and Hang C 2005 *Phys. Rev. E* **72** 036621
- [276] Aguero M, Frantzeskakis D J and Kevrekidis P G 2006 *J. Phys. A: Math. Gen.* **39** 7705
- [277] MacKay R S and Aubry S 1994 *Nonlinearity* **7** 1623
- [278] Alfimov G L, Brazhnyi V A and Konotop V V 2004 *Physica D* **194** 127
- [279] Levy H and Lessman F 1992 *Finite Difference Equations* (New York: Dover)
- [280] Pelinovsky D E, Kevrekidis P G and Frantzeskakis D J 2005 *Physica D* **212** 1
- [281] Pelinovsky D E, Kevrekidis P G and Frantzeskakis D J 2005 *Physica D* **212** 20
- [282] Lukas M, Pelinovsky D E and Kevrekidis P G 2008 *Physica D* **237** 339–50
- [283] Kevrekidis P G and Pelinovsky D E 2006 *Proc. R. Soc. A* **462** 2671
- [284] Alexander T J, Sukhorukov A A and Kivshar Yu S 2004 *Phys. Rev. Lett.* **93** 063901
- [285] Malomed B A and Kevrekidis P G 2001 *Phys. Rev. E* **64** 026601
- [286] Kevrekidis P G, Malomed B A, Chen Z and Frantzeskakis D J 2004 *Phys. Rev. E* **70** 056612
- [287] Neshev D N, Alexander T J, Ostrovskaya E A, Kivshar Yu S, Martin H, Makasyuk I and Chen Z 2004 *Phys. Rev. Lett.* **92** 123903
- [288] Fleischer J W, Bartal G, Cohen O, Manela O, Segev M, Hudock J and Christodoulides D N 2004 *Phys. Rev. Lett.* **92** 123904
- [289] Myatt C J, Burt E A, Ghrist R W, Cornell E A and Wieman C E 1997 *Phys. Rev. Lett.* **78** 586
- [290] Stenger J, Inouye S, Stamper-Kurn D M, Miesner H-J, Chikkatur A P and Ketterle W 1998 *Nature* **396** 345
- [291] Modugno G, Ferrari G, Roati G, Brecha R J, Simoni A and Inguscio M 2001 *Science* **294** 1320
- [292] DeMarco B and Jin D S 1999 *Science* **285** 1703
- [293] O'Hara K M, Hemmer S L, Gehm M E, Granade S R and Thomas J E 2002 *Science* **298** 2179
- [294] Strecker K E, Partridge G B and Hulet R G 2003 *Phys. Rev. Lett.* **91** 080406
- [295] Partridge G B, Li W, Liao Y A, Hulet R G, Haque M, Stoof H T C 2006 *Phys. Rev. Lett.* **97** 190407
- [296] Ballagh R J, Burnett K and Scott T F 1997 *Phys. Rev. Lett.* **78** 1607
- [297] Amoruso A, Meccoli I, Minguzzi A and Tosi M P 2000 *Eur. Phys. J. D* **8** 361
- [298] Roth R and Feldmeier H 2001 *J. Phys. B: At. Mol. Opt. Phys.* **34** 4629
- [299] Capuzzi P, Minguzzi A and Tosi M P 2003 *Phys. Rev. A* **67** 053605
- [300] Mineev V P 1974 *Zh. Eksp. Teor. Fiz.* **67** 263
Mineev V P 1974 *Sov. Phys. JETP* **40** 132
- [301] Hall D S, Matthews M R, Ensher J R, Wieman C E and Cornell E A 1998 *Phys. Rev. Lett.* **81** 1539
- [302] Pu H and Bigelow N P 1998 *Phys. Rev. Lett.* **80** 1130
- [303] Ho T-L and Shenoy V B 1996 *Phys. Rev. Lett.* **77** 3276
- [304] Esry B D, Greene C H, Burke J P Jr and Bohn J L 1997 *Phys. Rev. Lett.* **78** 3594
- [305] Pu H and Bigelow N P 1998 *Phys. Rev. Lett.* **80** 1134
- [306] Busch Th, Cirac J I, Pérez-García V M and Zoller P 1997 *Phys. Rev. A* **56** 2978
- [307] Graham R and Walls D 1998 *Phys. Rev. A* **57** 484
- [308] Esry B D and Greene C H 1998 *Phys. Rev. A* **57** 1265
- [309] Busch Th and Anglin J R 2001 *Phys. Rev. Lett.* **87** 010401
- [310] Öhberg P and Santos L 2001 *Phys. Rev. Lett.* **86** 2918
- [311] Kevrekidis P G, Nistazakis H E, Frantzeskakis D J, Malomed B A and Carretero-González R 2004 *Eur. Phys. J. D* **28** 181
- [312] Kevrekidis P G, Susanto H, Carretero-González R, Malomed B A and Frantzeskakis D J 2005 *Phys. Rev. E* **72** 066604
- [313] Deconinck B, Kevrekidis P G, Nistazakis H E and Frantzeskakis D J 2004 *Phys. Rev. A* **70** 063605
- [314] Porter M A, Kevrekidis P G and Malomed B A 2004 *Physica D* **196** 106
- [315] Trippenbach M, Goral K, Rzazewski K, Malomed B and Band Y B 2000 *J. Phys. B: At. Mol. Opt. Phys.* **33** 4017
- [316] Coen S and Haelterman M 2001 *Phys. Rev. Lett.* **87** 140401
- [317] Öhberg P and Stenholm S 1998 *Phys. Rev. A* **57** 1272
- [318] Esry B D and Greene C H 1999 *Phys. Rev. A* **59** 1457

- [319] Svidzinsky A A and Chui S T 2003 *Phys. Rev. A* **68** 013612
- [320] Malomed B A, Nistazakis H E, Frantzeskakis D J and Kevrekidis P G 2004 *Phys. Rev. A* **70** 043616
- [321] Malomed B A, Nistazakis H E, Kevrekidis P G and Frantzeskakis D J 2005 *Math. Comput. Simul.* **69** 400
- [322] Mertes K M, Merrill J, Carretero-González R, Frantzeskakis D J, Kevrekidis P G and Hall D S 2007 *Phys. Rev. Lett.* **99** 190402
- [323] Williams J, Walser R, Cooper J, Cornell E and Holland M 1999 *Phys. Rev. A* **59** 31(R)
- [324] Öhberg P and Stenholm S 1999 *Phys. Rev. A* **59** 3890
- [325] Son D T and Stephanov M A 2002 *Phys. Rev. A* **65** 063621
- [326] Jenkins S D and Kennedy T A B 2003 *Phys. Rev. A* **68** 053607
- [327] Park Q H and Eberly J H 2004 *Phys. Rev. A* **70** 021602(R)
- [328] Akhmediev N and Soto-Crespo J M 1994 *Phys. Rev. E* **4** 4519
- [329] Malomed B A, Skinner I M, Chu P L and Peng G D 1996 *Phys. Rev. E* **53** 4084
- [330] Mak W, Malomed B A and Chu P L 1997 *Phys. Rev. E* **55** 6134
- [331] Mak W, Malomed B A and Chu P L 1998 *Phys. Rev. E* **57** 1092
- [332] Mak W, Malomed B A and Chu P L 1998 *J. Opt. Soc. Am. B* **15** 1685
- [333] Albuch L and Malomed B A 2007 *Math. Comput. Simul.* **74** 312
- [334] Merhasin I M, Malomed B A and Driben R 2005 *J. Phys. B: At. Mol. Opt. Phys.* **38** 877
- [335] Chang M-S, Hamley C D, Barrett M D, Sauer J A, Fortier K M, Zhang W, You L and Chapman M S 2004 *Phys. Rev. Lett.* **92** 140403
- [336] Nistazakis H E, Frantzeskakis D J, Kevrekidis P G, Malomed B A, Carretero-González R and Bishop A R 2007 *Phys. Rev. A* **76** 063603
- [337] Leanhardt A E, Shin Y, Kielpinski D, Pritchard D E and Ketterle W 2003 *Phys. Rev. Lett.* **90** 140403
- [338] Ieda J, Miyakawa T and Wadati M 2004 *Phys. Rev. Lett.* **93** 194102
- [339] Ieda J, Miyakawa T and Wadati M 2004 *J. Phys. Soc. Japan.* **73** 2996
- [340] Li L, Li Z, Malomed B A, Mihalache D and Liu W M 2005 *Phys. Rev. A* **72** 033611
- [341] Zhang W, Müstecaplioglu Ö E and You L 2007 *Phys. Rev. A* **75** 043601
- [342] Uchiyama M, Ieda J and Wadati M 2006 *J. Phys. Soc. Japan.* **75** 064002
- [343] Dabrowska Büster J-W, Ostrovskaya E A, Alexander T J and Kivshar Y S 2007 *Phys. Rev. A* **75** 023617
- [344] Nistazakis H E, Frantzeskakis D J, Kevrekidis P G, Malomed B A and Carretero-González R 2008 *Phys. Rev. A* **77** 033612
- [345] Fetter A L and Svidzinsky A A 2001 *J. Phys.: Condens. Matter* **13** R135
- [346] Kevrekidis P G, Carretero-González R, Frantzeskakis D J and Kevrekidis I G 2004 *Mod. Phys. Lett. B* **18** 1481
- [347] Williams J E and Holland M J 1999 *Nature* **401** 568
- [348] Recati A, Zambelli F and Stringari S 2001 *Phys. Rev. Lett.* **86** 377
- [349] Sinha S and Castin Y 2001 *Phys. Rev. Lett.* **87** 190402
- [350] Madison K W, Chevy F, Bretin V and Dalibard J 2001 *Phys. Rev. Lett.* **86** 4443
- [351] Raman C, Abo-Shaer J R, Vogels J M, Xu K and Ketterle W 2001 *Phys. Rev. Lett.* **87** 210402
- [352] Frisch T, Pomeau Y and Rica S 1992 *Phys. Rev. Lett.* **69** 1644
- [353] Hakim V 1997 *Phys. Rev. E* **55** 2835
- [354] Jackson B, McCann J F and Adams C S 1998 *Phys. Rev. Lett.* **80** 3903
- [355] Jackson B, McCann J F and Adams C S 2000 *Phys. Rev. A* **61** 051603(R)
- [356] Winiecki T, McCann J F and Adams C S 1999 *Phys. Rev. Lett.* **82** 5186
- [357] Jackson B, McCann J F and Adams C S 2000 *Phys. Rev. A* **61** 013604
- [358] Carretero-González R, Kevrekidis P G, Frantzeskakis D J, Malomed B A, Nandi S and Bishop A R 2007 *Math. Comput. Simul.* **74** 361
- [359] Susanto H, Kevrekidis P G, Carretero-González R, Malomed B A, Frantzeskakis D J and Bishop A R 2007 *Phys. Rev. A* **75** 055601
- [360] Scherer D R, Weiler C N, Neely T W and Anderson B P 2007 *Phys. Rev. Lett.* **98** 110402
- [361] Whitaker N, Kevrekidis P G, Carretero-González R, Frantzeskakis D J 2008 *Phys. Rev. Lett.* **77** 023605
- [362] Carretero-González R, Anderson B P, Kevrekidis P G, Frantzeskakis D J and Weiler C N 2008 *Phys. Rev. A* **77** 033625
- [363] Berloff N G 2004 *J. Phys. A: Math. Gen.* **37** 1617
- [364] Simula T P, Virtanen S M M and Salomaa M M 2002 *Phys. Rev. A* **65** 033614
- [365] Lundh E 2002 *Phys. Rev. A* **65** 043604
- [366] Pu H, Law C K, Eberly J H and Bigelow N P 1999 *Phys. Rev. A* **59** 1533
- [367] Shin Y, Saba M, Vengalattore M, Pasquini T A, Sanner C, Leanhardt A E, Prentiss M, Pritchard D E and Ketterle W 2004 *Phys. Rev. Lett.* **93** 160406

- [368] Möttönen M, Mizushima T, Isoshima T, Salomaa M M and Machida K 2003 *Phys. Rev. A* **68** 023611
- [369] Penckwitt A A, Ballagh R J and Gardiner C W 2002 *Phys. Rev. Lett.* **89** 260402
- [370] Tsubota M, Kasamatsu K and Ueda M 2003 *Phys. Rev. A* **65** 023603
- [371] Kasamatsu K, Tsubota M and Ueda M 2003 *Phys. Rev. A* **67** 033610
- [372] Lobo C, Sinatra A and Castin Y 2004 *Phys. Rev. Lett.* **92** 020403
- [373] Kivshar Y S, Christou J, Tikhonenko V, Luther-Davies B and Pismen L M 1998 *Opt. Commun.* **152** 198
- [374] Fetter A L 1998 *J. Low Temp. Phys.* **113** 189
- [375] Svidzinsky A A and Fetter A L 2000 *Phys. Rev. Lett.* **84** 5919
- [376] Lundh E and Ao P 2000 *Phys. Rev. A* **61** 063612
- [377] Tempere J and Devreese J T 2000 *Solid State Commun.* **113** 471
- [378] Rokhsar D S 1997 *Phys. Rev. Lett.* **79** 2164
- [379] McGree S A and Holland M J 2001 *Phys. Rev. A* **63** 043608
- [380] Anderson B P, Haljan P C, Wieman C E and Cornell E A 2000 *Phys. Rev. Lett.* **85** 2857
- [381] Fedichev P O and Shlyapnikov G V 1999 *Phys. Rev. A* **60** 1779(R)
- [382] Abrikosov A A 1957 *Sov. Phys. JETP* **5** 1174
- [383] Madison K W, Chevy F, Wohlleben W and Dalibard J 2000 *J. Mod. Opt.* **47** 2715
- [384] Aref H, Newton P K, Stremmler M A, Tokieda T and Vainchtein D L 2003 *Adv. Appl. Mech.* **39** 1
- [385] Newton P K 2007 *Discrete Continuous Dyn. Syst. A* **19** 411
- [386] Carretero-González R, Kevrekidis P G, Kevrekidis I G, Maroudas D, Theocharis G and Frantzeskakis D 2005 *J. Phys. Lett. A* **341** 128
- [387] Tkachenko V K 1966 *Sov. Phys. JETP* **22** 1282
- [388] Coddington I, Engels P, Schweikhard V and Cornell E A 2003 *Phys. Rev. Lett.* **91** 100402
- [389] Matthews M R, Hall D S, Jin D S, Ensher J R, Wieman C E, Cornell E A, Dalfovo F, Minniti C and Stringari S 1998 *Phys. Rev. Lett.* **81** 243
- [390] Higbie J M, Sadler L E, Inouye S, Chikkatur A P, Leslie S R, Moore K L, Savalli V and Stamper-Kurn D M 2005 *Phys. Rev. Lett.* **95** 050401
- [391] Saito H and Ueda M 2005 *Phys. Rev. A* **72** 023610
- [392] Kasamatsu K, Tsubota M and Ueda M 2003 *Phys. Rev. Lett.* **91** 150406
- [393] Schweikhard V, Coddington I, Engels P, Tung S and Cornell E A 2004 *Phys. Rev. Lett.* **93** 210403
- [394] Simula T P, Engels P, Coddington I, Schweikhard V, Cornell E A and Ballagh R J 2005 *Phys. Rev. Lett.* **94** 080404
- [395] Proukakis N P, Schmiedmayer J and Stoof H T 2006 *Phys. Rev. A* **73** 053603
- [396] Hofer M A, Ablowitz M J, Coddington I, Cornell E A, Engels P and Schweikhard V 2006 *Phys. Rev. A* **74** 023623
- [397] Shvartsburg A B, Stenflo L and Shukla P K 2002 *Eur. Phys. J. B* **28** 71
- [398] Zak M and Kulikov I 2003 *Phys. Lett. A* **307** 99
- [399] Zak M and Kulikov I 2003 *Phys. Rev. A* **67** 063605
- [400] Damski B 2004 *Phys. Rev. A* **69** 043610
- [401] Pérez-García V M, Konotop V V and Brazhnyi V A 2004 *Phys. Rev. Lett.* **92** 220403
- [402] Kamchatnov A M, Gammal A and Kraenkel R A 2004 *Phys. Rev. A* **69** 063605
- [403] Menotti C, Kraemer M, Smerzi A, Pitaevskii L and Stringari S 2004 *Phys. Rev. A* **70** 023609
- [404] Dekel G, Fleurov V, Soffer A and Stucchio C 2007 *Phys. Rev. A* **75** 043617
- [405] Damski B 2004 *J. Phys. B: At. Mol. Opt. Phys.* **37** L85
- [406] Damski B 2006 *Phys. Rev. A* **73** 043601
- [407] Liberman M A and Yelikovich A L 1986 *Physics of Shock Waves in Gases and Plasmas* (Heidelberg: Springer)
- [408] Kodama Y 1999 *SIAM J. Appl. Math.* **59** 2162
- [409] Abdullaev F Kh, Caputo J G, Kraenkel R A and Malomed B A 2003 *Phys. Rev. A* **67** 013605
- [410] Kevrekidis P G, Theocharis G, Frantzeskakis D J and Malomed B A 2003 *Phys. Rev. Lett.* **90** 230401
- [411] Matuszewski M, Infeld E, Malomed B A and Trippenbach M 2005 *Phys. Rev. Lett.* **95** 050403
- [412] Whitham G B 1974 *Linear and Nonlinear Waves* (New York: Wiley)
- [413] Muryshev A E, van Linden van den Heuvell H B and Shlyapnikov G V 1999 *Phys. Rev. A* **60** 2665(R)
- [414] Carr L D, Leung M A and Reinhardt W P 2000 *J. Phys. B: At. Mol. Opt. Phys.* **33** 3983
- [415] Feder D L, Pindzola M S, Collins L A, Schneider B L and Clark C W 2000 *Phys. Rev. A* **62** 053606
- [416] Rosenbusch P, Bretin V and Dalibard J 2002 *Phys. Rev. Lett.* **89** 200403
- [417] García-Ripoll J J and Pérez-García V M 2001 *Phys. Rev. A* **63** 041603
- [418] Modugno M, Pricoupenko L and Castin Y 2003 *Eur. Phys. J. D* **22** 235
- [419] Ruostekoski J 2004 *Phys. Rev. A* **70** 041601(R)

- [420] Donnelly R J 1991 *Quantized Vortices in Helium II* (New York: Cambridge University Press)
- [421] Saffman P G 1992 *Vortex Dynamics* (New York: Cambridge University Press)
- [422] Ruostekoski J and Anglin J R 2001 *Phys. Rev. Lett.* **86** 3934
- [423] Zhai H, Chen W Q, Xu Z and Chang L 2003 *Phys. Rev. A* **68** 043602
- [424] Mueller E J 2004 *Phys. Rev. A* **69** 033606
- [425] Savage C M and Ruostekoski J 2003 *Phys. Rev. Lett.* **91** 010403
- [426] Wüster S, Argue T E and Savage C M 2005 *Phys. Rev. A* **72** 043616
- [427] Battye R A, Cooper N R and Sutcliffe P M 2002 *Phys. Rev. Lett.* **88** 080401
- [428] Law C T and Swartzlander G A 1993 *Optics Lett.* **18** 586
- [429] McDonald G S, Syed K S and Firth W J 1993 *Opt. Commun.* **95** 281
- [430] Pelinovsky D E, Stepanyants Yu A and Kivhsar Yu S 1995 *Phys. Rev. E* **51** 5016
- [431] Tikhonenko V, Christou J, Luther-Davis B and Kivhsar Yu S 1996 *Opt. Lett.* **21** 1129
- [432] Carr L D and Clark C W 2006 *Phys. Rev. A* **74** 043613
- [433] Ginsberg N S, Brand J and Hau L V 2005 *Phys. Rev. Lett.* **94** 040403
- [434] Sackett C A, Stoof H T C and Hulet R G 1998 *Phys. Rev. Lett.* **80** 2031
- [435] Sackett C A, Gerton J M, Welling M and Hulet R G 1999 *Phys. Rev. Lett.* **82** 876
- [436] Chiao R Y, Garmire E and Townes C H 1964 *Phys. Rev. Lett.* **13** 479
- [437] Moll K D, Gaeta A L and Fibich G 2003 *Phys. Rev. Lett.* **90** 203902
- [438] Parker N G, Martin A M, Cornish S L and Adams C S 2006 *Proc. Australian Institute of Physics 17th National Congress (Brisbane)* Paper 119
- [439] Trippenbach M, Matuszewski M and Malomed B A 2005 *Europhys. Lett.* **70** 8
- [440] Carr L D and Clark C W 2006 *Phys. Rev. Lett.* **97** 010403
- [441] Dodd R J 1996 *J. Res. Natl Inst. Stand. Technol.* **101** 545
- [442] Dodd R J, Edwards M, Williams C J, Clark C W, Holland M J, Ruprecht P A and Burnett K 1996 *Phys. Rev. A* **54** 661
- [443] Goodman R H, Holmes P J and Weinstein M I 2004 *Physica D* **192** 215
- [444] Maradudin A A 1966 *Theoretical and Experimental Aspects of the Effects of Point Defects and Disorder on the Vibrations of Crystal* (New York: Academic)
- [445] Lifshitz I M and Kosevich A M 1966 *Rep. Prog. Phys.* **29** 217
- [446] Dobson J F 1994 *Phys. Rev. Lett.* **73** 2244
- [447] Herring G, Kevrekidis P G, Carretero-González R, Malomed B A, Frantzeskakis D J and Bishop A R 2005 *Phys. Lett. A* **345** 144
- [448] Konotop V V, Pérez-García V M, Tang Y-F and Vázquez L 1997 *Phys. Lett. A* **236** 314
- [449] Konotop V V and Vekslerchik V E 1994 *Phys. Rev. E* **49** 2397
- [450] Parker N G, Proukakis N P, Barenghi C F and Adams C S 2004 *Phys. Rev. Lett.* **92** 160403
- [451] Oh Y-J 1989 *Commun. Math. Phys.* **121** 11
- [452] Oh Y-J 1989 *J. Diff. Eqns* **81** 255
- [453] Parker N G, Proukakis N P, Leadbeater M and Adams C S 2003 *Phys. Rev. Lett.* **90** 220401
- [454] Parker N G, Proukakis N P, Leadbeater M and Adams C S 2003 *J. Phys. B: At. Mol. Opt. Phys.* **36** 2891
- [455] Proukakis N P, Parker N G, Frantzeskakis D J and Adams C S 2004 *J. Opt. B: Quantum Semiclass. Opt.* **6** S380
- [456] Parker N G, Proukakis N P, Barenghi C F and Adams C S 2004 *J. Phys. B: At. Mol. Opt. Phys.* **37** S175
- [457] Kevrekidis P G, Carretero-González R, Theocharis G, Frantzeskakis D J and Malomed B A 2003 *Phys. Rev. A* **68** 035602
- [458] Theocharis G, Frantzeskakis D J, Carretero-González R, Kevrekidis P G and Malomed B A 2005 *Math. Comput. Simul.* **69** 537
- [459] Theocharis G, Frantzeskakis D J, Carretero-González R, Kevrekidis P G and Malomed B A 2005 *Phys. Rev. E* **71** 017602
- [460] Kevrekidis P G, Carretero-González R, Theocharis G, Frantzeskakis D J and Malomed B A 2003 *J. Phys. B: At. Mol. Phys.* **36** 3467
- [461] Bhattacharjee A B, Morsch O and Arimondo E 2004 *J. Phys. B: At. Mol. Phys.* **37** 2355
- [462] Kevrekidis P G, Malomed B A, Frantzeskakis D J and Carretero-González R 2004 *Phys. Rev. Lett.* **93** 080403
- [463] Carretero-González R, Kevrekidis P G, Malomed B A and Frantzeskakis D J 2005 *Phys. Rev. Lett.* **94** 203901
- [464] Alexander T J, Ostrovskaya E A, Sukhorukov A A and Kivshar Yu S 2005 *Phys. Rev. A* **72** 043603
- [465] Tung S, Schweikhard V and Cornell E A 2006 *Phys. Rev. Lett.* **97** 240402
- [466] Reijnders J W and Duine R A 2004 *Phys. Rev. Lett.* **93** 060401

- [467] Pu H, Baksmaty L O, Yi S and Bigelow N P 2005 *Phys. Rev. Lett.* **94** 190401
- [468] Estève J, Aussibal C, Schumm T, Figl C, Maillly D, Bouchoule I, Westbrook C I and Aspect A 2004 *Phys. Rev. A* **70** 043629
- [469] Wang D-W, Lukin M D and Demler E 2004 *Phys. Rev. Lett.* **92** 076802
- [470] Damski B, Zakrzewski J, Santos L, Zoller P and Lewenstein M 2003 *Phys. Rev. Lett.* **91** 080403
- [471] Roth R and Burnett K 2003 *J. Opt. B: Quantum Semiclass. Opt.* **5** S50
- [472] Roth R and Burnett K 2003 *Phys. Rev. A* **68** 023604
- [473] Guidoni L, Triché C, Verkerk P and Grynberg G 1997 *Phys. Rev. Lett.* **79** 3363
- [474] Guidoni L, Dépret B, di A Stefano and Verkerk P 1999 *Phys. Rev. A* **60** R4233
- [475] Sanchez-Palencia L and Santos L 2005 *Phys. Rev. A* **72** 053607
- [476] Gavish U and Castin Y 2005 *Phys. Rev. Lett.* **95** 020401
- [477] Schulte T, Drenkelforth S, Kruse J, Ertmer W, Arlt J, Sacha K, Zakrzewski J and Lewenstein M 2005 *Phys. Rev. Lett.* **95** 170411
- [478] Lye J E, Fallani L, Modugno M, Wiersma D S, Fort C and Inguscio M 2005 *Phys. Rev. Lett.* **95** 070401
- [479] Clément D, Varón A F, Hugbart M, Retter J A, Bouyer P, Sanchez-Palencia L, Gangardt D M, Shlyapnikov G V and Aspect A 2005 *Phys. Rev. Lett.* **95** 170409
- [480] Fort C, Fallani L, Guarrera V, Lye J E, Modugno M, Wiersma D S and Inguscio M 2005 *Phys. Rev. Lett.* **95** 170410
- [481] Clément D, Varón A F, Retter J A, Sanchez-Palencia L, Aspect A and Bouyer P 2006 *New J. Phys.* **8** 165
- [482] Anderson P W 1958 *Phys. Rev.* **109** 1492
- [483] Fisher M P A, Weichman P B, Grinstein G and Fisher D S 1989 *Phys. Rev. B* **40** 546
- [484] Scalettar R T, Batrouni G G and Zimanyi G T 1991 *Phys. Rev. Lett.* **66** 3144
- [485] Freedman R and Hertz J A 1977 *Phys. Rev. B* **15** 2384
- [486] Imry Y 1995 *Europhys. Lett.* **30** 405
- [487] Mézard M, Parisi G and Virasoro M A 1987 *Spin Glass and Beyond* (Singapore: World Scientific)
- [488] Lewenstein M, Sanpera A, Ahufinger V, Damski B, Sen A and Sen U 2007 *Adv. Phys.* **56** 243
- [489] Kuhn R C, Miniatura C, Delande D, Sigwarth O and Müller C A 2005 *Phys. Rev. Lett.* **95** 250403
- [490] Sanchez-Palencia L, Clément D, Lukan P, Bouyer P, Shlyapnikov G V and Aspect A 2007 *Phys. Rev. Lett.* **98** 210401
- [491] Paul T, Schlagheck P, Leboeuf P and Pavloff N 2007 *Phys. Rev. Lett.* **98** 210602
- [492] Fallani L, Lye J E, Guarrera V, Fort C and Inguscio M 2007 *Phys. Rev. A* **75** 061603(R)
- [493] Sanchez-Palencia L 2006 *Phys. Rev. A* **74** 053625
- [494] Lee D K K and Gunn J M F 1990 *J. Phys. Condens. Matter* **2** 7753
- [495] Bilas N and Pavloff N 2006 *Eur. Phys. J. D* **40** 387
- [496] Lukan P, Clément D, Bouyer P, Aspect A and Sanchez-Palencia L 2007 *Phys. Rev. Lett.* **99** 180402
- [497] Schwartz T, Bartal G, Fishman S and Segev M 2007 *Nature* **446** 52
- [498] Fallani L, Lye J E, Guarrera V, Fort C and Inguscio M 2007 *Phys. Rev. Lett.* **98** 130404
- [499] Lukan P, Clément D, Bouyer P, Aspect A, Lewenstein M and Sanchez-Palencia L 2007 *Phys. Rev. Lett.* **98** 170403
- [500] Huse D A and Siggia E D 1982 *J. Low Temp. Phys.* **46** 137
- [501] Dörre P, Haug H and Tran D B Thoi 1979 *J. Low Temp. Phys.* **35** 465
- [502] Kobe D H 1968 *Ann. Phys.* **45** 15
- [503] Goldman V V, Silvera I F and Leggett A J 1981 *Phys. Rev. B* **24** 2870
- [504] Griffin A 1996 *Phys. Rev. B* **53** 9341
- [505] Fetter A L and Walecka J D 1971 *Quantum Theory of Many-Particle Systems* (New York: McGraw Hill)
- [506] Blaizot J-P and Ripka G 1986 *Quantum Theory of Finite Systems* (Cambridge, MA: MIT Press)
- [507] Hutchinson D A W, Burnett K, Dodd R J, Morgan S A, Rusch M, Zaremba E, Proukakis N P, Edwards M and Clark C W 2000 *J. Phys. B: At. Mol. Opt. Phys.* **33** 3825
- [508] Proukakis N P, Morgan S A, Choi S and Burnett K 1998 *Phys. Rev. A* **58** 2435
- [509] Burnett K 1999 *Proc. Int. School of Physics—Enrico Fermi* ed M Inguscio *et al* (Amsterdam: IOS Press)
- [510] Hutchinson D A W, Dodd R J and Burnett K 1998 *Phys. Rev. Lett.* **81** 2198
- [511] Zaremba E, Nikuni T and Griffin A 1999 *J. Low Temp. Phys.* **116** 277
- [512] Kirkpatrick T R and Dorfman J R 1983 *Phys. Rev. A* **28** 2576
- [513] Stoof H T C 1999 *J. Low Temp. Phys.* **114** 11
- [514] Stoof H T C 1999 *Dynamics: Models and Kinetic Methods for Non-Equilibrium Many-Body Systems* ed J Karkheck (Dordrecht: Kluwer)
- [515] Stoof H T C 2001 *Coherent Atomic Matter Waves, Proc. Les Houches Summer School Session 72 (1999)* ed R Kaiser *et al* (Berlin: Springer)

- [516] Duine R A and Stoof H T C 2001 *Phys. Rev. A* **65** 013603
- [517] Gardiner C W and Zoller P 1997 *Phys. Rev. A* **55** 2902
- [518] Jaksch D, Gardiner C W and Zoller P 1997 *Phys. Rev. A* **56** 575
- [519] Gardiner C W and Zoller P 1998 *Phys. Rev. A* **58** 536
- [520] Jaksch D, Gardiner C W, Gheri K M and Zoller P 1998 *Phys. Rev. A* **58** 1450
- [521] Gardiner C W and Zoller P 2000 *Phys. Rev. A* **61** 033601
- [522] Lee M D and Gardiner C W 2000 *Phys. Rev. A* **62** 033606
- [523] Davis M J, Gardiner C W and Ballagh R J 1997 *Phys. Rev. A* **62** 063608
- [524] Stoof H T C and Bijlsma M J 2001 *J. Low Temp. Phys.* **124** 431
- [525] Pitaevskii L P 1959 *Sov. Phys.—JETP* **35** 282
- [526] Choi S, Morgan S A and Burnett K 1998 *Phys. Rev. A* **57** 4057
- [527] Buljan H, Segev M and Vardi A 2005 *Phys. Rev. Lett.* **95** 180401
- [528] Mitchell M, Chen Z, Shih M and Segev M 1996 *Phys. Rev. Lett.* **77** 490
- [529] Mitchell M, Segev M, Coskun T H and Christodoulides D N 1997 *Phys. Rev. Lett.* **79** 4990
- [530] Ahufinger V and Sanpera A 2005 *Phys. Rev. Lett.* **94** 130403
- [531] Merhasin I M, Malomed B A and Band Y B 2006 *Phys. Rev. A* **74** 033614
- [532] Jackson B, Proukakis N P and Barenghi C F 2007 *Phys. Rev. A* **75** 051601(R)
- [533] Jackson B, Barenghi C F and Proukakis N P 2007 *J. Low Temp. Phys.* **148** 387
- [534] Dziarmaga J, Karkuszewski Z P and Sacha K 2002 *Phys. Rev. A* **66** 043615
- [535] Dziarmaga J and Sacha K 2002 *Phys. Rev. A* **66** 043620
- [536] Dziarmaga J, Karkuszewski Z P and Sacha K 2003 *J. Phys. B: At. Mol. Opt. Phys.* **36** 1217
- [537] Law C K 2003 *Phys. Rev. A* **68** 015602
- [538] Kanamoto R, Saito H and Ueda M 2005 *Phys. Rev. Lett.* **94** 090404
- [539] Lee R-K, Ostrovskaya E A, Kivshar Yu S and Lai Y 2005 *Phys. Rev. A* **72** 033607
- [540] Shapiro B 2007 *Phys. Rev. Lett.* **99** 060602
- [541] Skipetrov S E, Minguzzi A, van Tiggelen B A and Shapiro B 2008 *Phys. Rev. Lett.* **100** 165301
- [542] Henseler P and Shapiro B 2008 *Phys. Rev. A* **77** 033624
- [543] Weller A, Ronzheimer J P, Gross C, Frantzeskakis D J, Theocharis G, Kevrekidis P G, Esteve J and Oberthaler M K 2008 *Preprint* [arXiv:0803.4352](https://arxiv.org/abs/0803.4352)
- [544] Becker C, Stellmer S, Soltan-Panahi P, Dörscher S, Baumert M, Richter E-M, Kronjäger J, Bongs K and Sengstock K 2008 *Preprint* [arXiv:0804.0544](https://arxiv.org/abs/0804.0544)